NUREG/CR-3091
BNL-NUREG-51630
Vol. 1

Review of Waste Package Verification Tests

Semiannual Report Covering the Period April - September 1982

Prepared by G. T. Bida, D. Eastwood, H. Jain, B. Siskind, P. Soo

Brookhaven National Laboratory

Prepared for
U.S. Nuclear Regulatory Commission

GPO Printed copy price: $ 6.00

NUREG/CR-3091
BNL-NUREG-51630
Vol. 1

Review of Waste Package Verification Tests

Semiannual Report Covering the Period April - September 1982

Manuscript Completed: November 1982
Date Published: April 1983

Prepared by
G. T. Bida, D. Eastwood, H. Jain, B. Siskind, P. Soo

Brookhaven National Laboratory
Nuclear Waste Management Division
Upton, NY 11973

Prepared for
Division of Waste Management
Office of Nuclear Material Safety and Safeguards
U.S. Nuclear Regulatory Commission
Washington, D.C 20555
NRC FIN A3167

ABSTRACT

The current study is part of an ongoing task to specify tests that may be used to verify that engineered waste package/repository systems comply with NRC radionuclide containment and controlled release performance objectives. Work covered to date describes tests for demonstrating that chemical and mechanical failure modes in TiCode-12 containers and bentonite- and zeolite-based packing materials do not compromise the approximately 1000-year containment period for these engineered barriers.

CONTENTS

CONTENTS (Cont'd)

CONTENTS (Cont'd)

CONTENTS (Cont'd)

TABLES

FIGURES

FIGURES (Cont'd)

ACKNOWLEDGMENTS

The authors gratefully acknowledge the skills and patience of Bernadette Christian, Sharon M. Moore and Grace Searles in the typing and preparation of this report.

EXECUTIVE SUMMARY

This Biannual Progress Report addresses the testing requirements to demonstrate compliance with the NRC performance objective in 10 CFR 60 for radionuclide containment which states that radionuclides should be contained within the waste package for approximately 1000 years after repository closure. Both the metal container and packing material systems in the waste package have the potential to contain radionuclides but a borosilicate glass waste form itself does not, since it will always have a finite leach rate when contacted by groundwater. At the present time efforts in this study have focused on defining those container system and packing material system tests which may be used to show that each of these components complies with the 1000-year containment requirement. In specifying the tests, potential failure or degradation modes for the waste package components are necessarily addressed.

The first part of the study addresses the relevant corrosion test requirements for a TiCode-12 container system in order for this component to comply with the containment criterion after emplacement in salt and basalt repositories. Corrosion failure modes for this material include uniform and pitting corrosion, crevice corrosion, stress-corrosion cracking, hydrogen embrittlement, galvanic corrosion, and selective leaching.

Uniform corrosion is not expected to be a major problem, but its understanding as a function of various parameters will help in evaluating other types of corrosion. Pitting of TiCode-12 has not been observed to date. Testing for long durations under accelerated corrosion conditions will be needed to confirm this. Crevice corrosion in brine has only recently been observed and needs to be studied further under more prototypic conditions.

For stress-corrosion cracking, two broad categories of test are recommended: static and dynamic. Static testing methodologies are outlined including the use of smooth-bar, pre-cracked, and residual-stress specimens. In the dynamic test category, slow-strain-rate and the fatigue-crack-growth-rate methods are described. Long term testing on the order of years is recommended for stress-corrosion in TiCode-12 using statically loaded specimens under expected repository conditions.

Hydrogen from fabrication processes or radiolysis of groundwater can be seriously detrimental to the TiCode-12 container. Fracture mechanics tests for the determination of the threshold stress intensity factor K_{Th} are needed; other tests will be useful to supplement this information under anticipated elastic-plastic conditions.

Relatively little work has been done on either galvanic corrosion or selective leaching of titanium and its alloys. It is recommended that long term testing for these failure modes be carried out.

The two major attributes that a packing material should possess in order to comply with the containment criterion are: (1) groundwater flow control, and (2) retardation of radionuclide migration. Experimentally measurable properties associated with these attributes are evaluated to determine those that should be included in testing for containment. Available test methods that provide necessary licensing information are also discussed, and additional testing and data needs are identified. In this work, only two candidate packing materials are addressed, bentonite and synthetic zeolites. A review of the status of packing material testing has resulted in two general conclusions: (1) packing material properties and performance have not been determined under the range of conditions expected in a repository. For this reason, the available data base is currently insufficient to assure 1000-year containment of radionuclides, and (2) although some test methods are available for quantifying the important packing material attributes, no standard, generally-accepted methods appear to exist within the technical community. Some degree of test methodology standardization (e.g., a Materials Characterization Center-type approach) and interlaboratory data generation and statistical comparison seem essential.

From a groundwater flow control point of view, the design life of packing material can be divided into two time periods: (1) the time required to completely saturate the material and (2) the time for water to migrate through the backfill after saturation. Because of the swelling behavior of bentonite upon hydration and the complex interdependence of swelling pressure with other packing material properties, the first time period is a complex function of clay properties. In order to predict the long term behavior of expandable clays, more extensive testing is required to address these properties and the variables upon which they depend. The situation will probably be less complicated for non-expanding materials such as synthetic zeolites.

After saturation, groundwater flow through a material such as bentonite will depend on the hydraulic conductivity through the material. Thus, prediction of the long term behavior of fluid motion through saturated bentonite will require elucidation of the principal mode(s) of transport (Darcian, non-Darcian, or diffusion), and determination of diffusion rates for radionuclides and groundwater ions and the functional dependence of hydraulic conductivity on the hydraulic gradient.

Containment by the packing material will be significantly influenced by the presence of cracks since they act as fast flow paths for groundwater. Also, hydrologic erosion and liquefaction of the packing material will compromise its capability to retard radionuclides. These mechanical failure modes may occur as a result of heating of the packing materials by nuclear decay heat, either with or without drying, followed by intrusion of groundwater. Standard test methods for determining the liquid limit, plastic limit, and the shrinkage factors are briefly described and the use of the first two to test bentonite subjected to wet-dry cycling is discussed. Procedures which have provided information on the self-sealing properties of bentonite are described, and a method which has been used to investigate the ability of the backfill to slow or prevent the migration of water between the host geology

and the waste container system is delineated. Measurements of the self-sealing properties at higher temperatures and for longer time periods are recommended, as are direct measurements of the rate of flow of the permeating fluid through the packing material under conditions simulating the repository environment. In particular, it is urged that realistic values of the hydraulic gradients be used. It is concluded that even experiments lasting for several years may not be of adequate duration to demonstrate definitively the absence of mechanical failure of the packing material for the full 1000-year containment period specified in 10 CFR 60.

1. INTRODUCTION

The NRC Rule for the Disposal of High Level Waste in Geologic Repositories (10 CFR 60) specifies two main performance objectives for the engineered system:

a. "The containment of high level waste within the high level waste package will be substantially complete for a period of 1000 years after permanent closure of the geologic repository, or such other period as may be approved or specified by the Commission."

b. "The release rate of any radionuclide following the containment period shall not exceed one part in 100,000 per year of the inventory of that radionuclide calculated to be present at 1000 years following permanent closure, or such other fraction of the inventory as may be approved or specified by the Commission; provided, that this requirement does not apply to any radionuclide which is released at a rate less than 0.1% of the calculated total annual release at 1000 years following permanent closure."

In order to show compliance with these performance objectives the license applicant will need to provide a data base and analyses to quantify anticipated behavior of the waste package/repository system after permanent closure. This will necessarily involve research and testing programs to evaluate the likely modes by which engineered system components will degrade or fail by chemical or mechanical means. Knowledge of the ways in which the engineered barriers fail will permit estimates to be made regarding the containment capability of the waste package and the radionuclide release rate from the engineered system. Below is listed a logical sequence of events leading to loss of containment and the release of radionuclides:

a. Groundwater enters the engineered repository system
b. Groundwater penetrates the geologic packing material (discrete backfill)
c. Groundwater penetrates the containment system
d. Groundwater leaches radionuclides from the waste form
e. Radionuclides are transported through the failed container system, packing material and disturbed host rock to the near field environment.

Figures 1.1 and 1.2 outline the failure/degradation modes which may occur during the sequence of events leading to loss of containment and the release of radionuclides. Chemical (corrosion) and mechanical failure modes are given for each of the barriers in the engineered system. The ones ultimately found to be applicable will depend on specific waste package/repository designs, temperatures, water chemistry and flow rate, design geometries and sizes, and materials selected, etc.

The objective of the current study is to specify the types of test that may be used to demonstrate compliance with the containment and radionuclide release performance objectives for engineered systems. At this time only the containment criterion is addressed in this report; future activities will involve the specification of test requirements for demonstrating compliance with the release criterion.

Figure 1.1 serves as the basis for specifying containment verification tests for waste package components. Currently, borosilicate glass waste forms, titanium and Type 304L stainless steel containers, and bentonite- and zeolite-based packing materials are emphasized for evaluation in basaltic and salt repositories. Future work will include low carbon steel, which is now likely to be the main DOE container materials and tuff repository environments. Initially, the tests that will be described for verification of barrier performance will assume that the individual barriers (containers and packing material) are designed to meet the approximately 1000-year radionuclide containment requirement. The recommended tests specified to show compliance will outline the test variables to consider and the test methodology. Where appropriate, tests being developed by the Materials Characterization Center (MCC) will be evaluated and any limitations specified. Future research to develop additional testing methodologies will also be given.

In future work in this program, the use of more than one barrier component to meet NRC performance objectives will be discussed. This is an important consideration since the license applicant may choose to use, for example, a container/packing material system to meet the approximately 1000-year radionuclide containment time, or a waste form/packing material system to demonstrate that the release rate is less than 1 part in 10^5 per year. In such cases, bicomponent tests will be required in addition to single-component tests to quantify interaction effects. A recent report by Davis (1982) describes the demonstration of compliance with NRC engineered barrier performance objectives through the use of single and multiple waste package components.

Reference

NUREG/CR-2951, BNL-NUREG-51588, "Draft Staff Technical Position, Subtask 1.1: Waste Package Performance After Repository Closure," M. S. Davis and D. G. Schweitzer, Brookhaven National Laboratory, September 1982.

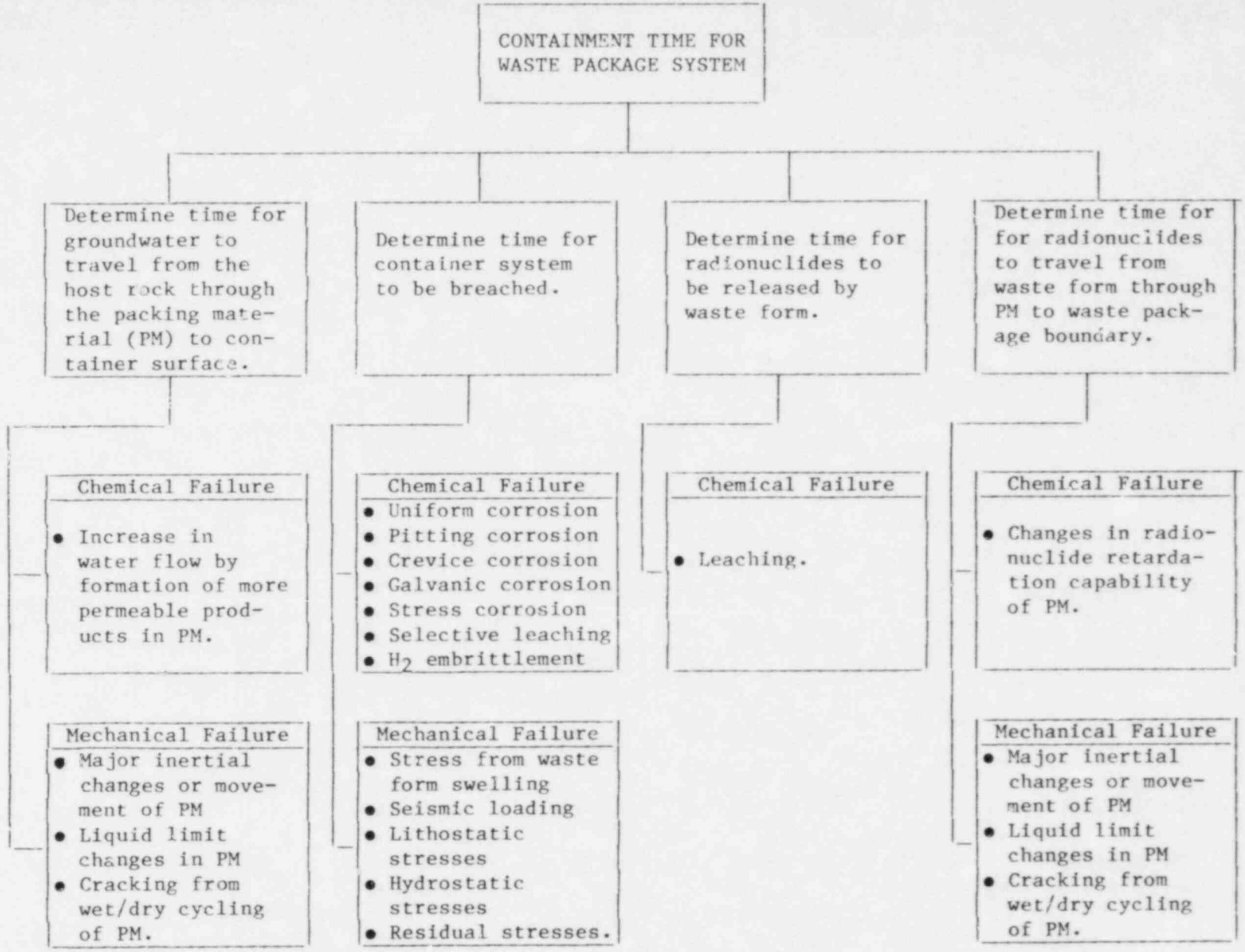

Figure 1.1 Chemical and mechanical failure/degradation modes affecting containment of radionuclides by the waste package system.

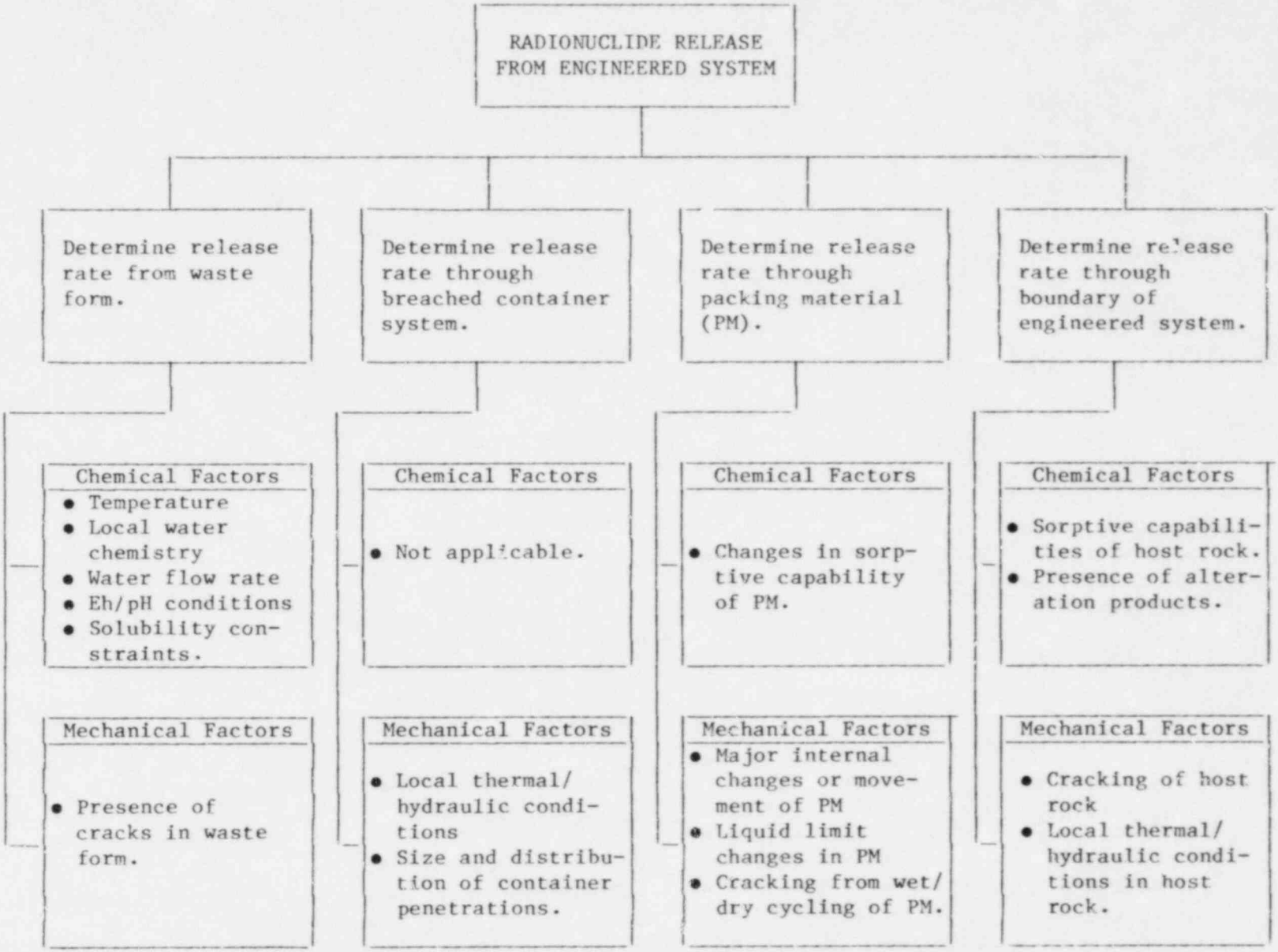

Figure 1.2 Factors affecting radionuclide release from the engineered repository system.

2. WASTE FORM TESTING REQUIREMENTS FOR DEMONSTRATION OF COMPLIANCE WITH THE CONTAINMENT CRITERION

Of the three principal waste package components (waste form, container, and packing material) the reference DOE borosilicate glass waste form has no radionuclide containment capability because of its finite leach rate upon contact with groundwater. On the other hand, the container system and packing material will prevent radionuclide migration until they are compromised by chemical or mechanical processes. In the sections below are described tests which could be used to show that a container or packing material meets the approximately 1000-year containment performance objective.

3. CONTAINER SYSTEM TESTING REQUIREMENTS FOR DEMONSTRATION OF COMPLIANCE WITH THE CONTAINMENT CRITERION

Titanium alloys have been identified as possible candidates for high level nuclear waste package applications in which relatively thin (<2 cm) corrosion-resistant sections are required. At least one of the current conceptual designs for a high level nuclear waste package incorporates a titanium alloy as part of the overpack structure (AESD-TME-3113, 1981). In the present report, the testing of one of these alloys, TiCode-12 (ASTM Grade 12),* for possible modes of corrosion is discussed. The composition of ASTM Grade 12 titanium nominally 0.3% molybdenum and 0.8% nickel, is given in Table 3.1. It should be noted that although TiCode-12 has been a leading candidate material for the waste package container, other materials such as low carbon steel are being considered. Considerations common to all of the tests are presented in the next two sections, 3.1 and 3.2. Each subsequent section contains a discussion specific to a particular corrosion failure mode. The discussion of each of these corrosion modes begins with some general introductory remarks about the testing for that mode. Some examples of testing of titanium or its alloys for the particular corrosion mode are then given so that the reader may be given some idea of the current status of such testing; testing of TiCode-12 is emphasized when such information is available. Finally, recommendations are made for further testing of TiCode-12 for these modes of corrosion in the context of demonstrating that a container of this material is capable of containing radionuclides for 1000 years.

Table 3.1 Composition of ASTM Grade 12 titanium.[a]

Element	Composition, %
Nickel	0.6 to 0.9
Molybdenum	0.2 to 0.4
Iron, max.	0.30
Carbon, max.	0.08
Oxygen, max.	0.25
Hydrogen, max.	0.015
Nitrogen, max.	0.03
Residuals (each), max.[b]	0.1
Residuals (total), max.[b]	0.4
Titanium	remainder

[a]From ASTM (1981b).
[b]A residual is an element present in a metal or an alloy in small quantities inherent to the manufacturing process but not added intentionally.

*American Society for Testing and Materials standard specification B265-79.

3.1 Relevant Test Environment Variables

Two kinds of repositories are presently under consideration for this report: (a) a salt repository where the container may come in contact with brine and (b) a basalt repository where it may come in contact with basaltic groundwater. Besides this basic difference, there are other variables, namely, temperature, pH, Eh, composition, and flow rate of the corroding groundwater; radiation, and new products generated due to irradiation, which must be considered in a laboratory test to simulate the field conditions.

Siskind and Hsieh (NUREG/CR-2780, Part 1, 1982) have recently reviewed near-field conditions for basalt and salt repositories. Their report lists available information on the ranges of different parameters which are likely to influence the life of TiCode-12. Groundwater chemistry and hydraulic properties are of concern with the basalt repository, whereas brine inclusion migration is specific to a salt repository. To ensure compliance of TiCode-12 to the containment criterion, respective corrosion and hydrogen embrittlement tests should be performed over the anticipated ranges of each of the above mentioned parameters. This will provide suitable data for extrapolation, to prototypic repository design conditions.

Some of the parameters may influence the corrosion life of TiCode-12 indirectly. For example, the temperature dependence of the uniform corrosion rate may be larger in a lower pH solution. Such interactions need to be considered to determine overall corrosion rates.

The presently available information on either basalt or salt repository conditions is not complete (NUREG/CR-2780, Part 1, 1982), which means that the respective testing conditions are also ill defined. The lack of information is most importantly due to uncertainties in the final design of the high level waste package itself. For example, relevant repository conditions will be vastly different depending on whether a radiation shield is used in the container system.

Shao and Soo (NUREG/CR-2780, Part 2, 1982) have reviewed available uniform and pitting corrosion data for TiCode-12 under different conditions. Though TiCode-12 has shown superior resistance to uniform and pitting corrosion, it is concluded that not all the possible repository conditions have been given enough attention. Major areas where further information is needed are:

- Effect of gamma radiation directly on the corrosion process or indirectly through changes in the corroding atmosphere due to radiolysis, etc.
- Correlation between microstructural variables of the alloy and corrosion rates.
- Stability of the oxide film which is primarily responsible for the corrosion resistance of TiCode-12.

- Reliability of the predictions of the lifetime of TiCode-12, based on data which are collected only during the very early stage of corrosion.

Similar conclusions are drawn by Lee and Ahn for crevice corrosion and hydrogen embrittlement, respectively, in the biannual BNL FIN A-3164 report under preparation.

3.2 General Experimental Considerations

To perform corrosion testing under the high temperature and high pressure conditions expected for the repositories, special laboratory apparatus is needed. Berry (1971) has discussed the basic types of testing arrangements, including autoclaves with a window or irradiation accessories. The experimental setup used at Rockwell International (RHO-BWI-ST-15, 1981) and Pacific Northwest Laboratory (PNL) (Pitman, S.G., 1981) are shown in Figures 3.1 and 3.2, respectively, for corrosion tests in simulated groundwater. For basalt repository conditions, as used at these organizations, one needs a high pressure autoclave system where a flow of solution is maintained. In the PNL setup, the groundwater was purged with N_2 or argon and passed through a column of basalt to create oxygen fugacity comparable to what is found in repository water. However, it was noted by Anderson (RHO-BWI-ST-15, 1981) that crushed basalt did not produce equilibrium values of oxygen concentration. In this respect, Hart (1971) has discussed the use of a galvanic cell to evaluate and then control the concentration of dissolved oxygen in the brine.

The uniform corrosion results reported from experiments at Rockwell International and PNL are preliminary; only weight changes for several alloys are reported without defining what these represent in terms of actual metal thickness loss. PNL plans to perform further tests under gamma radiation conditions (see Figure 3.3). The system at Rockwell International (Figure 3.1) appears to have a good access capability for solution analysis; the addition of an irradiation facility would be highly desirable.

Brine inclusions in salt repository have much smaller movement compared to water in a basalt repository. Therefore, having an autoclave with flowing brine is not necessary. BNL (NUREG/CR-2317, Vol. 1, No. 3, 1981), PNL (Pitman, S. G., 1981), and Sandia National Laboratories (SNL) (SAND79-2023C, 1979) have used closed systems, producing static corrosion data. Corrosion of TiCode-12 in geothermal brines is also being evaluated both in static (PB81-104564, 1980) and flowing autoclaves. The brines used in these tests are different from brines considered typical of salt repositories. Nevertheless, some of the experimental details are common and can be considered for the evaluation of corrosion in repository brines.

The material of the system in which corrosion tests are to be carried out, should ideally have negligible corrosion rates compared to that of the test specimens. When system corrosion is not negligible, corrosion products from the system can interfere with the sample corrosion process and produce

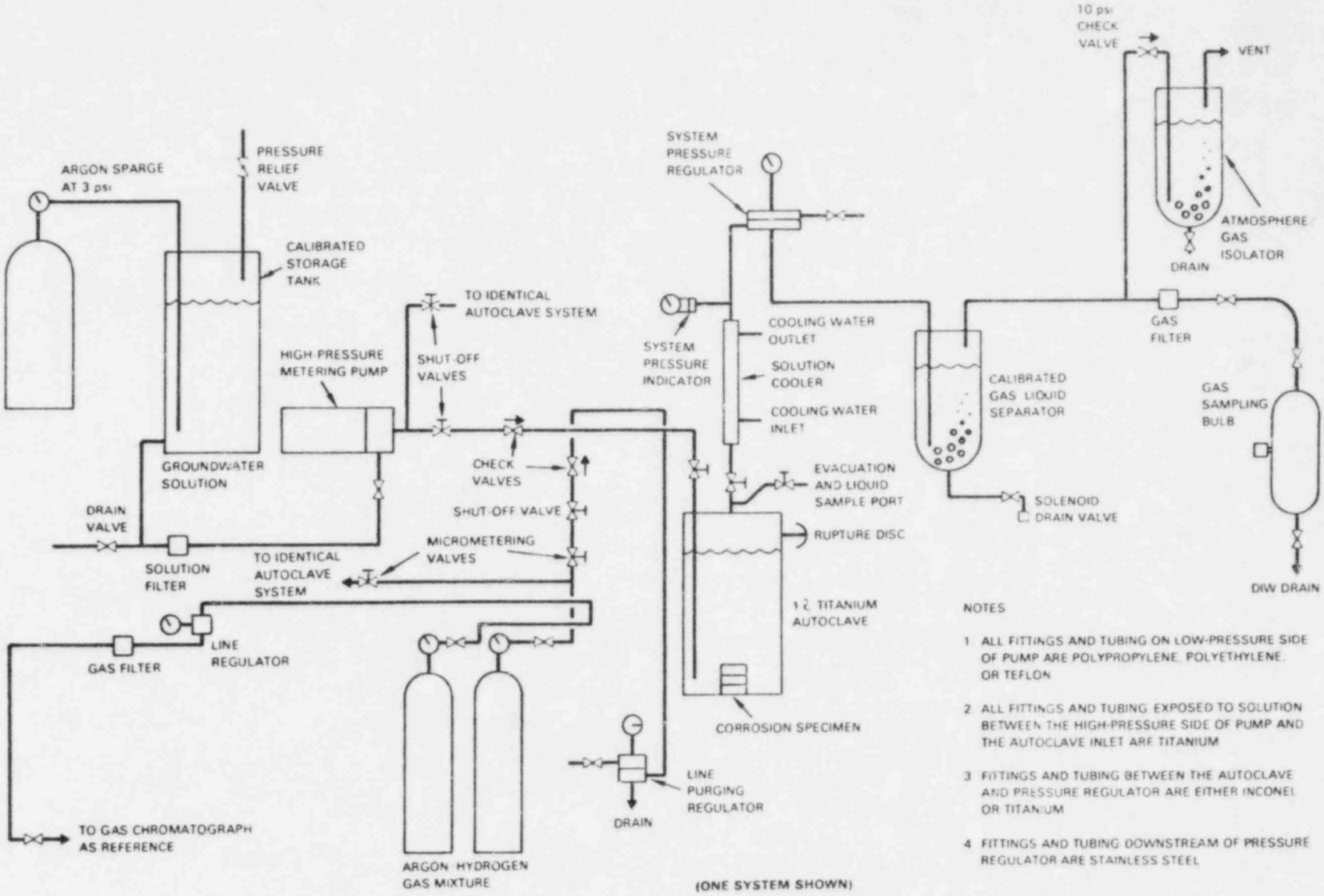

Figure 3.1 Rockwell corrosion testing system for container/overpack materials screening tests (RHO-BWI-ST-15, 1981).

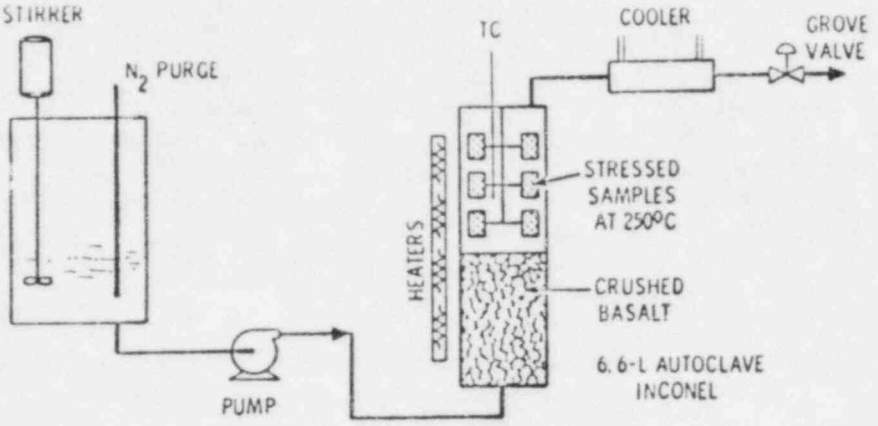

Figure 3.2 PNL autoclave system (PNL-3484, 1980.).

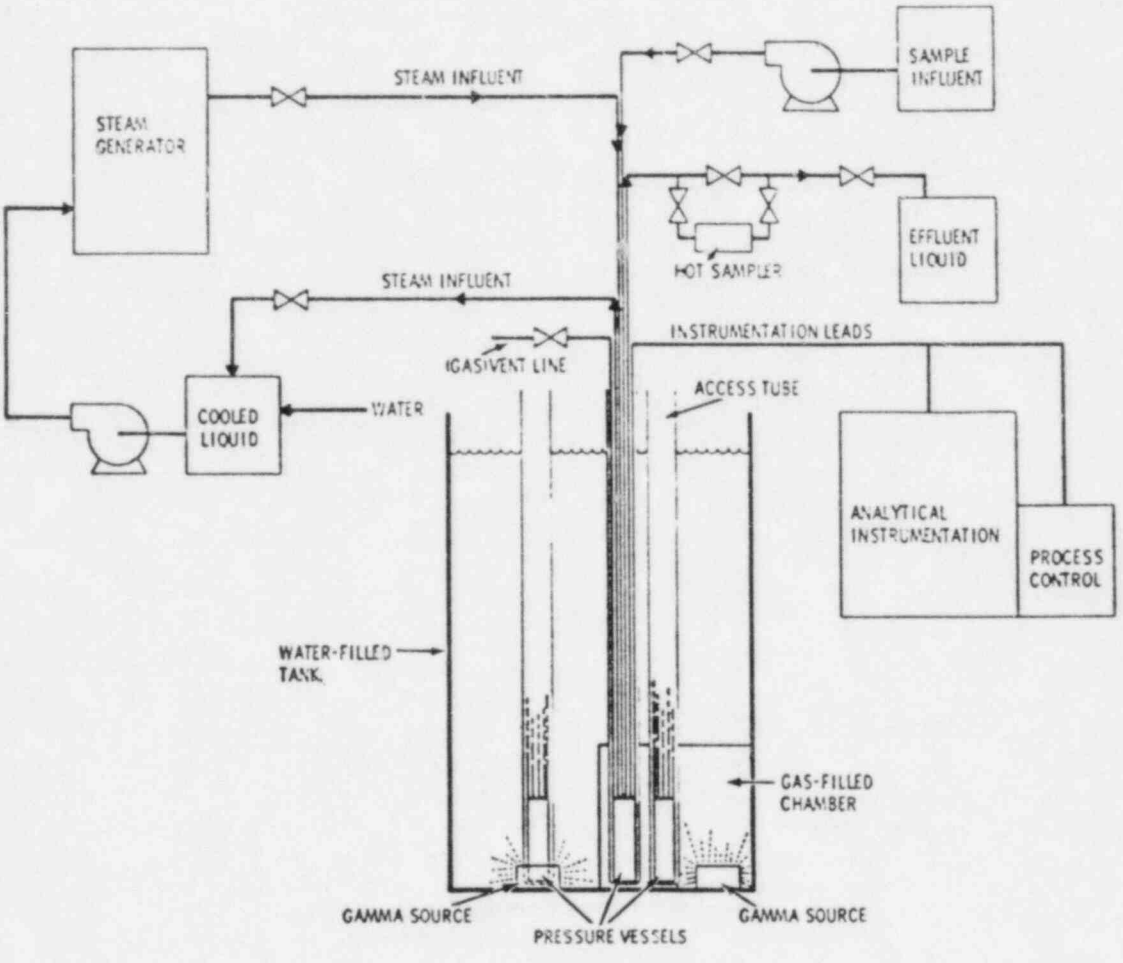

Figure 3.3 PNL radiation test facility (PNL-3484, 1980. ,.

incorrect results. For example, oxides of nickel and molybdenum originating from a Hastelloy autoclave were found to be deposited on TiCode-12 specimens in oxygenated brine (SAND79-2023C, 1979). Such deposition will not only give an incorrect change in weight of the sample, but may also affect the corrosion/passivation mechanism. PTFE Teflon is a commonly used liner material which does not corrode at room temperature. However, at elevated temperatures (>200°C), Teflon must be used with caution. Titanium or TiCode-12 liners for autoclaves may be an alternative. In summary, one should take precautions in selecting the testing equipment material so that it does not interfere with the corrosion process of the samples.

WIPP Brine A is a commonly used test solution which is considered to be representative of a salt repository. It is more corrosive (Braithwaite, J. W., 1980) than WIPP Brine B or seawater presumably due to its lower pH at high temperature. Compositions of these brines and seawater are listed in Table 3.2. The compositions listed in this table are indicative of equilibrium concentrations of various chemical species at room temperature. At elevated temperatures, the equilibrium concentration will be much higher due to higher solubility of various salts. For example, the fraction of total dissolved solids in Brine A at 25°C is 25.46 weight percent (using a density of 1.202 g/cc) (Stewart, D. B., 1978) which increases to 34.0 weight percent at 200°C. Further, it is concluded that bitterns near the waste containers will most probably contain 35 to 55 weight percent total dissolved solids and values as high as 75 weight percent are possible (Stewart, D. B., 1978). Clearly, the presently performed corrosion experiments at high temperatures in Brine A grossly underestimate the concentration of corrosive species which the container may encounter in a salt repository. Therefore, it is suggested that some testing be conducted as a function of temperature in brines which are in equilibrium at that temperature.

Temperature, radiation, and pressure are the major parameters which should be explicitly considered in evaluating corrosion of TiCode-12. Of these, the effect of radiation is least studied. For example, radiation will change the corrosion rate mainly by altering the chemistry of brines by radiolysis. The production of NaOH and hydrogen due to irradiation of salt has been postulated (Swyler, K. J., 1980) In this regard, one may consider two cases: (1) effect of radiation on brine and (2) effect of radiation on solid salt which eventually reacts with brine. The radiolysis products may or may not be the same for the two cases. It will be useful to check this point before continuing with elaborate experimentation with radiation.

When groundwater or brine reaches the container, its composition might also be modified due to the presence of packing material such as bentonite. However, a simple experiment demonstrating that brine composition does not change significantly after coming in contact with the packing material at appropriate temperature and pressure will be a desirable first step.

Table 3.2 Representative corrosion solution compositions (major ions).

Ion	Seawater (ppm)	Brine A[a] (ppm)	Brine B[b] (ppm)
Na^{+}	10,651	42,000	115,000
K^{+}	380	30,000	15
Mg^{+2}	1,272	35,000	10
Ca^{+2}	400	600	900
Sr^{+2}	13	5	15
Cl^{-}	18,980	190,000	175,000
SO_4^{-2}	884	3,500	3,500
I^{-}	0.05	10	10
HCO_3^{-}	146	700	10
Br^{-}	65	400	400
BO_3^{-3}	--	1,200	10
pH[c]	8.1	6.5	6.5
Eh[d]	--	mildly oxidizing	mildly oxidizing
Total Dissolved Solids	35 g/L	306 g/L	297 g/L

[a]Brine A is a high Mg, K, and Na chloride brine and is representative of water which might intrude into the proposed (WIPP) site by percolation through an overlying zone containing potash. It is also considered tentatively representative of minute brine inclusions found in bedded salt formations.

[b]Brine B is a nearly saturated, predominately NaCl brine representative of dissolved, bedded salt at the 800 m horizon of the proposed WIPP site.

[c]These pH values are taken at room temperature; they decrease with increasing temperature (e.g., seawater solution quenched from 270°C measured 3.3 at room temperature).

[d]From SAND80-2416C, 1980.

TiCode-12 has superior corrosion resistance compared to unalloyed titanium, presumably due to a change in anodic potential at the alloy surface caused by the alloying elements. Details of this mechanism are not known. Chemical analysis of specimens of TiCode-12 at BNL has shown (NUREG/CR-2317, Vol. 1, No. 3, 1982) considerable variation in the concentrations of iron and nickel. This compositional variation is likely to affect the corrosion rates of TiCode-12. To compare the results of different investigators, the source of their material should be reported, and preferably the same material used until the influence of alloying elements on corrosion is understood.

3.3 Tests for Uniform Corrosion

3.3.1 Introduction

In general, titanium and its alloys are very reactive; their surfaces readily transform into one of the oxides of titanium. The superior corrosion resistance of TiCode-12 is primarily due to the inertness and stability of this oxide film. When the oxide film is not stable, e.g., in air free dilute HCl or H_2SO_4 (where the corrosion potential is in the electrochemically active region) titanium corrodes rapidly. Determination of corrosion resistance of TiCode-12, therefore, concerns the properties of the oxide film during corrosion. Characterization of the oxide film under various corrosion conditions, though a very difficult task, is of vital importance.

Uniform corrosion tests should involve determination of the growth and/or dissolution rate of the oxide film as well as its stability. One may approach this problem either by focusing on the oxide film, or the remainder of the alloy not yet corroded. For the purpose of predicting the lifetime of the alloy, both approaches should be equally acceptable. Experimentally, the problems with each approach may be significantly different and one may obtain different results if the experimental conditions are not well understood.

In August of 1980, the Materials Characterization Center (MCC) held a workshop to prepare guidelines for corrosion testing of engineered barrier metals. The suggestions made by the MCC in its summary report (PNL-3720, 1981) are not specific to TiCode-12, but most of these are applicable to this alloy. The MCC Workshop considered various available testing procedures and recommended that the following hierarchy may be adopted to determine uniform corrosion rates: (1) gravimetric tests, (2) polarization resistance tests, (3) surface analysis for film thickness, (4) metallurgical examination, (5) surface analysis for characterization, (6) interferometry and ellipsometry techniques, and (7) solution analysis. Each of these test procedures are relevant to TiCode-12 as discussed below.

3.3.2 Gravimetric Measurements

The gravimetric or weight change method of determining uniform corrosion is based on estimating the loss of metal or alloy by measuring its weight before and after corrosion. It is recommended that the surface finish, thermal history, etc. of the laboratory specimen be representative of the container to

be used in the repository. To evaluate the effects of any microstructural or other changes during welding, additional testing on welded samples is necessary and may be carried out as suggested by ASTM (ASTM Designation G58-78, 1981).

In most cases, uniform corrosion produces oxide or some other form of loosely attached scale on the metal surface. In such cases, the loss in sample weight after removing the corrosion product is obtained to calculate the corrosion rate. The standard procedure for such a measurement is described by ASTM (ASTM Designation G1). In the case of TiCode-12 however, a strongly adhering oxide layer is formed. Removal of this oxide layer (which may be quite thin) can easily remove some of the metal as well, thus introducing a large error in weight loss. Discrepancies in the results of different authors (PNL-3484, 1980; RHO-BWI-ST-15, 1981) may be partly due to this reason. A preferred method for TiCode-12 would be to measure the gain in weight of the sample as the oxide layer is formed. However, note that the weight-gain method assumes: (1) all of the oxide adheres to the surface and (2) it does not dissolve in the corrosive solution.

Although uniform corrosion is often expressed as the change in weight for a given set of experimental conditions and test duration, for the purpose of estimating the life of a TiCode-12 container, it is more appropriate to describe corrosion in terms of loss of container thickness per year (μm/year). The conversion from weight-change to thickness-loss requires the knowledge of: (1) the area of the sample exposed to corrosive solution and (2) the nature of the corrosion film. The area of a sample is easy to determine, but the oxide film on TiCode-12 has hardly been characterized. In the simplest case, the weight gain is assumed entirely due to the addition of oxygen and thus the corresponding weight of titanium reacted with oxygen can be easily calculated if the type of oxide is known. From the weight of corroded titanium, finding the loss of thickness per year is straightforward.

In a complex system such as TiCode-12 in a brine containing 15 or more reactive ions, it is probably an incorrect assumption that corrosion produces only a TiO_2 film. For example, Braithwaite and others (SAND79-2023C, 1979) have found oxides of nickel and molybdenum in the corrosion layer and Ahn and Soo (NUREG/CR-2317, Vol. 1, No. 4, 1982) have found significant amounts of Mg and Si on the surface layer of TiO_2 formed from corrosion in WIPP Brine A. The latter authors also found that thickness of the film was twice the value predicted from weight measurements.

These observations suggest that for uniform corrosion of TiCode-12 in relevant solution, the weight gain cannot be easily converted to corrosion rate. To achieve such a conversion correctly, one should first correlate weight gain with loss of thickness of the alloy determined from an independent experiment.

As mentioned above, porosity of the film or adsorption of elements from solution, introduce error in the determination of alloy thickness lost due to corrosion. A more important consequence of adsorption of elements from solu-

tion is their effect on the stability of the oxide film. Such adsorption may mean that uniform corrosion does not produce an absolutely uniform oxide film and may lead to localized corrosion in time. This question will be considered further in the sections on non-uniform corrosion, but it may be noted that characterization of the oxide film produced by uniform corrosion is important even for other kinds of corrosion.

3.3.3 Electrochemical Measurements

3.3.3.1 Polarization Resistance Tests

The linear polarization technique is based on the relationship (Callow, L., 1976):

$$I_{corr} = B/R_p$$

where I_{corr} is the corrosion current which is directly proportional to the uniform corrosion rate, R_p is the experimentally determined polarization resistance and B is a constant related to Tafel slopes of the cathodic and anodic processes.

The sample in the appropriate corroding solution is polarized by applying a voltage of a few mV from the corrosion potential and then measuring the resulting current. Assuming that Ohm's law is applicable, the ratio of the two gives R_p. There are commercial instruments available which measure R_p and convert the results directly to the uniform corrosion rate in mils per year. The measurement can be done remotely and the corrosion process monitored without removing the sample from the autoclave or corrosion system. Thus, this method appears to be a simple, easy to use technique.

Due to departure from Ohm's law and uncertainty in the value of B, the results from the linear polarization method are considered to be only reliable to within a factor of two (Callow, L., 1976). Danielson (1980) has found that when oxygen is introduced into the solution, one may underestimate actual corrosion rates by as much as a factor of five because the corrosion rate is now controlled by mass transport at the cathode. Unfortunately, the results of polarization resistance do not give any indication that the corrosion mechanism and hence the value of B, has changed considerably. This method has not been used on TiCode-12 either for salt or basalt repository conditions. Due to different chemistries and conditions in the two repositories, one would need to determine the value of the constant B separately.

The polarization technique described above uses a dc signal. Detailed information about the corrosion mechanisms particularly in high resistivity groundwater can be obtained by measuring ac impedance over a wide range of frequencies. In several cases, the faradaic process is frequency dependent and one determines from "complex impedance analysis" the charge transfer resistance which then correlates well with the corrosion rate (Epelboin, I., 1981; Haruyama, S., 1981).

3.3.3.2 Other Electrochemical Measurements

In these measurements, one determines the voltage-current (voltammogram) response of the corrosion system under the relevant conditions of pH, temperature, etc. The results can be used to predict the corrosion behavior of an alloy by comparing with the voltage that would be expected in an actual situation. For example, titanium samples having an oxide layer prepared by thermal oxidation and anodization show different corrosion resistances. This observation is directly connected with polarization characteristics (Schutz, R. W., 1981). The corrosion resistance of an oxide film under different conditions can be estimated from the magnitude of the corrosion current after passivation.

Common experimental instrumentation for potentiostatic or potentiodynamic measurements is relatively simple and commercially available. Standard procedures for these measurements are described by ASTM (ASTM Designation G3 and G5, 1981). Substantial modification from the ASTM procedure is required to test TiCode-12 in a repository simulated environment. General problems of measurements above 100°C are discussed by Jones and Masterson (Jones, D. de G., 1970). Some measurements of TiCode-12 at high temperature and pressure using an autoclave are under way at BNL (NUREG/CR-2317, Vol. 1, No. 3, 1982) and SNL (SAND79-2023C, 1979). These results are very preliminary, and further experiments will be required before drawing any conclusions regarding the mechanisms of corrosion.

MacDonald, Syrett, and others (MacDonald, D. D., 1979; Syrett, B. C., 1980) have performed electrochemical measurements on TiCode-12 in geothermal brines at temperatures up to 250°C. Sweeping the voltage from the noble to the active region several times produces cyclic voltammograms such as that shown for TiCode-12 in Figure 3.4. From the complexity of Figure 3.4, it is clear that interpretation of such electrochemical measurements for alloys in complex corrosive solutions is not straightforward. However, cyclic voltammograms do indicate the changes which might be overlooked in a single sweeping of voltage. It is suggested here that to represent steady state behavior, the voltage sweeping rates be as slow as possible.

The corrosion potential for TiCode-12 was found to become more active when the temperature of the brine was increased, but started to become nobler with time (MacDonald, D. D., 1979) . It is believed that at higher temperatures, dissolved oxygen is consumed more readily and subsequent retardation in corrosion may be related to the formation of a surface film which inhibits the anodic reaction. Thus, the amount of dissolved oxygen is an important parameter and is reflected in the time dependence of voltammograms. It would be desirable to regulate the dissolved oxygen and then understand its effect on corrosion in a controlled manner. There are no experiments in basalt groundwater reported to date on voltammograms for TiCode-12. Due to fewer reactants than in brine, the data will probably be simpler and more useful. However, in this case, one would like to know explicitly the effect of dissolved oxygen on electrochemical parameters. Finally, in situations where enough supporting thermodynamic data about various reacting species in the

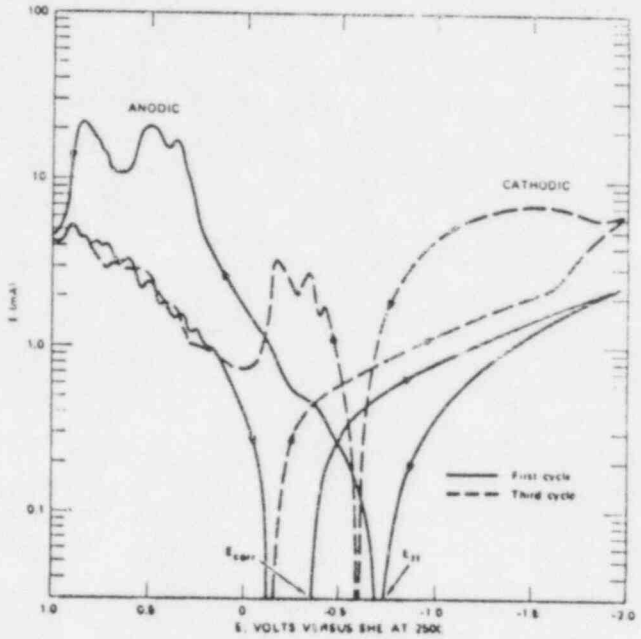

Figure 3.4 Cyclic voltammogram for TiCode-12 in high salinity brine at 250°C after 146 hours exposure (MacDonald, D. D., 1979).

corrosion solution are available (unfortunately to date not for TiCode-12), one can construct useful Pourbaix diagrams from voltammogram data (see MacDonald, D. D., 1979 and references therein).

3.3.4 Film Thickness Measurements

Uniform corrosion of TiCode-12 involves the growth of an oxide film on its surface and to a limited extent dissolution of this oxide film. Hence, the change in the thickness of a sample due to corrosion is the direct measurement for this type of corrosion. The MCC Workshop has suggested (PNL-3720, 1981) the following thickness measurement tests (in order of preference) for this purpose.

3.3.4.1 Surface Analyses

In this method, thickness of the oxide film is determined by sputtering the film off the sample. Since it is possible to perform this experiment in conjunction with Auger or ESCA (electron spectroscopy chemical analysis) facilities, one can also study the composition and structure of the film. Sputtering is a complex phenomenon and its rate may depend both on chemical compositions and physical condition of the film. However, once the rate of

sputtering is standardized for the given situation, the method can be easily used for similar specimens; corrosion specimens from basalt and salt solutions would probably need to be standardized separately. This method may be particularly attractive for TiCode-12 corrosion where film thickness will usually be very small.

3.3.4.2 Metallographic Examinations

It is always desirable to examine a metallographically sectioned and polished corrosion sample under an optical microscope. This will confirm the uniformity of the corrosion film as well as show any development of nonuniform corrosion. One can use this method to determine corrosion films thicker than 1 μ. However, since the film thickness on TiCode-12 is usually very small, use of an optical microscope may not be the ideal technique for thickness determination.

3.3.4.3 Interference and Ellipsometry Methods

These optical methods are appropriate for very thin oxide films and possibly appropriate for TiCode-12 corrosion study. In interferometric methods, the thickness of the oxide film is measured in terms of interference-fringe shift due to the optical path difference with respect to uncorroded surfaces. Sometimes, however, the fringes are not significantly shifted and are difficult to relate to absolute thickness. This method has not been commonly used in the past and only should be considered for TiCode-12 corrosion under special circumstances.

The above mentioned oxide thickness determination methods examine the film after the completion of corrosion. The ellipsometric method, however, can be used for in situ measurements during the growth of the film. In this fashion, one can observe the kinetics of film growth at very early stages. There are no measurements currently available on TiCode-12, but a titanium-aluminum alloy has been studied using ellipsometry under external stress and voltage (NAVSHIPRANDLAB 8-730, 1971). To investigate the uniform corrosion of TiCode-12, one would first need to determine the optical properties of the oxide film in relation to film thickness. Due to the possible deposition of some impurities from the corrosion solution, it is suggested that the films from basalt water and brine be calibrated separately if such techniques are employed.

3.3.5 Solution Analyses

In this method, uniform corrosion of an alloy is estimated from chemical analysis of the corrosion solution containing dissolved metal. Shortcomings of this technique were pointed out by the MCC (PNL-3720, 1981). For TiCode-12 corrosion in brine or basalt water, the corrosion solution is very complex and the dissolution rate of the alloy, if any, is very small. Therefore, this testing method is not expected to provide reasonably accurate uniform corrosion rates. However, chemical analysis of the solution may be useful to determine changes in solution such as those due to precipitation of compounds on specimens and autoclave walls.

3.3.6 Conclusions and Recommendations

Salient features, possible problems, and important precautions for the measurement of uniform corrosion of TiCode-12 using the general methods outlined by the MCC are discussed above. With this information, modifications of above methods in conjunction with new techniques can be readily adopted. For example, at BNL the thickness of oxide films on TiCode-12 after exposure to WIPP Brine A was determined by examining the transverse sections of the sample under the scanning electron microscope (NUREG/CR-2317, Vol. 1, No. 4, 1982). At the same time, energy dispersive spectroscopy techniques were used to identify any impurities in the corrosion scale. Since such instruments are versatile and very common, their usage may be preferred over the older techniques such as interferometry.

Most of the thickness measurement methods described above concentrate on the observation of the corrosion layer on TiCode-12. However, the basic parameter of interest is the loss in thickness of TiCode-12, which should be obtained as a function of time, temperature, radiation, pH, Eh, etc. One can measure this parameter most simply by examining the cross section of the corrosion sample. This is similar to the approach recently adopted at BNL except that the emphasis should be on the metal loss rather than the oxide growth. One may determine the alloy loss by measuring the position of its metallic surface from a pre-marked inert "reference", before and after corrosion. The "reference" can be a small part of the surface which was not exposed to corrosion, or a fine line on a side surface of the sample. Of course, it should be assured that the corrosion process is not altered due to the presence of the "reference".

3.4 Tests for Pitting Corrosion

3.4.1 Introduction

Pitting is a form of corrosion where the metal corrodes locally, at discrete locations on the surface. It occurs where the passivating film breaks locally, due to some flaw in the film, the metal below it, or even statistical fluctuation in corrosion solution. Thus, pitting is a highly statistical phenomenon, and testing results will depend on the area examined or number of the samples used. Extreme value statistical analysis (Gumbel, E. J., 1958) has been shown to reasonably predict the time of perforation of long metal tubes, from laboratory data on small samples (Finley, H. F., 1967; Ishikawa, Y., 1981). The same analysis may be applied here but, first, enough data on maximum pit depths should be collected to show that it obeys this analysis.

Since TiCode-12's corrosion resistance is due to the passivating TiO_2 film, this alloy may be susceptible to pitting. In general, pitting is aided by chloride ions. Therefore, a salt repository environment will be much more conducive to pitting than basalt water. Currently available data have not shown any signs of pitting corrosion of TiCode-12 in either environment, though several variables (e.g., irradiation, Eh and water flow rate in basalt

water, etc.) have not been evaluated (NUREG/CR-2780, Part 2, 1982). It is a well known fact that pitting may occur after an induction or incubation period which is not known for TiCode-12. The induction period may depend on the solution characteristics. Once started, a pit grows rapidly in an autocatalytic fashion. Long term tests on TiCode-12 should be carried out to determine the likelihood of pitting. It may be noted that due to the more corrosive environment inside a crevice, pitting could be more severe in this region.

The MCC summary report (PNL-3720, 1981) has listed the methods for non-uniform corrosion testing by dividing them into conventional and nonconventional techniques in flowing or static solutions. The distinction between static and flowing solutions is important because pitting may depend on the flow rate, e.g., there is a decrease in the pitting of a stainless steel as the flow rate of seawater increases (Beck, T. R., 1981). Apparently, the flowing solution changes the local conditions and the pit growth is arrested. However, uniform corrosion may be higher as the solution flow rate is increased. The MCC report has further identified following hierarchy of screening tests for pitting:

1. Mechanical breakdown of the passive layer.
2. Sustained electrochemical tests.
3. Immersion tests under chemical potentiostatic control.
4. Systems tests.

The above hierarchy is reasonable if the ease and time for testing are considered and should be appropriate for screening purposes. The tests in the first two categories are accelerated by externally applied mechanical or electrochemical perturbation. Besides being much faster, these tests are also appropriate for understanding the mechanisms of pitting. Important features and problems of all the test methods in the above categories are discussed next for pitting of TiCode-12 in basalt and salt repositories. General experimental considerations for pitting tests are almost the same as for uniform corrosion discussed earlier and are, therefore, not repeated here; only relevant differences will be pointed out.

3.4.2 Test Methods

3.4.2.1 Mechanical Breakdown of the Passive Layer

Since pitting is a result of local breakdown of the passivating layer, one can study the pitting behavior of TiCode-12 by artificially rupturing the titanium oxide film in a limited area (to maintain large cathode/anode area ratio) and observe the changes in surface properties. Ahn and others (NUREG/CR-2317, Vol. 1, No. 3, 1982) have made use of this test on titanium and TiCode-12 in 1 M HCl at 80°C. A scratch was made on the surface of these alloys using a diamond tipped scriber. From the open circuit potential transient measurement on a fully abraded surface the active/passive state of the sample could be determined as a function of time. These measurements were relatively fast and particularly useful in comparing the performance of titanium and TiCode-12, and may be used to compare TiCode-12 corrosion

resistance in various solutions. So far only preliminary testing has been done using the "scratch" method.

The method described above will provide some information about the mechanisms of pitting on TiCode-12. In this regard, it will be useful to produce a single pit and simultaneously observe it under an optical microscope. Bech and Chan (1981) have studied growth of small pits on stainless steel in this fashion. The flow rate of corrosion solution was varied in their experimental setup, which could be of use for tests relevant to a basalt repository. Alternatively, one may simply rotate the specimen at varying speeds if solution chemistry does not change during the test.

3.4.2.2 Sustained Electrochemical Tests

One purpose of an electrochemical test is to determine potential vs current characteristics of a corrosion cell for given conditions. An example is shown (Posey, F. A., 1967) in Figure 3.5 for titanium in chloride solution. Pitting occurs when a specific potential is reached. It is often necessary to identify the potential at which pitting starts and the one at which a pit repassivates; the two are different because it takes a more corrosive environment to initiate a pit than to sustain an established pit. When enough information is collected from polarization curves, regimes of passivation and pitting may be obtained as a function of test conditions.

There are several variations for electrochemical testing (NACE, 1977), but these may be divided into two broad categories, namely, controlled current and controlled potential. In the former, constant current is passed through a corrosion cell and the potential of the specimen is measured. The polarization curve is then obtained by changing the applied current, either in steps (galvanostatic) or by continuous sweeping (galvanodynamic). In many cases the sweeping rate will affect the current-potential response of the cell; the time dependence of potential (or current) may be useful information to describe the kinetics of pit growth (Greene, N. D., 1959). In the case of controlled potential, one applies a predetermined potential on the specimen and measures the resulting current. Due to the different time responses for the two types of tests, each has its own advantages and disadvantages (Dear, S. W., 1971). For metals which show an active/passive transition such as TiCode-12, the constant potential (potentiostatic or potentiodynamic) technique is most commonly used. However, it is useful to compare the results with galvanodynamic data, as was demonstrated in the determination of pitting and repassivation potentials of Incoloy in water containing chloride and phosphate ions (Hickling, J., 1981). Braithwaite and others (SAND79-2023C, 1979) have carried out some potentiodynamic measurements of passive layer breakdown potential of TiCode-12 in seawater, Brine A, and Brine B. Increasing temperature showed the strongest adverse effect, then lack of oxygen, followed by increasing salt content.

To obtain an estimate of the effect of surface preparation on the susceptibility of TiCode-12 to pitting, the "anodic breakdown residual potential test" (ABRPT) method by Murphy (1970) may be used. It is a galvanodynamic

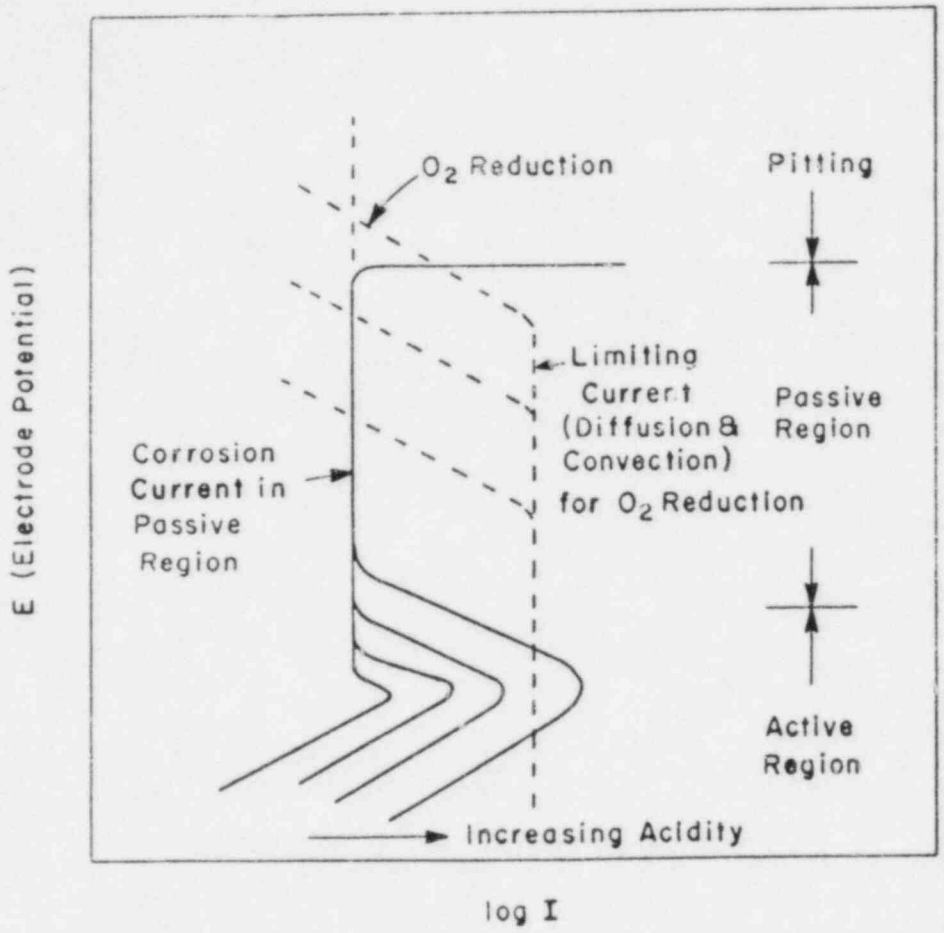

Figure 3.5 Schematic diagram of polarization curves for commercially pure titanium in chloride solution (Posey, F. A., 1967).

method in which the potential of the sample is measured as the applied current is gradually (within one hour) increased to 1000 μA. The minimum value of potential after anodic breakdown is taken as a measure of pitting susceptibility.

It cannot be overemphasized that electrochemical data are best suited for making comparisons of the pitting tendency of TiCode-12 under different conditions. The results may depend on the surface condition, rate of measurement, solution conditions, etc. Very often this makes it very difficult to compare results from different laboratories. Sometimes the mechanisms of pitting may be different in the actual situation and accelerated laboratory tests. Therefore, a correlation between actual pitting and electrochemical observations must be established for the latter to be directly useful. Nevertheless, several recently developed electrochemical and other techniques possess excellent capabilities to study the mechanisms of pitting. They are briefly described below:

- During pitting corrosion current flows between the anodic area inside the pit and the cathodic part of the sample. Figure 3.6 illustrates how the potential may vary across a pit on an inhomogeneous surface. The potential distribution on a pitting sample can be measured by scanning the sample surface with a microtip electrode (Isaacs, H. S., 1980; 1981). Alternatively, the microelectrode is kept fixed and a cylindrical sample is rotated to scan its circumference (Gainer, L. G., 1979). The testing system can be designed to map the potential across the whole surface directly, but is not available commercially. If it is possible to correlate the observed potential peak at the center of a pit to the corrosion current, the technique may be used to quantitatively determine pitting characteristics.

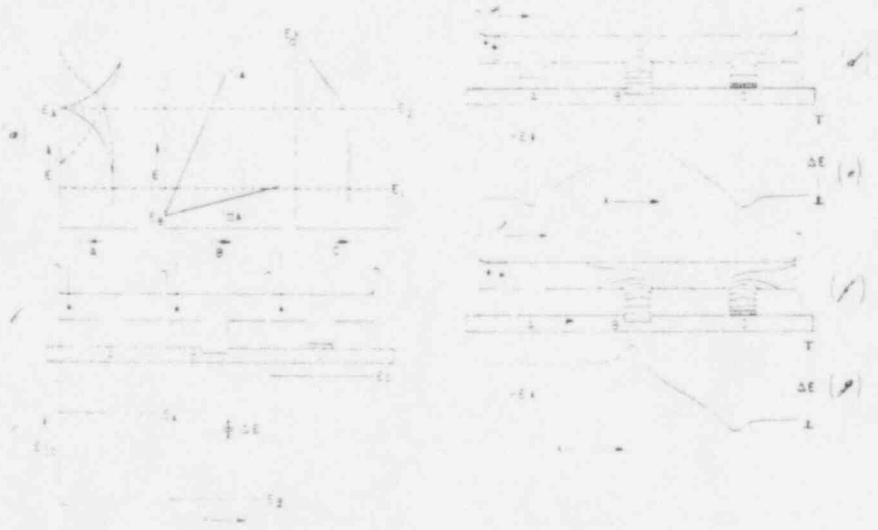

(a) Polarization diagrams for each exposed area
    A - passive surface supporting anodic and cathodic reactions
    B - local "pitting" anode with either high (I) or low (II) polarization
    C - metal-coated area supporting only a cathodic reaction.
(b) Areas exposed to separate solutions.
(c) Open-circuit potentials in solutions between "iron" and the reference electrodes.
(d) Equipotential lines in solution when area B has low polarization (II).
(e) Potential variations on scanning across the sample for case (d).
(f) Equipotential lines in solution when area B has high polarization (I).
(g) Potential variations on scanning across the sample for case (f).

Figure 3.6 Schematic variations of the potential in a solution above a partially coated "iron" surface (Issacs, H. S., 1981).

- Alternating current impedance measurements (MacDonald, D. D., 1981) are often used in corrosion studies to understand elementary processes such as dissolution, passivation, inhibition, mass transfer, etc. These measurements are particularly useful for high resistivity solutions, but so far a direct correlation between ac results and pitting has not been established.

Pitting on TiCode-12 results from local failure of the titanium oxide film. Therefore, the structure, stability, composition, etc. of this film should be characterized to understand the pitting phenomenon. It is not possible to achieve this goal with the exclusive use of the electrochemical techniques described above, and one should consider using modern surface analysis techniques to complement the electrochemical information. Optical and electron microscopy for film morphology, X-ray emission and electron spectroscopy for composition and film thickness, reflection high energy electron diffraction (RHEED) for the structure of the film, and Auger spectroscopy in conjunction with sputtering for layer by layer structure can virtually provide all the supporting information one might need for film characterization. By comparing the results of surface analysis techniques with the observed electrochemical conditions of various stages of pitting, one can predict the pitting with greater confidence or even suggest appropriate methods to improve pitting resistance (see MacDougal, B, 1982). Initially, such experiments will have to be limited to simpler corrosion conditions than expected for TiCode-12 in a repository, or the result may become too complex to be interpreted.

3.4.2.3 Immersion Tests Under Chemical Potentiostatic Control

These tests may be performed in the laboratory by exposing the specimens to the test solutions and allowing them to pit unaided by external electrochemical potentials. The pitting corrosion may then be evaluated following ASTM Standard Recommended Practice (ASTM Designation G46-76, 1981). The first step would be to obtain morphological information (size and shape, and then distribution) by visual examination or with a simple microscope; any correlation with surface heterogeneity should be recorded. There are other nondestructive methods (such as X-ray radiography, deflection of electromagnetic or ultrasonic waves around a pit, and penetration of a dye into the pits), which can be used to supplement direct observations of pitting. In the case of highly pitting resistant TiCode-12, however, these methods may not be of much help.

In determining the lifetime of a TiCode-12 container, pit sizes and depths are of foremost importance. ASTM Standard Practice (ASTM Designation G46-76, 1981) suggests the following categories of methods for pit depth measurements:

- Metallographic - a vertical section is cut through the deepest part of a pit. The pit depth is then measured from the surface to the bottom of the pit with an optical microscope.

- Micrometer or Depth Gauge - a micrometer with a pointed needle, or a depth gauge directly measures the pit depth with respect to the unaffected flat part of the surface. As an alternative, one may use a calibrated microscope and determine the depth by focusing it at the lip and the bottom of the pit.

- Machining - a sample with major faces parallel to each other is used. After pitting exposure and cleaning is over, one of the sample's surface is removed in small steps by parallel machining and the number of pits at each step counted until all the pits are removed. The difference between two successive steps gives the number of pits with the average depth of that particular step. This method is somewhat tedious but it gives information about the depth distribution as well as maximum pit depth.

To describe the extent of pitting on a surface, ASTM does not recognize any fixed procedure. However, to have a qualitative description, it is useful to describe the pit pattern with reference to ASTM standard chart (ASTM Designation G46-76, 1981). To describe susceptibility of pitting of an alloy, a pitting factor defined as the deepest metal penetration/average metal penetration is reported. In TiCode-12 the two penetrations may not be comparable and there can be large uncertainty in the pitting factor.

3.4.3 System Test

For the final determination of pitting corrosion life of TiCode-12 containers, MCC suggests that the testing be done on a full size container in an environment having as many features of a working repository as practical. Such testing will have to wait until all the details of repository design are completed. Meanwhile, testing should be initiated under laboratory conditions.

3.4.4 Conclusions and Recommendations

Many of the testing methods discussed above assume that pitting occurs on TiCode-12, even though none of the tests have so far shown (NUREG/CR-2780, Part 2, 1982) any sign of this type of corrosion. Since pitting may have long incubation periods, it is suggested that the tests be continued for periods of up to several years. To induce pitting, the testing should also be done under accelerating conditions (e.g., lower pH, higher temperature, etc. than those expected either in a salt or a basalt repository).

3.5 Tests for Crevice Corrosion

3.5.1 Introduction

Crevice corrosion can occur when stagnant corrosive solution is present in a crevice between the metal and some other surface. In this situation, the metal inside the crevice corrodes in an autocatalytic fashion similar to pitting on an open surface. This type of corrosion can be minimized by

restricting crevices around a nuclear waste container. However, the container will likely be in contact with packing material or other engineered barriers so that a crevice geometry may be unavoidable. Therefore, the testing of TiCode-12 for crevice corrosion is essential.

Crevice corrosion of commercial titanium in salt solution was detected by Griess (1968) many years ago. It was also confirmed that additional small amounts of nickel, molybdenum, or palladium would reduce the metal's susceptibility to this type of attack. It would, therefore, appear that TiCode-12 should be highly resistant to crevice corrosion. In fact, the SNL experiments (SAND79-2023C, 1979) did not show any sign of crevice corrosion on TiCode-12 in seawater at 300°C. However, recent results from BNL (NUREG/ CR-2317, Vol. 2, No. 1, 1982) have shown significant amounts of crevice corrosion. Assuming a constant rate of corrosion (though unlikely), they found that in 1000 years ~10 cm of metal could be lost inside the crevice. Since there is very little other data available on crevice corrosion of TiCode-12 and this form of corrosion is a potential failure mode (particularly in salt repositories), extensive testing will be needed to predict the life of the container.

3.5.2 Variables Affecting Crevice Corrosion

Oldfield and Sutton (1978 a) have listed most of the relevant parameters which influence crevice corrosion (Figure 3.7). With reference to TiCode-12 under repository conditions, we may add to this list radiation from the waste form, and lithostatic pressure. Traditionally, most crevice corrosion testing has been performed on steels where a crevice is associated with the presence of chloride or some other halide ion (Bates, J. F., 1973; Sedricks, A. J., 1979). For similar reasons, crevice corrosion on TiCode-12 will likely be more severe in a salt repository than under basaltic conditions. Naturally, in the initial stages, the testing should be done in brines.

Among the factors shown in Figure 3.7 to affect crevice corrosion, except for temperature (and radiation), all are fixed by the properties of TiCode-12 and the repository. The temperature depends on waste loading conditions.

3.5.3 Test Methods

From the point of view of basic mechanisms, crevice corrosion is very similar to pitting corrosion. In fact, pitting may be considered as crevice corrosion in which the pit is a self-induced crevice. It has been stated (Fontana, M. G., 1978) that if an alloy is susceptible to pitting, it will also show crevice corrosion; though the converse may not be true. Due to this similarity, the electrochemical tests described in the last chapter to understand the mechanism of pitting can usually be used for crevice corrosion. However, because of large differences in the physical nature of a pit and a crevice, direct tests for crevice corrosion are distinct and will be discussed next. The electrochemical tests will be discussed only to the extent that they are different from those for pitting.

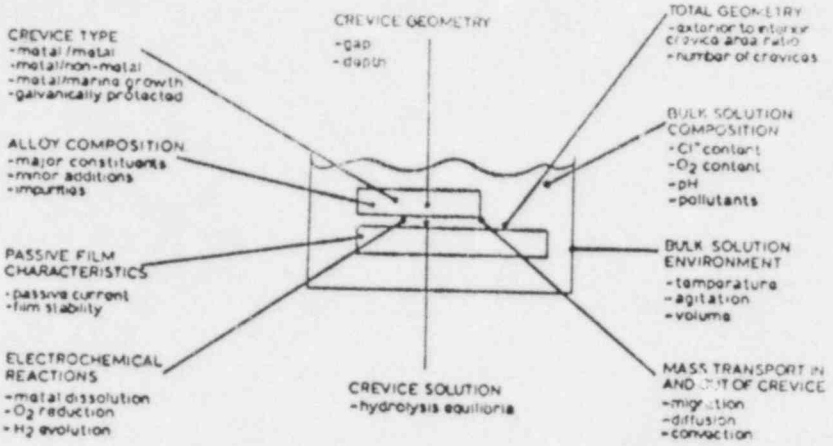

Figure 3.7 Factors affecting crevice corrosion (Oldfield, J. W., 1978 a).

3.5.3.1 Direct Tests

As with uniform and pitting corrosion tests, one can expose a TiCode-12 crevice sample to simulated repository conditions, and then examine the material loss either by weight change or some other methods discussed in the previous two sections. However, considering that TiCode-12 is highly corrosion resistant, and did not show crevice corrosion in SNL experiments (SAND79-2023C, 1979), it may become necessary to conduct the testing under accelerating conditions. This is desirable especially because crevice corrosion may have a long incubation period before active attack begins. From the results of Griess (1978), it is suggested that of the several variables listed in Figure 3.7, temperature, pH, and Cl^- concentration will be most effective for accelerating the corrosion. However, one should be cautious because in some instances, low pH and high Cl^- variables may not necessarily give an increase in crevice corrosion (Oldfield, J. W., 1978 b).

To test for crevice corrosion in the laboratory, an artificial crevice can be made either between two pieces of TiCode-12 or one piece of TiCode-12 and another inactive material. It is known (Brigham, R. J., 1981) that different surfaces can nucleate a crevice with varying degrees of effectiveness. In a repository, TiCode-12 will be most likely in contact with the packing material, which may enhance crevice corrosion. It is difficult, however, to predict the effect the packing material will have. Experiments should be conducted to scope the problem.

In the absence of any fundamental restrictions on crevice geometry, there have been virtually as many kinds of crevices as there are crevice corrosion investigations (Shreir, L. L., 1976; Day, K. J., 1976; France, W. D., 1968; Lizlovs, E. A., 1970; Diegle, R. B., 1982). For the sake of illustration, some crevice configurations are shown in Figure 3.8. A common deficiency in most of the crevices is the lack of knowledge of their actual width or area.

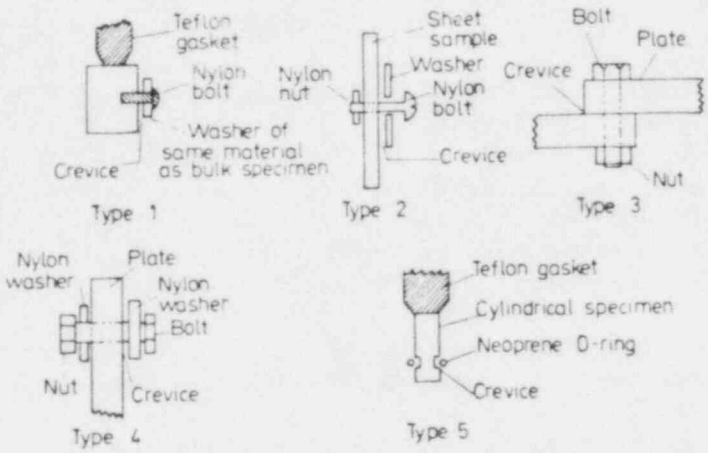

(Taken from Day, K. J., 1976.)

(a)

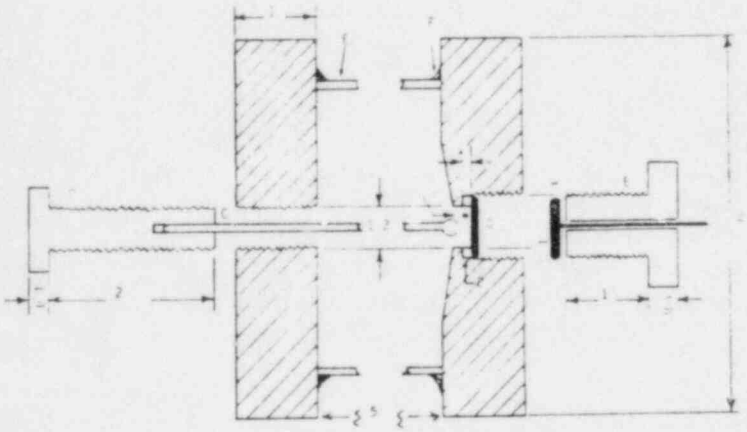

Taken from Lizlovs (1970)

A. Teflon bolt
B. PVC bolt
C. Glass rod with glass bead at the end
D. Teflon gasket
E. Glass tubing
F. Silicone rubber mount
G. Stainless steel working electrode
H. Copper disk with copper lead wire.

(b)

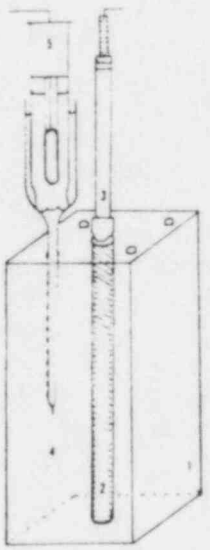

Taken from France and Greene (1968)

1. Plexiglass block
2. Specimen
3. Electrode holder
4. Potential probe
5. Saturated calomel reference.

(c)

Figure 3.8 Various types of crevices used for investigating crevice corrosion.

This has caused poor reproducibility even in determining if crevice corrosion exists under the "same" experimental conditions (Griess, J. C., 1968) and suggestions are made to include statistical analysis of the scatter in data. Therefore, in the methods not having a crevice with well defined area and width, an experiment should be performed on multiple similar samples and the range of results recorded. Figure 3.8(b) shows a crevice design which is purported to give reproducible crevice geometry. The France-Greene assembly (Figure 3.8(c)) has an added feature that potential can be measured along the length of the crevice. Many of the crevice designs referenced here may have the limitation that they cannot be used at temperatures as high as expected in a repository and may require certain modifications.

All the crevice designs mentioned above form a closed system in which the corrosion can be observed only by interrupting the test and dismantling the specimen. In these designs, the crevice region corrodes anodically, whereas the outside surface acts as a cathode. Lee (1981) has separated the anodic and cathodic areas by enclosing a small thin sheet specimen between two transparent acrylic blocks and then electrically connecting it to a freely exposed, much larger piece of the same metal. When the whole assembly is exposed to the corroding atmosphere, the small piece along with plastic blocks represents the inside of the crevice and the big piece acts as a cathode. In this way, he could observe the crevice corrosion in situ and obtain a better understanding of the corrosion mechanisms.

To investigate the severity of crevice corrosion, one can measure either the loss in weight or the thickness of the sample. To convert weight loss into a corrosion rate, one would need to know the area of the effective crevice. Then, it will be necessary to make an assumption that all the affected area corrodes at the same rate. Considering recent results on TiCode-12, which show a corrosion gradient within the crevice, this assumption may need careful evaluation. In thickness measurements, one may prefer to determine the maximum rather than the average reduction in thickness, using one of the methods described in the last section on pitting.

3.5.3.2 Electrochemical Tests

Crevice corrosion is usually considered to proceed in four stages: (1) consumption of oxygen within the crevice without any replenishment from outside, thus, an oxygen concentration cell is formed, (2) increase in acidity and chloride concentration within the crevice, (3) breakdown of the oxide passivation film and initiation of fast corrosion, and (4) propagation of crevice corrosion. By simply observing the crevice, one can identify the third and fourth stages of corrosion and correlate them with large changes in current. In this way, the incubation time and the time of rapid corrosion are known individually. With this information, the rate of crevice corrosion can be calculated more accurately rather than by simple averaging over the total test period; the error can be substantial in alloys having long incubation periods.

In the open crevice configuration (Lee, T. S., 1981) described earlier (also see Diegle, R. B., 1982), a zero impedance ammeter is connected between the cathode and anode. Thus, the current between the cathode and anode may be monitored continuously as crevice corrosion proceeds. This current may be a good measure of corrosion, since its correlation with direct weight loss was observed for stainless steels in seawater. This method of testing is not an electrochemical type in the sense it is described in earlier sections, but it can provide information about the corrosion mechanisms. With respect to the corrosion potential (E_{corr}) large changes (Figure 3.9) occur during breakdown of passivity. Therefore, measurements of E_{corr} (Oldfield, J. W., 1978 b) can also be used to determine the beginning of rapid crevice corrosion. Note that all the observations of micropitting and coalescing of pits shown in Figure 3.9 are specifically for Type 316 stainless steel, and may not be applicable to TiCode-12. Although E_{corr} shows time variation for different stages of crevice corrosion, the corrosion current can give quantitative data on corrosion rates as well.

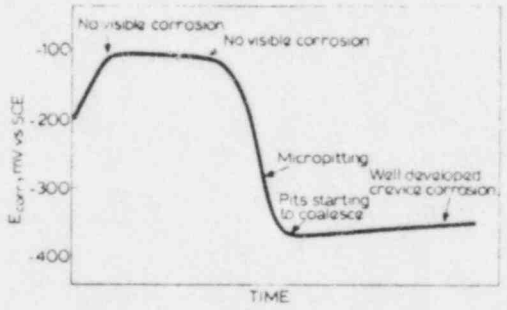

Figure 3.9 Schematic composite E_{corr}/time curve showing the development of corrosion of Type 316 stainless steel crevices (Oldfield, J. W., 1978 b).

The basic objectives for ordinary potentiostatic (dynamic) or galvanostatic (dynamic) testing for crevice corrosion is the same as those for pitting described in the previous section. Therefore, we shall examine only new considerations which are specially relevant to crevice corrosion. For the given corrosion conditions, a generally adopted electrochemical parameter is the protection potential below which a pit or crevice will repassivate. However, values of this potential may depend to some extent on the method of measurement and, hence, it may not be a unique quantity. Wilde (1972) has compared his cyclic potentiodynamic results on stainless steel samples having artificial crevices, with long term direct weight loss measurements. He concludes that the severity of crevice corrosion in an alloy increases with the area of the hysteresis loop on the voltage vs log (current) cyclic curve. This is an important observation in quantifying crevice corrosion of TiCode-12 under varying conditions. However, it must be realized that Wilde's

conclusion is based on empirical observations. Therefore, it needs to be shown that TiCode-12 also obeys such an empirical formulation.

In spite of the close similarity between pitting and crevice corrosion, there are some obvious differences. Crevice corrosion occurs in a small solution volume whose characteristics can be changed much more readily than those of pitting which will probably occur in the presence of a much larger volume of solution. However, within a pit the local chemistry may be substantially altered compared to the bulk solution. As a result, the kinetics and probably some details of the mechanisms of pitting and crevice corrosion can be substantially different. Therefore, when making any potential measurements, it will be desirable, to differentiate between pitting and crevice corrosion. Garner (1978) found for stainless steels, that in a potentiostatic study after applying a temporary voltage more positive than the pitting potential, the decay characteristics of the open circuit potential depended on whether pit- ting or crevice corrosion had been initiated. Depending on whether the steady state potential was in active or passive region, the presence or absence of crevice corrosion could be determined. It cannot be predicted if similar observations will be found for TiCode-12, but studies of potential-time transients may be a helpful and simple means of evaluation.

Since a crevice (at least the ones prepared artificially) is much larger than a pit, the conditions of corrosion within a crevice can be studied more easily. An important parameter concerning crevice corrosion is the actual pH of solution within the crevice at which corrosion starts, since this information can be used to conduct further tests in an open solution at this pH. Griess (1968) measured in situ pH in a titanium crevice at 150°C (in an autoclave) by withdrawing a very small volume (~.05 ml) of crevice solution. To do this, he had welded a titanium capillary to the center of the crevice, passing through the head of the autoclave.

Some observations from Griess' study (1968) on titanium and its alloys are very relevant for the testing of TiCode-12:

1. He determined the changes in pressure and composition of autoclave gases. In this way, he could determine what fractions of oxygen reduction and formation of hydrogen reactions were responsible for the cathodic half of the electrochemical reaction.

2. In principle, it is considered that a metal can be brought to an active state by the application of a proper external potential. However, Griess could not induce an active state by either cathodic or anodic polarization in a solution in which crevice corrosion occurred. He then suggested that an active crevice must have an acid concentration greater than 10^{-3} M.

3. Highly cathodic polarization produced hydride on the surface, which soon decomposed reforming a metallic surface.

4. Generally, it is difficult to clean the oxide film from the surface of titanium and its alloys. To obtain an anodic polarization curve in acidified brine, the solution was deoxygenated and the metal was pickled lightly in an HNO_3-HF solution.

5. The relative degree of resistance of titanium (and hence very likely TiCode-12) to acid chloride solutions to be found in a crevice could be determined from anodic polarization curves at temperatures below which crevice corrosion is a major problem.

6. Finally, the activity of hydrogen ions, rather than the concentration, determined the rate of attack. Actually, the anion associated with acid was of little importance as long as acidity existed. The activity coefficient of hydrogen increases as the concentration of sodium chloride in solution increases. Thus, indirectly, composition of brine or groundwater is an important parameter in influencing the rate of crevice corrosion.

3.5.3.3 Other Measurements

Since the occurrence of crevice corrosion in TiCode-12 was demonstrated only recently, this form of corrosion has hardly been characterized. Therefore, along with any direct or electrochemical testing on TiCode-12, materials characterization techniques such as optical and electron microscope, microprobe, X-ray diffraction, etc. should be used to obtain supplementary information. This approach at BNL (NUREG/CR-2317, Vol. 2, No. 1, 1982) has shown the presence of some lower oxides of titanium and that there is a potential/chemical gradient within the crevice. Thus, it may not be appropriate to treat a crevice as a homogeneous entity. Confirmatory experiments will be desirable for a spatially uniform crevice such as shown in Figure 8(b). Some other questions concerning the effect of surface oxide layers on crevice corrosion were raised, which may be answered by correlating surface studies with cathodic polarization behavior.

Concentration of dissolved oxygen is an important consideration because the initial stage of crevice corrosion involves depletion of oxygen. Hence, the larger the amount of dissolved oxygen, the longer it should take for crevice corrosion to occur. In relation to crevice corrosion in a repository, it may be noted that due to radiolysis, concentration of dissolved oxygen may be considerably affected. When oxygen or some other oxidizing agent is one of the radiolysis products, it is possible that the crevice is continuously buffered by them, thus delaying the initiation of crevice corrosion. The details of this possibility are discussed elsewhere (BNL-NUREG-31775, 1982) Testing under irradiation will be necessary to evaluate this aspect of crevice corrosion of TiCode-12.

3.5.4 Conclusions and Recommendations

Crevice corrosion of TiCode-12 under simulated repository conditions has been recently shown (NUREG/CR-2317, Vol. 2, No. 1, 1982) to occur and hence is

a potential mode of container failure. Whereas relatively extensive testing of TiCode-12 has been performed on uniform corrosion, crevice attack has not been adequately addressed. Therefore, from the standpoint of the life of a TiCode-12 container, extensive testing on crevice corrosion is required under realistic conditions.

Generally, depletion of oxygen from the crevice may be considered a prerequisite for the initiation of corrosion. Under radiation conditions some oxidizing agents may be produced by radiolysis within the crevice and hence delay the onset of corrosion. On the other hand, radiolysis might lower the solution pH and hence expedite crevice attack. At a later stage, or in some areas where effective radiolysis is negligible, crevice corrosion may occur early. Thus, testing needs to be performed under both conditions.

Finally, high concentrations of anions (mostly Cl^-) and temperature and low pH are expected to accelerate crevice corrosion, and may be used to reduce the incubation time for initiation of rapid crevice corrosion. Testing as a function of these parameters both by direct as well as electrochemical methods will be useful. As these tests proceed, an input should be obtained from other materials characterization techniques to determine further testing requirements.

3.6 Tests for Stress Corrosion Cracking

3.6.1 Introduction

Stress-corrosion cracking (SCC) is potentially one of the most significant of the failure modes which can compromise the integrity of the metallic components of the waste package (PNL-3915, 1981). This failure mode is difficult to quantify, and difficult to eliminate as a potential failure mode during the course of a short (in comparison with 1000 years) laboratory study, because there are two phases to the SCC process--crack initiation and crack growth--and each phase may be controlled by a different mechanism. A discussion of these mechanisms is given by Shao elsewhere in this program (BNL-NUREG-31771, 1982).

Quantification of the time of penetration of the metallic barrier and, the elucidation of the mechanisms of SCC provide the rationale for the testing of a potential barrier material for SCC. Such predictions are necessary to demonstrate the compliance (or lack of compliance) with the 1000-year containment criterion. In this section, after some general introductory comments about SCC testing, the DOE's SCC testing program on TiCode-12 will be reviewed, and recommendations will be made for future work.

3.6.2 Real-Time Testing vs Accelerated Testing

There are several limitations on the use of laboratory data on SCC to predict the probability of 1000-year containment by a metallic barrier. Real-time data are limited by experimental constraints, e.g., the length of time a test can be conducted, the constancy of steady-state crack-growth rates, and

the uncertainty in the threshold stress integrity for crack propagation. For example, the present experimental capability for measuring crack-growth rates (10^{-8} mm/sec or about 300 mm/1000 years) is insufficient for 1000-year life predictions (PNL-3720, 1981). Thus, attempts have been made to observe SCC in candidate metals by changing the value of some key environmental parameter in order to accelerate the SCC process. The validity of extrapolating such accelerated data back to the real-time conditions is open to question, however, if the real-time SCC mechanism cannot be shown to be the same as the accelerated SCC mechanism.*

Parameters which have been suggested by a Materials Characterization Center (MCC) workshop as suitable for accelerating SCC at constant temperature are pH, Eh (and O_2 concentration), stress, strain rate, and halide concentration (PNL-3720, 1981). Temperature was not considered a suitable accelerating parameter because temperature increases were deemed likely to introduce mechanisms not relevant to real-time SCC. As noted by the BNL group (NUREG/CR-2333, Vol. 4, Appendix A, 1982), even for the isothermally accelerated testing it would be necessary to show that neither the metal nor the metal-solution interface would undergo any structural, physical, or chemical change that could alter the corrosion rate over the time period in question. In two of the tests to be discussed later in this report, the slow-strain rate (SSR) and the fatigue-crack-growth rate (FCGR) tests acceleration of the fracture process is attempted by varying the strain rate and the cyclic stress intensity, respectively, on the test specimens in order to induce a breakdown of any passivating surface film and thus expose fresh metallic surface to the environment.

As noted by the MCC, a testing program for SCC may be divided into two phases. In the first phase, the SCC resistance of a variety of candidate materials should be determined by surveying the literature and by performing relatively simple, inexpensive screening tests. Susceptibility to SCC is often evaluated by real-time testing using stressed corrosion coupons (e.g., U-bends or C-rings). Accelerated testing may also be part of the screening process (PNL-3720, 1981; PNL-3915, 1981).

In the second phase of a SCC testing program, fracture mechanics testing should be conducted on those materials selected as a result of the screening phase of the program. Real-time testing may be performed on statically loaded, pre-cracked specimens (e.g., the wedge-opening-load test) in order to determine threshold stress intensities for crack propagation. As already noted, any crack-growth rates measurable in the laboratory on real-time test specimens would be too high for 1000-year barrier service. On the other hand, the threshold stress intensity for short term tests may be much larger than for longer term tests. Accelerated testing (e.g., the FCGR method) should also be part of this phase of the program. Fracture resulting from purely mechanical failure may be observed during these tests, but any environmentally enhanced cracking, i.e., any increase in crack-growth rate in a simulated re-

---

*Use of the term "real-time testing" is in no way meant to imply that there is anything "unreal" about accelerated testing.

pository environment over the rate in a reference environment (often referred to as an "inert" environment), usually air, may be indicative of the susceptibility of the material to SCC (PNL-3720, 1981; PNL-3915, 1981). According to some workers, only metallographic examination of the fractured surface (e.g., by scanning electron microscopy) can be used to unequivocally determine whether SCC is present (Payer, J. H., 1976; SAND79-2023C, 1979).

In the present report, it is assumed that TiCode-12 has been selected as a material for further consideration as a result of the screening phase of the SCC testing program. For completeness, test methods from both phases of the testing programs will be described in the following sections. The test methods may be grouped into two broad categories, static and dynamic. In static testing, either smooth-bar or pre-cracked specimen geometries may be used. The former, in particular, are frequently used for screening purposes because of their relative simplicity. The pre-cracked fracture mechanics geometries in a sense provide for accelerated testing with stress intensity as the isothermal accelerating parameter and in some cases, e.g., wedge-opening load and cantilever beam, are also relatively simple and compact. The dynamic tests considered, SSR and FCGR, are conservative accelerated tests requiring complex external loading devices. In the following section, static SCC testing with smooth-bar and pre-cracked specimens and dynamic SCC testing by the SSR and FCGR methods are described with emphasis on SCC testing of TiCode-12 in a simulated nuclear waste repository environment.

3.6.3 Static Tests

Two types of static testing are considered to be conventional methods for evaluating the susceptibility of a material to SCC: static load using smooth-bar specimens and static load using pre-cracked specimens (PNL 3720, 1981). A statically loaded specimen which exhibits no cracking when exposed to simulated repository conditions is considered to have low susceptibility to SCC. The use of pre-cracked static specimens provides a complementary test method which defines an experimentally determined threshold stress-intensity factor and a crack-growth rate which together can provide design-related data (PNL-3990, 1982).

There are four SCC specimen designs accepted for smooth-bar SCC testing: U-bend (ASTM G30-72)*, C-ring (ASTM G38-73), bent beam (ASTM G39-79), and direct tension (ASTM G49-76). Two of these designs, the U-bend and the C-ring, have been adopted by the Materials Characterization Center as MCC-103S, SCC Susceptibility Test Method. These two specimen designs were selected because they are: (1) generally small so that many specimens can be tested in a restricted volume, (2) generally of simple design and therefore inexpensive to

---

*Designations such as ASTM G30-72 refer to standard practices or standard test methods issued by the American Society for Testing and Materials (ASTM, 1981a).

make, and (3) bolt loaded requiring no external fixture to apply the strain as is sometimes the case for direct-tension or bent-beam specimens. A summary of the advantages and disadvantages is given with rough sketches of the specimen geometries in Figure 3.10 for each of these smooth-bar methods.

A companion fracture test method (MCC-104) is in preparation which can be used both to test resistance to crack propagation and to provide design-related data on threshold-stress intensities and crack-growth rates. An MCC workshop has considered four types of pre-cracked specimens for SCC testing: cantilever, compact tension (ASTM E399), wedge-opening load, (WOL) and cantilever beam. A summary of this is given with rough sketches of the specimen geometries in Figure 3.11 for each of these pre-cracked specimen methods.

In the present discussion of static testing, a description of some smooth-bar and pre-cracked fracture mechanics test methods will be given and their use in testing for SCC in TiCode-12 will also be considered. In addition, a brief comment will be made about residual stress specimen tests.

3.6.3.1 Smooth-Bar Tests: U-Bend and C-Ring

As noted in ASTM G 30-79, the U-bend specimen may be used for any metal alloy sufficiently ductile to be formed into the U-shape without mechanically cracking. The specimen usually contains large amounts of elastic and plastic strain and thus provides one of the most severe tests available for smooth stress-corrosion test coupons. Because a wide range of stresses exist in a single stressed specimen, the U-bend geometry is not suitable for determining the effects of different applied stresses on SCC or for variables which have and economical to make and use and are thus suitable for large scale screening to ascertain large differences in the SCC susceptibility of:

1. Different metals in the same environment.
2. One metal in different metallurgical conditions in the same environment.
3. One metal in several environments.

The U-bend specimen is most easily made from strip or sheet stock, but it is also possible to use plate, bar, castings, and weldments. The specimens may be cut from rolled stock material either transversely or longitudinally to the direction of rolling; since the SCC susceptibility may be anisotropic, the orientation of the test specimen must be defined.

The C-ring, as noted in ASTM G 38-73, is another versatile, economical specimen for determining the susceptibility to SCC of alloys. It is particularly suited for making transverse tests of tubing and rod. The C-ring is usually used as a constant strain specimen with tensile stress produced on the extension of the ring by tightening a bolt centered on the diameter of the ring. Other methods of stressing have been developed to produce a nearly constant load and to create a tensile stress on the inside surface (Figure 3.12). The C-ring specimens can be stressed with high precision and accuracy by application of a measured deflection, but the stress calculated from this

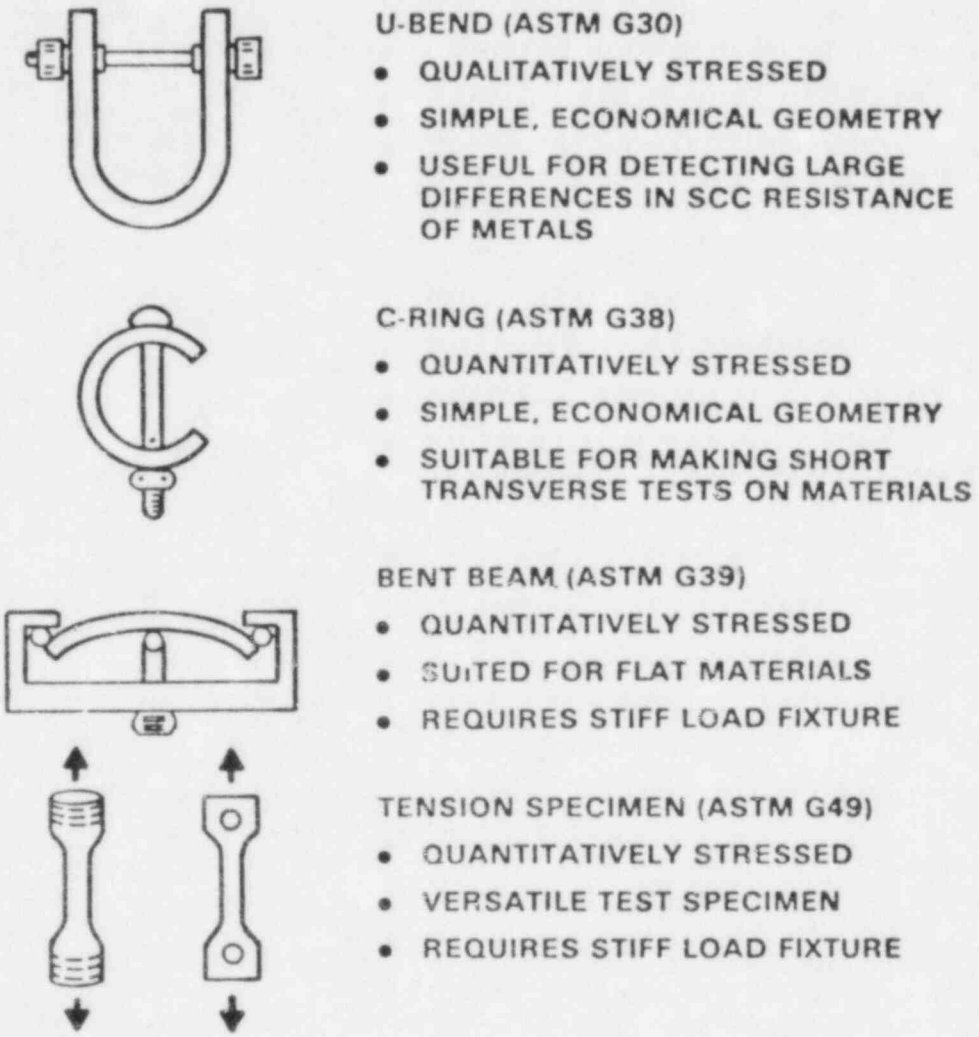

Figure 3.10 Smooth-bar specimens for SCC testing (PNL-3720, 1981).

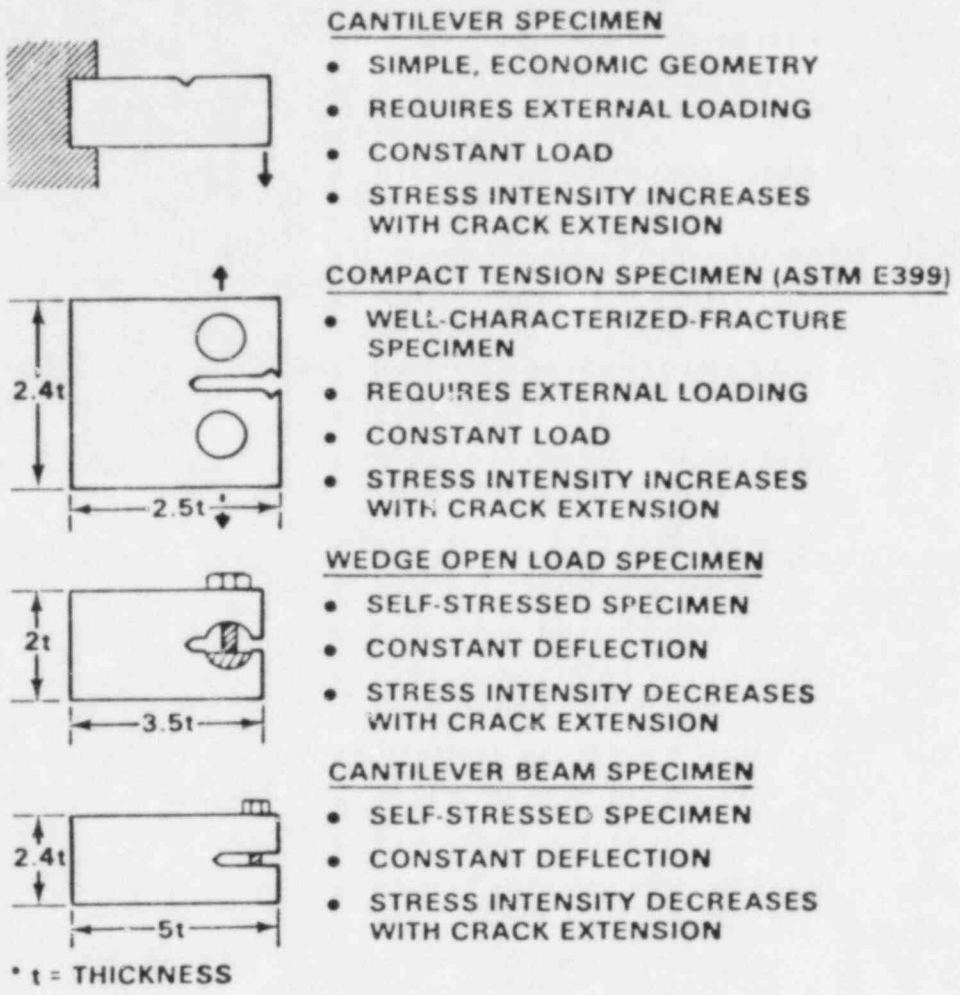

Figure 3.11 Pre-cracked specimens for SCC testing (PNL-3720, 1981).

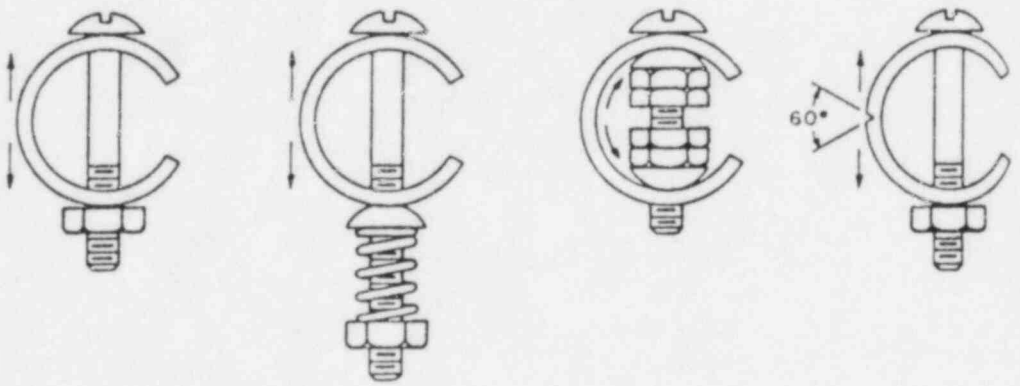

(a) (b) (c) (d)

Constant Strain Constant Load Constant Strain Constant Load

Figure 3.12 Methods of stressing C-rings. Note that for (d) a similar notch chould be used on the tension side of (b) or (c) (Adapted from ASTM, 1981a).

deflection does not apply if cracking is initiated. The C-ring, because of its small size and simplicity, can be exposed to almost any kind of corrosion environment. The specimen should be electrically insulated from any other metals in the system to avoid galvanic effects, unless such effects on SCC are to be studied (see Section 3.7.3, below).

A screening study using specimens in the U-bend configuration was carried out at Pacific Northwest Laboratories (PNL). A tungsten-inert gas welding torch was used to melt through the sheet material prior to fabrication and bending in order to create a weld bead. Two water chemistries were used in this study: a simulated Hanford basaltic groundwater and a simulated WIPP brine (Table 3.3). The requirement of total immersion of the specimens in an aqueous phase at a high test temperature (250°C) necessitated the use of a pressurized autoclave system. For the tests in the simulated basalt environment, a flow of simulated groundwater was maintained through a basalt rock layer in the bottom of the autoclave and over the corrosion specimens at rates of 30 to 300 mL/h (Figure 3.2 in Section 3.2). The tests in the simulated brine environment were run in a static brine solution (PNL-3484, 1980).

3.6.3.2 Pre-Cracked Specimen Tests

There are two major objectives in performing SCC testing with fracture mechanics type pre-cracked specimens. First, the SCC threshold stress intensity for a specific material and orientation in a specific environment may be

Table 3.3 Brine solution composition and synthetic Hanford groundwaters formulations.[a]

Brine Solution		Synthetic Hanford Groundwaters Formulations				
			August 1979 to May 1980		May 1980 to July 1980	
Component	Makeup	Component or Property	Makeup, mg/L	Effluent Analyses,[b] mg/L	Makeup, mg/L	Effluent Analyses,[b] mg/L
Mg^{2+}	34.98 g/L	Al^{3+}	0	10	0	6
Na^{+}	41.34 g/L	Na^{+}	139	140	111	127
K^{+}	29.95 g/L	Mg^{2+}	0.5	0.05	0.5	0.05
Ca^{2+}	0.60 g/L	Ca^{2+}	1.6	0.1	2.5	0.1
Li^{+}	20 mg/L	K^{+}	13	55	13	21
Rb^{+}	20 mg/L	CO_3^{2-} (total)	167	210	167	240
Sr^{2+}	5.3 mg/L	SiO_2	36	210	36	331
Cs^{+}	0.8 mg/L	Cl^{-}	52	50	52	58
Cl^{-}	191.3 g/L	F^{-}	8	8	8	8
SO_4^{2-}	3.51 g/L	SO_4^{2-}	0.8	--	0.8	5
BO_3^{3-}	1.24 g/L	O_2	<1	--	<0.05	--
Br^{-}	0.39 g/L					
I^{-}	10 mg/L	pH	9.5	8.5	9.0	7.7
Fe^{2+}	2 mg/L	Conductivity, μMHo	475	55	630	600

[a]From PNL-3484 (1980).
[b]Effluent was cooled before sampling. The water passed through a bed of crushed basalt at 250°C in the autoclave, which increased the Al and Si, and decreased pH, Ca, and Mg. The units of concentration (mg/L) do not apply to the pH or conductivity.

determined. As a second objective, the rate of SCC propagation, da/dt, as a function of the mechanical crack driving force may be determined under controlled test conditions (Sprowls, D. O., 1976). The parameter "a" represents the length of the crack.

Two convenient types of specimen for determining SCC propagation rates are the double-cantilever beam (DCB) and the wedge-opening-loading (WOL) geometries (Figure 3.11). Both are loaded for a constant displacement (called "constant deflection" in Figure 3.11) to a stress intensity at or just below the critical stress intensity required for crack propagation. At high stress intensity, SCC will start quickly in highly susceptible materials. Since the displacement across the notch is held constant by a bolt or other loading device, crack propagation causes the loading on the specimen and thus the stress intensity at the crack tip to decrease. When stress corrosion crack growth stops, the stress intensity at the crack tip has dropped to the threshold value for SCC (K_{Iscc}). This stress intensity level associated with crack arrest can be computed. Alternatively, a pre-cracked fracture mechanics specimen may have a constant load imposed upon it. Under a constant-load constraint, the stress intensity factor increases as the crack extends (if crack growth occurs) (Sprowls, D. O., 1976; Clark, W. G., Jr., 1976).

At PNL, WOL specimens were used to evaluate the susceptibility of TiCode-12 to SCC. A load-retaining wedge rather than a bolt was used to load the specimen (Figure 3.13). The external load was recorded during the wedge loading process so that the stress intensity could be determined. The crack length at the specimen surface was also recorded before the specimens were put into an autoclave. The specimens were exposed for 89 days at 250°C in a simulated Hanford groundwater repository environment (PNL-3484, 1980).

At Sandia National Laboratories (SNL), a series of tests was conducted on pre-cracked fracture mechanics specimens of the compact tension geometry (Figure 3.14) using the constant displacement technique. (This geometry, which is an ASTM standard described in E 399-81, is considered by an MCC workshop (PNL-3720, 1981) to be a constant load rather than constant displacement type of specimen.) The specimens were fatigue pre-cracked over a stress-intensity range of 2 to 11 $MN/m^{3/2}$ and exposed to the environment prior to loading. A heavy load ring with bolt-mounted clevises* across its diameter was used to load the specimen to 65 to 90% of the measured overload stress intensity (37 $MN/m^{3/2}$) in brine and dry salt plus 100% relative humidity air, for 1024 to 2000 hours. The specimens were electrically insulated from the clevises (SAND79-2023C, 1979).

3.6.3.3 Residual Stress Specimen Tests

Many SCC problems are associated with residual stresses developed in the metal during heat treatment, fabrication, and welding (Craig, H. L., 1971).

---

*A clevis is a U-shaped yoke at the end of a chain or rod, between the ends of which the specimen can be pinned or bolted. In the present case, two clevises are used to pull the "jaws" of the specimen apart.

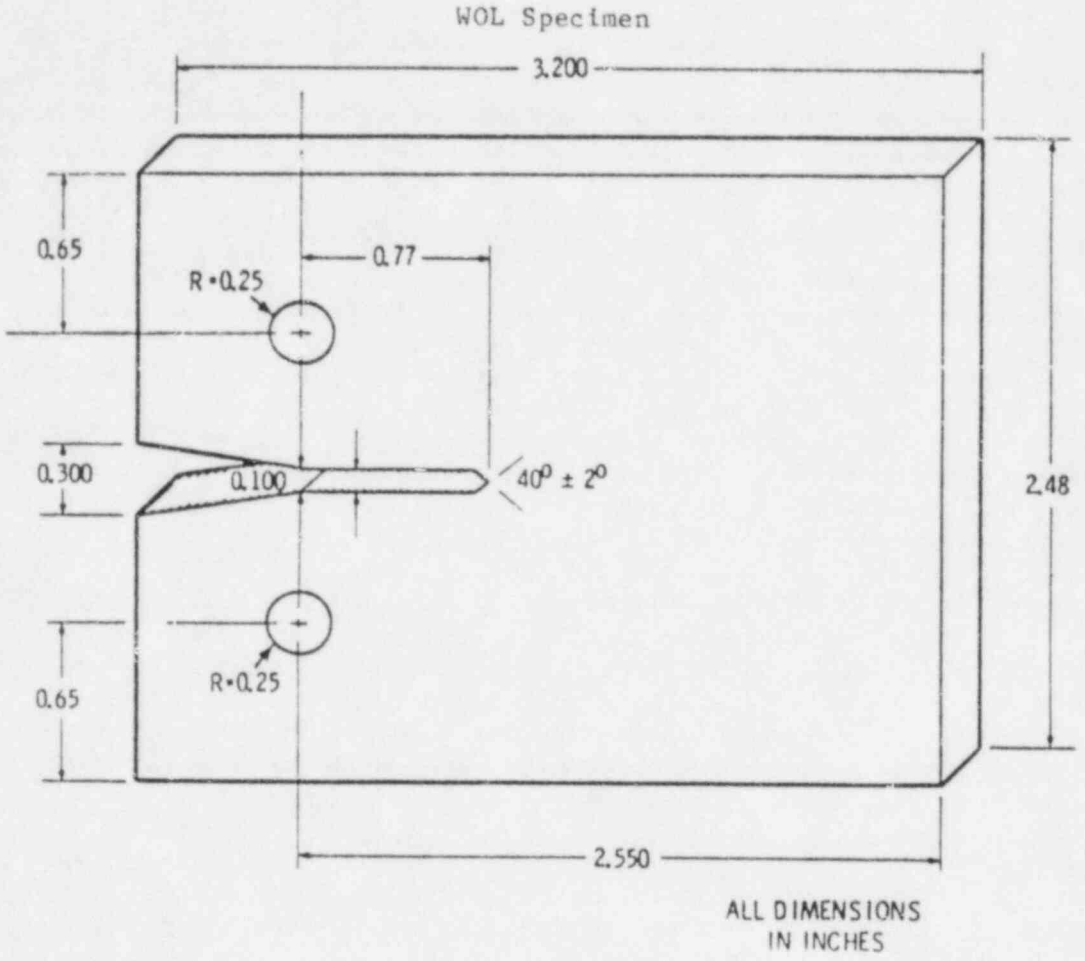

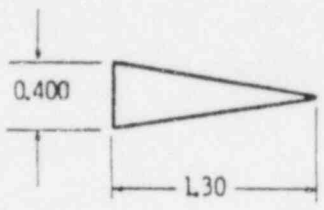

Figure 3.13 Wedge-opened specimen used for stress-corrosion-cracking evaluation in autoclave tests (PNL-3484, 1980).

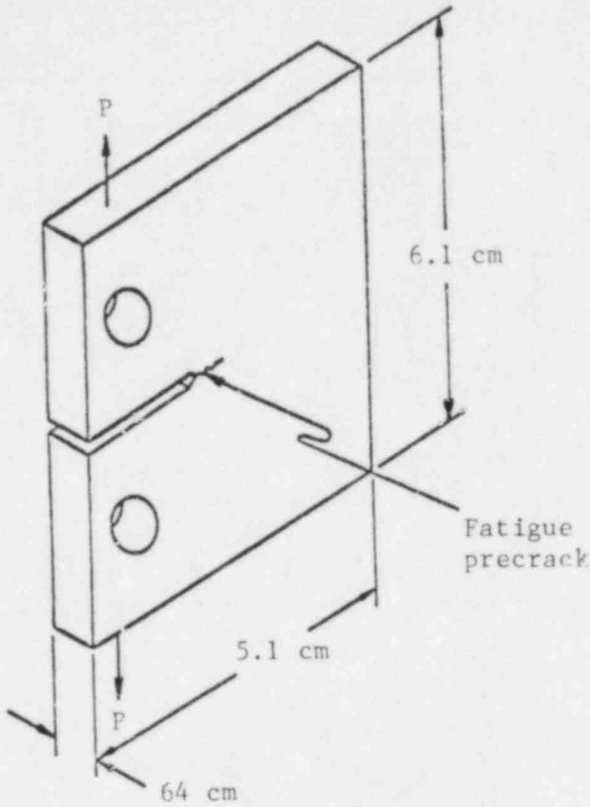

Figure 3.14 Pre-cracked fracture mechanics specimen with the compact tension geometry (SAND79-2023C, 1979).

As already noted above, a weld bead was produced on U-bend specimens as part of a screening study at PNL. In addition, residual stress specimens (Figure 3.15) were included in autoclave tests. The specimens were plastically deformed in compression, then allowed to spring back, thus producing residual tensile stresses. The specimens were exposed for 89 days at 250°C to simulated basaltic groundwater (PNL-3484, 1980).

3.6.4 Dynamic Testing

3.6.4.1 Slow-Strain-Rate Testing

The slow-strain-rate (SSR) test is an accelerated test relative to statically loaded tests, but it is qualitative in nature. Data from SSR testing can be used to show susceptibility to SCC in a particular environment, but the data may not be useful in a quantitative sense for design (PNL-3915, 1981).

The SSR technique consists of subjecting a specimen to a slow, constant strain rate under controlled environmental conditions. Typically, strain rates range from 10^{-8} to 10^{-4} sec^{-1}. SCC will be promoted if the strain rate is within a critical range of values for which a balance is maintained at the crack tip between deformation, dissolution, film formation, and diffusion.

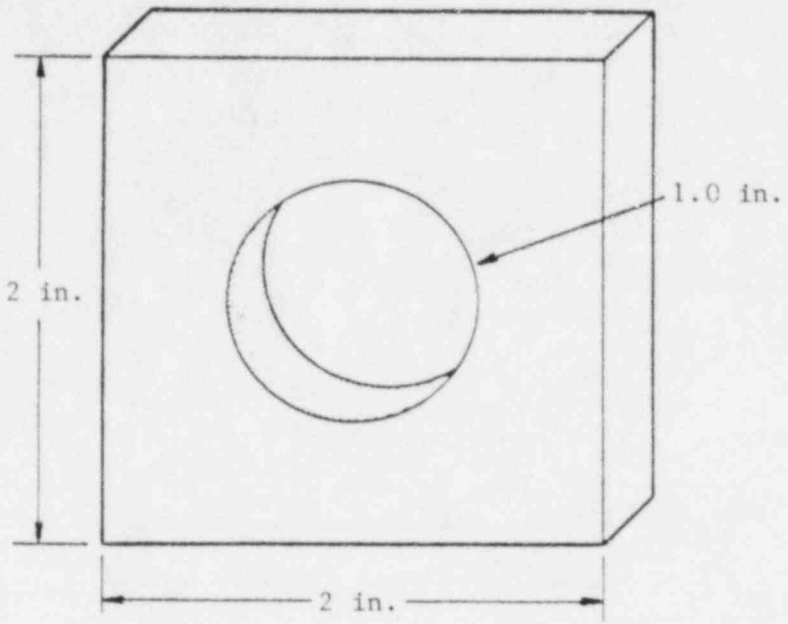

Figure 3.15 Residual-stress specimen used in SCC testing (PNL-3484, 1980).

(For a further discussion of the mechanism of SCC, see the BNL report by Shao (BNL-NUREG-31771, 1982)). The SSR apparatus must provide reproducible, constant strain rates over the 10^{-8} to 10^{-4} sec^{-1} range (Payer, J. H., 1976).

The slow-strain apparatus used at PNL consists of a gear-driven loading device with which constant extension rates are applied to the specimen (Figure 3.16). The load is measured in a load cell external to an autoclave containing the sample, and displacement is measured on a linear variable differential transformer (LVDT) between the autoclave and the loading rod. The load-vs-displacement data were plotted for each test so that deformation characteristics could be determined (PNL-3915, 1980).

Tensile specimens fabricated from sheet metal material were used to conduct the SSR tests at 250°C (Figure 3.17). Simulated Hanford groundwater was passed into the bottom of an autoclave and through a layer of crushed basalt before reaching the specimen (Figure 3.16). The dissolved oxygen content was 6 ppm. The tests were performed at strain rates ranging from 10^{-7} to 10^{-4} sec^{-1}. The fracture surfaces were examined by scanning electron microscopy for evidence of SCC (PNL-3000-10, 1981; PNL-SA-9543, 1981).

For the purpose of evaluating the SCC (and hydrogen embrittlement) behavior of TiCode-12, an SSR testing program has been carried out at SNL. The SSR tests were conducted on electrically insulated specimens (Figure 3.17) inside Hastalloy C-276 autoclaves. In the first series of tests, the specimens

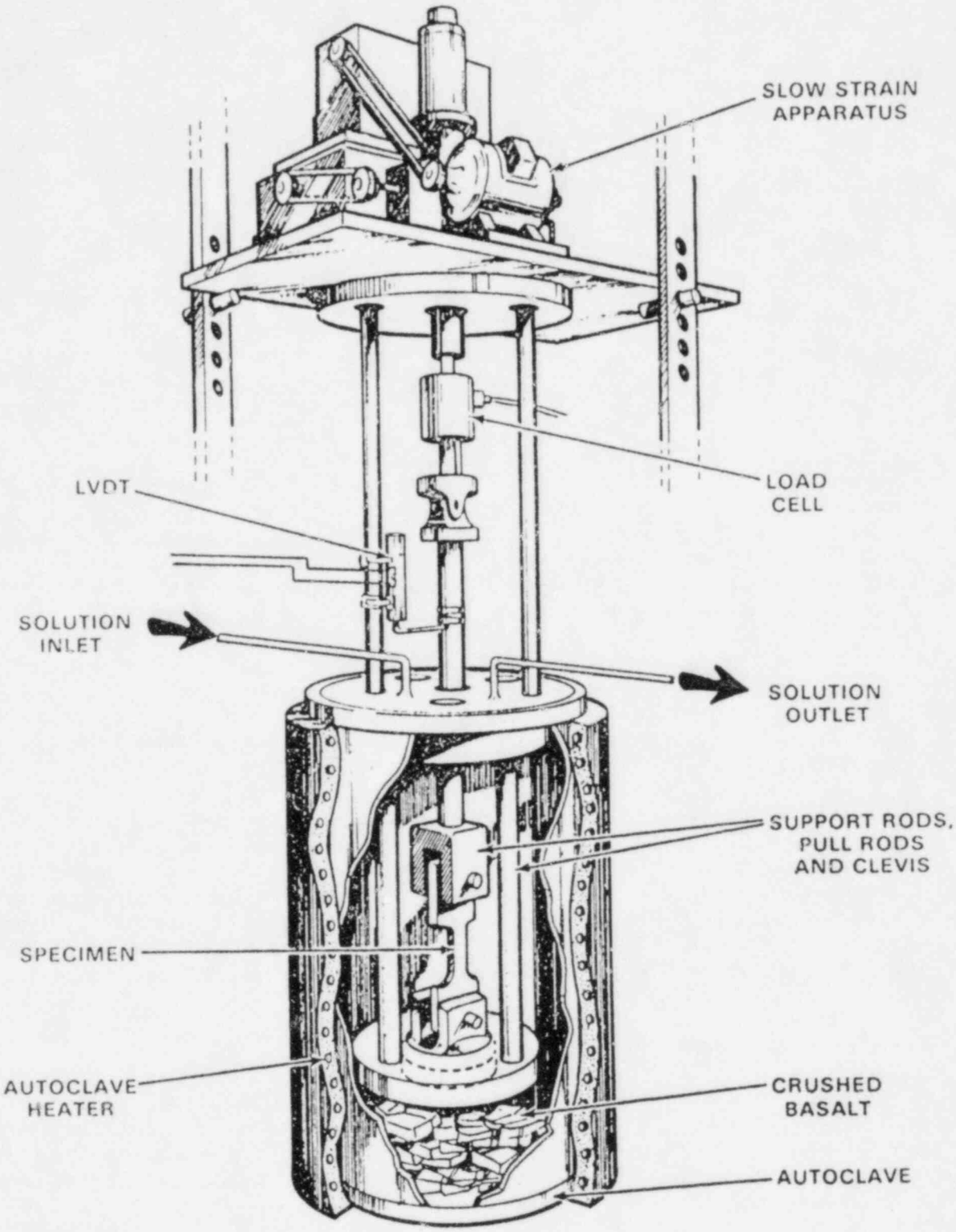

Figure 3.16 Slow-strain-rate test system (PNL-3915, 1981).

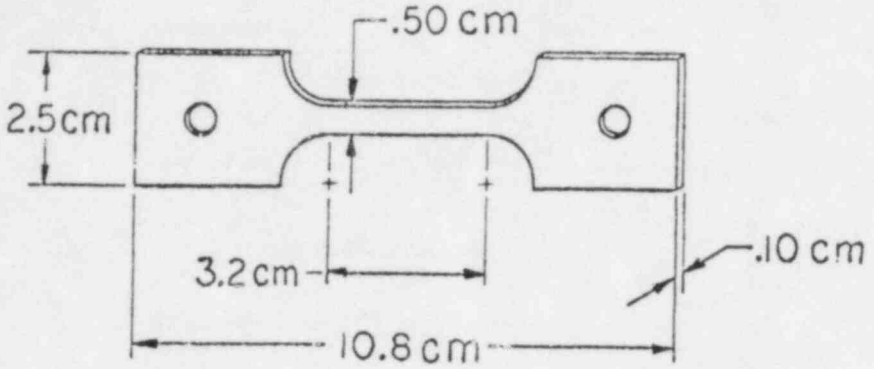

Figure 3.17 Slow-strain-rate test specimen (SAND80-1738C, 1980).

were subjected to initial strain rates ranging from 5×10^{-7} to 1×10^{-4} sec^{-1}, a temperature of 250°C, and an environment of air, dry salt, and saturated brine. Additional testing was carried out at a strain rate of 1×10^{-5} sec^{-1} at 250°C in oxygenated brine (~500 ppm O_2), deoxygenated dry salt (~0.003 ppm O_2 in any condensed solution) and dry salt plus 2% H_2O. In the second series of tests a constant strain rate from 10^{-7} to 10^{-4} sec^{-1} was maintained by means of a gear-reducer and electric motor coupled to the load cell so that recordings of applied load vs time could be obtained. The testing environments were synthetic seawater and simulated WIPP brine solutions (Table 3.2 in Section 3.2, above). The testing solutions had been deaerated by bubbling argon through them for eight hours prior to testing in order to reduce the dissolved oxygen content to ~30 ppb (SAND79-2023C, 1979; SAND80-1738C, 1981).

Susceptibility to SCC was assessed by measuring time to failure (i.e., total strain at fracture), the ultimate tensile strength, and reduction in cross-sectional area. The resulting experimental data for these three parameters were then divided by the values obtained for the corresponding parameters in air, which is the reference environment; ratios significantly less than unity were to be taken as an indication of susceptibility to SCC. The results indicate that SCC is an unlikely failure mode for the test conditions used.

3.6.4.2 Fatigue-Crack-Growth Rate Testing

The FCGR method, as its name implies, is a technique to determine the growth rates of cracks produced as a result of metal fatigue. Fatigue cracking, however, is a mechanical failure mode of interest in assessing the failure of metal structures subjected to cyclic stresses, and these are not anticipated in the repositiory environment. The FCGR method is of interest in the present context, however, because use of this method accelerates the SCC process in susceptible metals by the mechanical breakdown of the passivating film at the crack tip.

As noted by Pitman (PNL-3915, 1981), in FCGR testing, a crack is forced to grow by cycling the tension load on a notched, pre-cracked specimen and the rate of growth of this crack is measured. The new data are usually presented as crack extension per tension cycle (da/dn). The effects of a simulated repository environment on the crack-growth rate may be evaluated by the dependence of da/dn on the cyling frequency and by the acceleration of da/dn relative to its value in a reference environment (often referred to as an "inert" environment) such as air. An accelerated crack-growth rate may be indicative of SCC. In addition, the microscopic structure of the fracture surfaces should be examined for evidence of SCC (Payer, J. H., 1976; SAND79-2023C, 1979). FCGR data may be used with fracture toughness data and anticipated stress levels to predict the growth of a crack under repository conditions.

Crack-growth rates for Ti-6Al-4V plate have been found by Bania and Antolovich (1976) to obey an Arrhenius-like relationship:

$$(da/dt)_{SCC} = A\, e^{-(Q_{SCC}/RT)}$$

where

$(da/dt)_{SCC}$ = crack extension rate

A = constant

Q_{SCC} = apparent activation energy.

Note that Q_{SCC} is found to decrease linearly with K^2, where K is the stress intensity, and is thus only an apparent activation energy. Keeping in mind the possibility of failure mechanism changes under accelerated conditions, data from the FCGR method could, in principle, be used to obtain crack-growth rates for SCC in TiCode-12, assuming that the resulting crack-growth rate data as a function of temperature would also obey such an Arrhenius-like relationship. Also note that FCGR data are obtained under cyclic stressing and thus may be applicable to stress conditions which are much more severe than those reasonably expected in a repository environment. Further discussion of the SCC mechanism implied by the above Arrhenius-like relationship is presented in the original paper.

FCGR testing at PNL was conducted both in air and in simulated basalt groundwater. Compact tension specimens (Figure 3.18) were used to characterize the FCGR of TiCode-12 plate in air at 20°C at a stress-cycling frequency of 10 Hz. Center-crack tension specimens (Figure 3.19) were used to evaluate the crack-growth characteristics of TiCode-12 sheet in air at frequencies of 5 and 10 Hz.

The first series of FCGR tests in a simulated repository environment was conducted at 87 to 90°C on sheet specimens of TiCode-12 (Table 3.4). A system was designed to circulate pre-heated simulated basalt groundwater solution through a chamber surrounding the cracked area of the specimen (Figure 3.20).

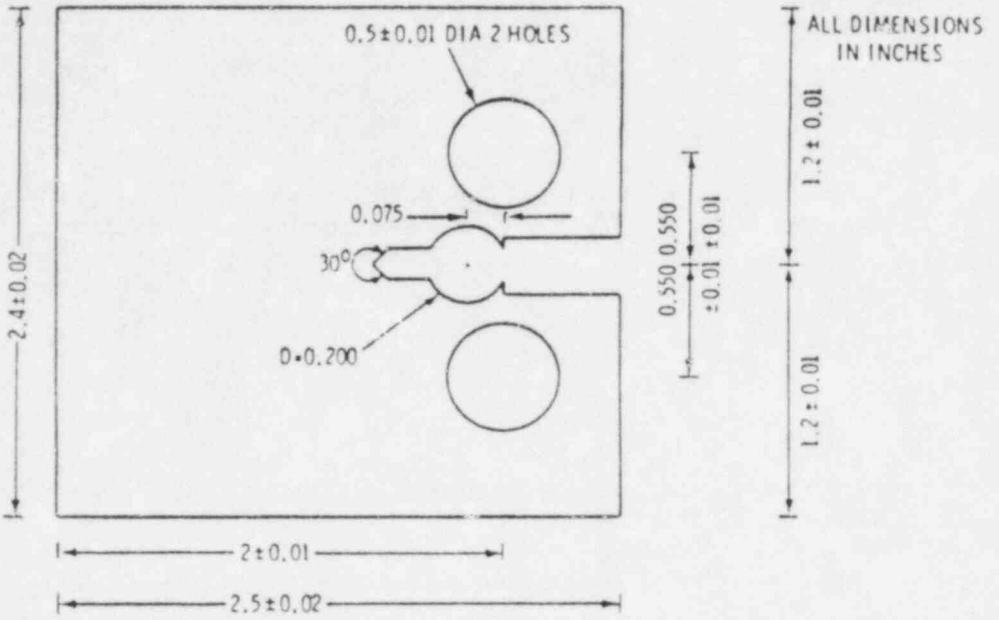

Figure 3.18 Compact tension specimen (ASTM E399) modified to accept a clip gauge for load-time displacement measurement (PNL-3484, 1980).

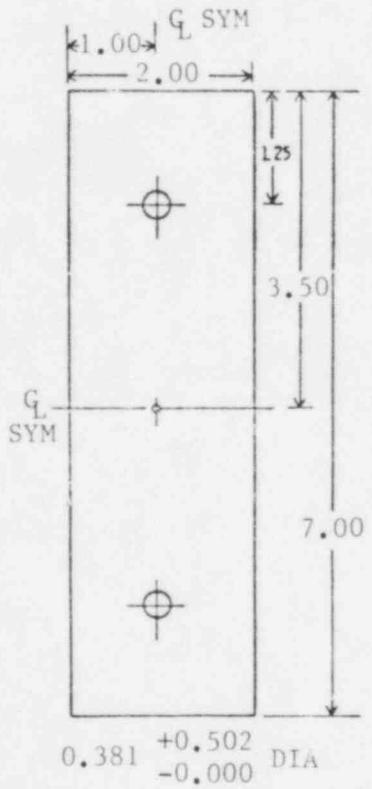

Figure 3.19 Center-cracked tension specimen (all dimensions in inches) (PNL-3484, 1980).

Table 3.4 Summary of environmental fatigue-crack-growth rates tests at PNL.[a]

Specimen Number	Material	Orientation[b]	Temperature (°C)
M267	Ti-12	LT	87 to 90
M268	Ti-12	TL	90
M269	Ti-2	LT	90
M270	Ti-2	TL	90
M271	Ti-2	TL	90
M272	Ti-12	TL	90
M273	Ti-2	TL	90

[a]From PNL-3484 (1980).
[b]The first letter refers to the direction of loading, i.e. in this case, longitudinal (rolling direction). The second letter refers to the direction of crack propagation, in this case, transverse (perpendicular to the rolling direction).

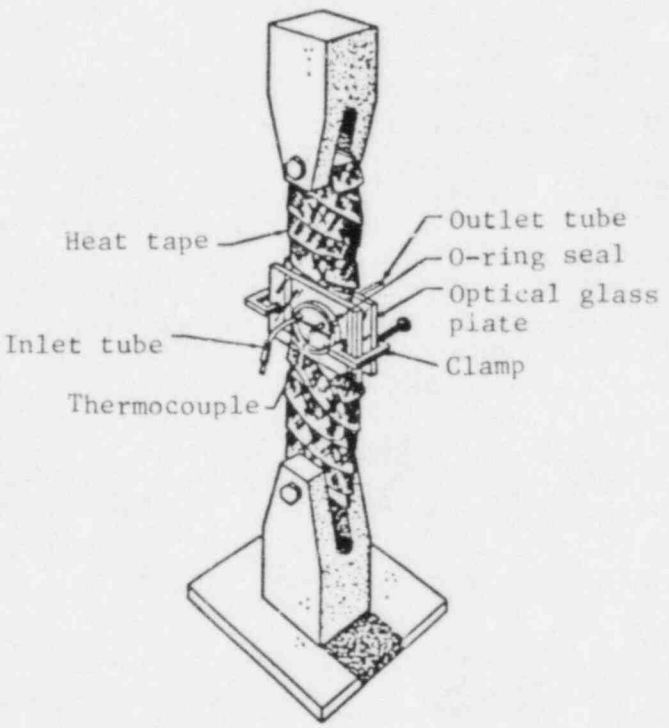

Figure 3.20 Environmental test system for fatigue-crack-growth-rate testing using CCT specimens (PNL-3484, 1980).

The temperature of the specimen was maintained by the heating tapes and monitored for control by the thermocouple. The flowing environmental solution was pre-heated by wrapping the inlet tube around the heating elements. The composition of the simulated Hanford groundwater used in this series of tests is given in Table 3.5.

Table 3.5 Chemical analysis of simulated Hanford repository water used for FCGR testing at PNL.[a] (pH: 9.50; conductivity (μMho): 472).

Solution Makeup	Concentration (ppm)
HCO_3^-	139.8
CO^{2-}	22.0
SO^{2-}	1.2
F^-	6.7
Cl^-	43.9
Ca^{2+}	1.5
Mg^{2+}	0.63
Na^+	100
Si	0.2

[a]From PNL-3484 (1980).

A more elaborate version of the environmental chamber was developed at PNL for further FCGR testing (Figure 3.21) (PNL-3915, 1981). A gravity feed system provides flowing solution to the chamber, and the flow rate is controlled using an in-line metering device. A once-through flow rate of approximately 10 mL/h is maintained. The solution in the chamber is heated to 90°C by Pyrex-covered electrical resistance wire. The temperature is monitored for control by a thermocouple. No metal or conducting parts are in contact with the wet portion of the specimen. The composition of the simulated basalt groundwater is given in Table 3.6. (Note that in both series of FCGR tests, the simulated groundwater was exposed to air before and during the tests; no attempt was made to control the concentration of dissolved oxygen.) The tests were conducted at frequencies of 1.0, 0.1, and 0.01 Hz, the last expected to be the most severe in the series (PNL-3000-10, 1981; PNL-3000-11, 1981; PNL-SA-9543, 1981). The stress intensity was varied sinusoidally with the maximum and minimum stress intensities 554 and 55.4 kg, respectively.

3.6.5 Discussion

3.6.5.1 Advantages and Disadvantages of the Test Methods

The advantages and disadvantages of the various SCC test methods discussed above have been considered by a Workshop on Corrosion of Engineered Barriers (PNL-3720, 1981) sponsored by the MCC:

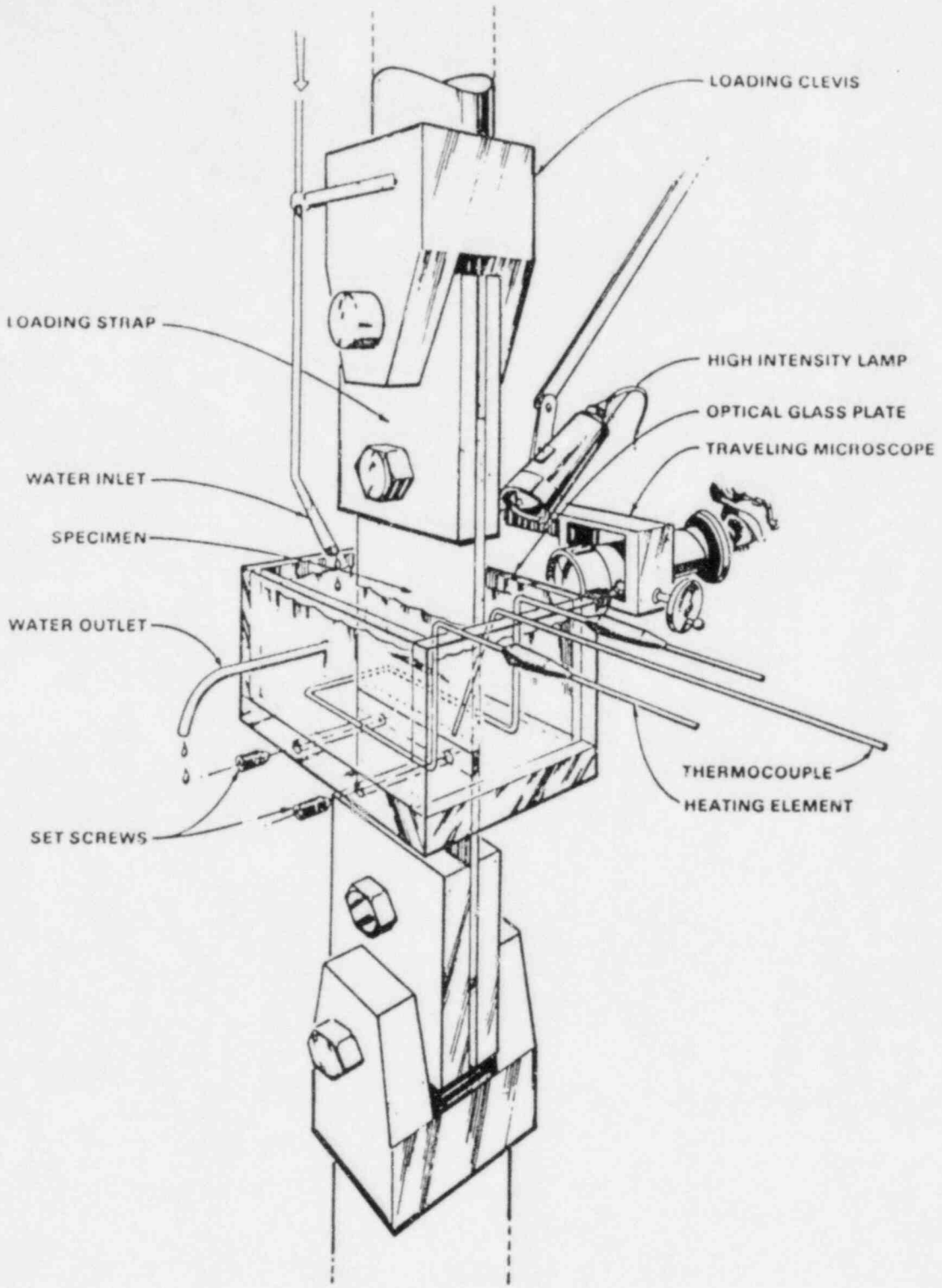

Figure 3.21 Environmental chamber used in fatigue-crack-growth-rate tests (PNL-3915, 1981).

Table 3.6 Typical inlet and outlet composition of simulated basaltic groundwater in SSR and FCGR at PNL.[a]

Component	Concentration (ppm)[b] Inlet	Outlet
B	0.02	0.03
Ca^{2+}	1.2	0.4
K^{+}	3	42
Mg^{2+}	0.31	<0.05
Na^{+}	285	267
Si	63	173
Sn	0.1	0.1
SO_4^{2-}	115	112
F^{-}	37	37
Cl^{-}	153	162
pH	9.84	9.46

[a]From PNL-3915 (1981).
[b]Except pH.

U-Bend and C-Ring Tests

Advantages:

- Low-cost specimens.
- Multiple specimens permitted in a single test.
- Suitable for accelerated electrochemical tests.
- Sensitive to crack initiation.
- Suited for autoclave and radiation tests.
- ASTM standards for specimen geometry.
- Good for evaluating the effects of pitting on SCC.

Disadvantages:

- Sensitive to surface preparation.
- Questionable repeatability.
- Uncertainty about the time a test should last to show SCC susceptibility.
- Uncertainty in starting stress.
- Stress gradient through the thickness.

Pre-Cracked Fracture Mechanics Tests

Advantages:

- Threshold stress intensity determined in these tests is useful for quality-assurance inspection of containers.
- Good for evaluating both hydrogen embrittlement and stress corrosion.
- ASTM standard for specimen geometry.
- Good reproducibility.
- Multiple WOL specimens permitted in a single test.

Disadvantages:

- Experimental limitations in extrapolating crack-growth rate results to 1000 years.
- More costly than smooth-bar specimens.
- The externally loaded, compact-tension specimens not suited for autoclave and gamma-radiation testing.
- Doubt about results from accelerated electrochemical tests on pre-cracked specimens.
- The compact-tension specimen limited to single-specimen tests.

Slow-Strain-Rate Tests

Advantages:

- Potential accelerated test, although requires verification of applicability to various classes of material.
- Good for screening, but examination needed for several parameters (strain rate in particular).
- Good for hydrogen embrittlement (external).
- Good for accelerated electrochemical tests.
- ASTM standard for the tensile specimen geometry.
- Good reproducibility.

Disadvantages:

- Any lifetime predictions will depend on modeling the appropriate failure mechanisms.
- May be too severe a test since a large dislocation density is being introduced in the material.
- Not well suited for testing in a radiation field.

Fatigue-Crack-Growth Rate Tests

Advantages:

- Generally considered to give a more conservative (lower value) stress-intensity threshold than do static methods.
- Reproducible threshold values.

3.6.6 Conclusions and Recommendations

The ideal test for SCC would yield data which could be used to predict the crack initiation time and the crack propagation rate under repository conditions, assuming that TiCode-12 is indeed susceptible to SCC under such conditions. As a practical matter, deriving such quantitative predictions from the experimental data is beset with difficulties. As noted by Wei, Novak, and Williams (1972), for example, the existence of an incubation period (a period of crack-growth rate much less than 10^{-6} in/min) and of a non-steady-state crack-growth period can lead to an underestimation of the steady-state rate of crack growth (and thus to an overestimation of the operating life of the barrier) as well as to erroneous values of K_{Iscc}.

We, therefore, recommend long term real-time testing of statically loaded specimens under expected repository conditions. "Long term" here means on the order of years. Such long term testing need not delay the progress of the waste disposal program, but can and should be carried out in parallel with the design and development of the waste package and repository.

As a result of such a long term testing program, data would be obtained on the crack initiation time and on the rate of crack growth for SCC of TiCode-12 under repository conditions (assuming that any measurable rate of SCC is found). Such data may be used to generate emperical predictive equations, from which extrapolations of the SCC data to 1000 years and confidence limits for the time to failure of a TiCode-12 containment barrier may be obtained. The work by Bania and Antolovich (1976), discussed in Section 3.6.4.2 above, provides an example of the use of SCC test data, in this case from short term dynamic testing, to generate predictive equations. There is, of course, no a priori reason to assume that long term static test data for TiCode-12 under repository conditions will necessarily obey the Arrhenius-like relationship found by these authors.

We further recommend that SCC testing of TiCode-12 be carried out under expected repository conditions in the presence of a radiation field so that any combined effects of both the repository environment and the radiation field may be observed. We note that PNL has constructed an autoclave test apparatus in a radiation facility (PNL-3484, 1980; PNL-3000-11, 1981) (shown schematically in Figure 3.3 in Section 3.2 and Figure 3.22) and has undertaken a preliminary study of the effects of γ-irradiation on the chemistry of simulated basaltic groundwater (PNL-SA-9543, 1981). Statically loaded specimens such as U-bend, C-ring, or WOL are the most appropriate specimen geometries for this type of facility. We particularly recommend that multi-year long term testing be carried out under the combined effects of the repository environment and the radiation field and that any crack surfaces which may develop be examined fractographically to check for microscopic evidence of SCC.

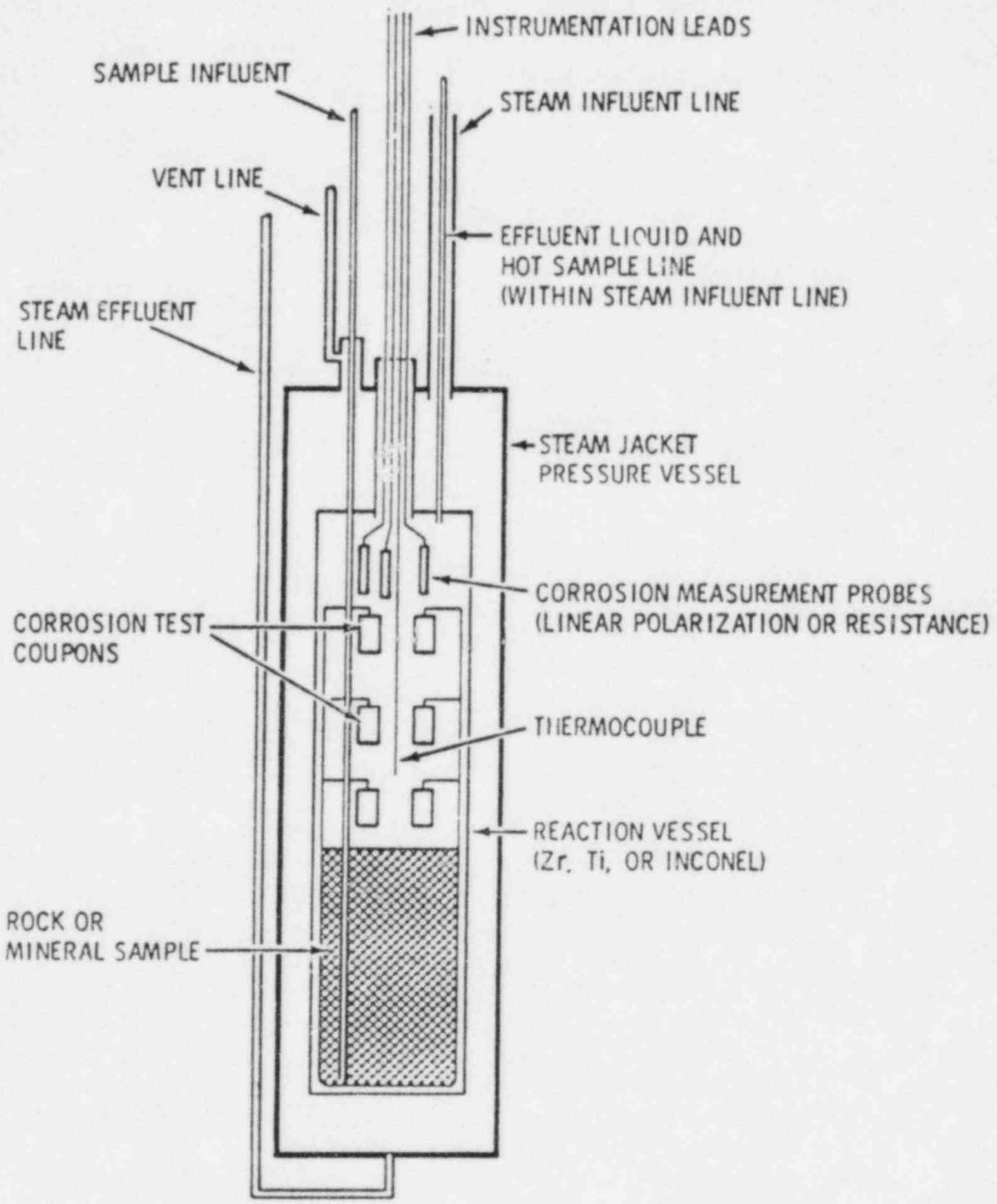

Figure 3.22 Reaction chamber for radiation/corrosion test facility (PNL-3484, 1980).

3.7 Tests for Galvanic Corrosion

3.7.1 Introduction

Galvanic corrosion results from the chemical reaction which occurs when two (or more) dissimilar metals are in physical or other electrical contact in a conductive solution. Such a situation could arise in a repository if packing material is not used or if the position of the container shifts with time as a result of the cracking or liquefaction of the packing material In either case, TiCode-12 could come into contact with the emplacement sleeve. This mode of corrosion has not been considered significant in the context of nuclear waste package performance because it is considered likely that it can be avoided by proper materials selection (NUREG/CR-2333, 1982).

In contrast to stress-corrosion cracking, which, for TiCode-12 has been investigated at several DOE laboratories, very little work has been done on the galvanic corrosion of this alloy. For example, galvanic corrosion was not addressed (for any material) by a workshop on corrosion of engineered barriers sponsored by the MCC (PNL-3720, 1981). Nevertheless, some additional data requirements characterizing the galvanic corrosion behavior of TiCode-12 are suggested by Shao (BNL-NUREG-31771, 1982). In the present report, a brief account will be given of galvanic corrosion test methods, in particular, those which have been used on titanium and its alloys coupled with other metals. The applicability of such test methods, suitably modified, to the above-mentioned data requirements will be considered.

3.7.2 Current Status of Galvanic Corrosion Testing

In order to measure galvanic corrosion, the two metals of interest are placed in electrical contact and the galvanic couple is them immersed in the electrolyte of interest under specified conditions. If the electrical contact is created by actual physical contact of the two specimens, then conditions which may be conducive to crevice corrosion must be avoided. Corrosion rates may be determined directly by measuring weight loss and indirectly, as well, by measuring the average galvanic current densities.

For example, Macki and Kochen (1971) measured the galvanic corrosion behavior of a selected group of alloys (Table 3.7), including Ti-6Al-4V, in ocean water and hydrochloric acid by gravimetrically measuring the corrosion rates of galvanically coupled specimens and by measuring electrode potentials for these couples. The alloy specimens were disks 1 inch in diameter by 0.080 inch in thickness. After being machined, the disks were abraded (to ensure good contact between the electrically connected faces of the two disks in the galvanic couple), measured to the nearest 0.001 inch, cleaned with acetone, dried, and weighed to the nearest 0.1 mg. A pair of disks was then assembled into a galvanic couple by mounting the pair in an insulated nylon clamp (Figure 3.23). The exposed edges of the disks were coated with a silicone adhesive so only one face of each disk was exposed to the environment; the adhesive also isolated the circle of contact between the exposed edges of the two disks from any possible crevice corrosion. The electrical resistance of each couple

Table 3.7 Alloys used in galvanic tests.[a]

Tuballoy (depleted uranium)	U-10 wt% Mo
U-4.5 wt% Nb	7178 Al
U-6 wt% Nb	Ti-6Al-4V
U-8 wt% Nb	4340 steel
Mulberry (U-7.5 wt% Nb-2.5 wt% Zr)	Type 304 SS (passivated)

[a]From J. M. Macki (1971).

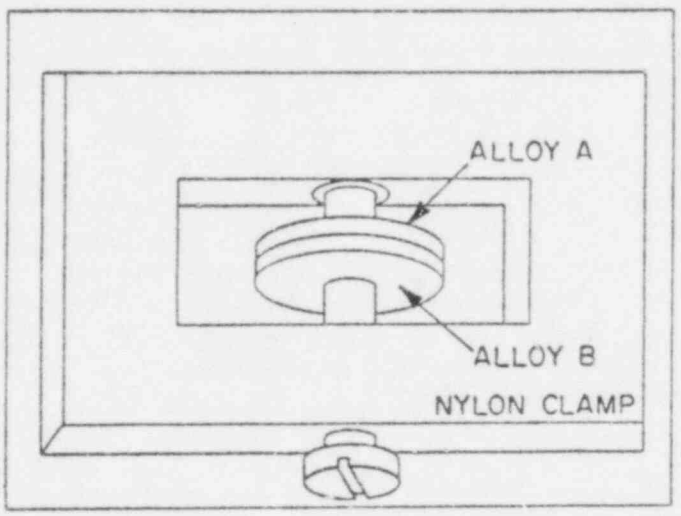

Figure 3.23 Apparatus used for gravimetric-galvanic corrosion tests (Macki, J. M., 1971).

was measured before and after exposure to the electrolyte in order to ascertain the degree of electrical contact between the disks. After exposure to the electrolyte (up to 96 hours in 0.1 N HCl) each couple was disassembled, the disks were cleaned in distilled water and acetone, dried, and reweighed to determine the weight loss, if any. A galvanic series for the alloys in each electrolyte was established by measuring the electrical potentials relative to a saturated calomel electrode generated by disks of each alloy immersed in the particular electrolyte (e.g., ocean water at 25°C).

Another discussion of the galvanic corrosion properties of titanium in NaCl and HCl solutions is given by Schlain (1953). In this series of experiments, the metal specimens were cut to size (10 cm x 2.5 cm x 0.13 cm for Ti), vacuum annealed at 900°C for two hours, and cleaned with solvent. The equipment used included an open two-liter beaker, a rotating specimen holder, and an aerator. The strips were fastened to the rotating holder, electrically coupled through a calibrated 0.62 ohm resistor, immersed in a 3% NaCl solution, and rotated at speeds up to 150 rpm. During the course of the test, voltage readings were taken across the calibrated resistor in order to estimate the size of the galvanic current. The weight loss of the specimens was

also noted. All of these measurements were performed at room temperature (20-25°C).

Another study of the galvanic corrosion behavior of titanium was conducted by Shalaby (1971). Diagrams of the test system and corrosion cell used in this study are presented in Figures 3.24 and 3.25, respectively. The materials studied were 99.5% Ti and the four alloys described in Table 3.8. Measurements were taken, over a period of one month, of the corrosion current densities of the couples in a 32.7 g/l NaCl solution at 90°C with oxygen gas bubbled through the solution. Micrographs of the coupled specimens were compared with those of uncoupled specimens subjected to the same conditions.

Mansfeld and others (1974) studied the galvanic interactions between several aluminum alloys and various metals, including Ti-6Al-4V in air-saturated 3.5% NaCl solution by means of weight-loss measurements and continuous monitoring of the galvanic current in 24-hour tests. The test specimens were flat coupons which were mounted in a Lucite holder so that an area of about 20 cm^2 of each specimen was exposed to the electrolyte. The corrosion potential of the two specimens, as yet uncoupled, was followed for 15 minutes after immersion. The specimens were then electrically connected via a zero-impedance ammeter, the output of which is proportional to the galvanic current. The ammeter output and the potential for the couple were monitored by recorder for 24 hours. Because the titanium alloy was considered to be more noble than the aluminum alloys, only the weight losses of the latter were noted when they were coupled with the titanium alloy.

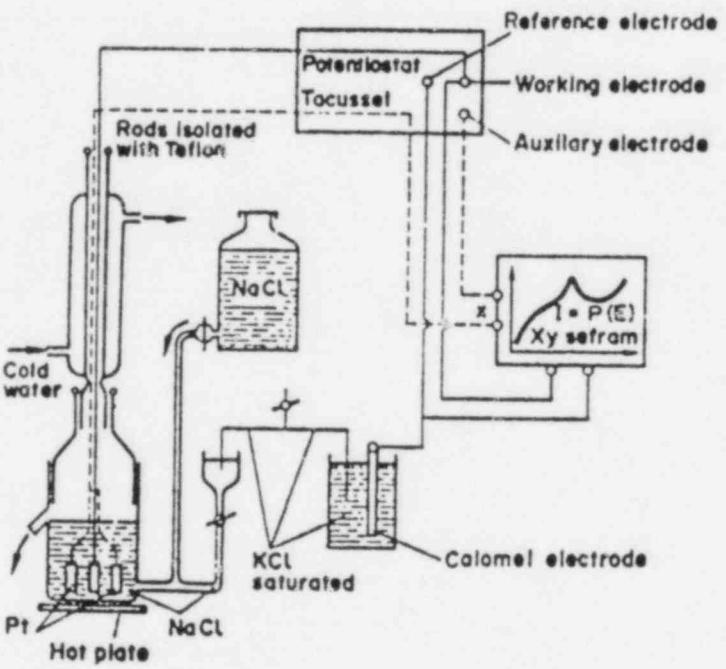

Figure 3.24 Galvanic corrosion test system used by Shalaby (1971). *

*Excerpted from "Corrosion Science", 11,767-778.

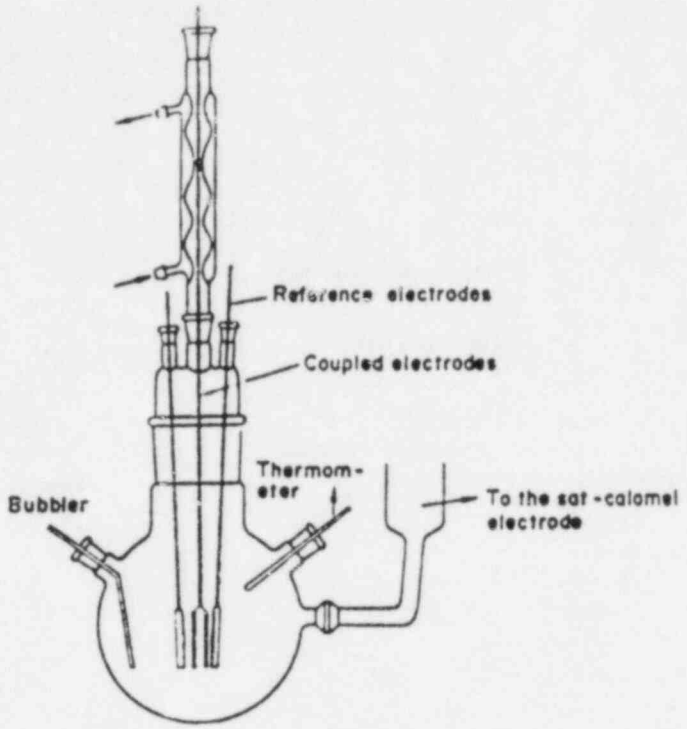

Figure 3.25 The corrosion cell used by Shalaby (1971).

Table 3.8 Four alloys investigated by Shalaby (1971).

	Cu	Zn	Ni	Al	Fe	Mg	Sn	Si	As	Mn
Admirality brass	69-9	28-77	--	--	--	--	1-01	--	0-02	--
Al-brass	74-1	23-5	--	2-35	--	--	--	--	0-02	--
Cu-Ni	89-4	0-04	9-44	--	0-52	--	--	0-036	--	0-49
Ag-Mg	--	--	--	97-0	--	2-9	--	--	--	0-01

None of the above studies are directly applicable to the galvanic corrosion of TiCode-12 in a nuclear waste repository environment and are mentioned only to provide the reader with a general impression of the kind of galvanic corrosion testing which has been done on titanium and its alloys. In the context of the nuclear waste package program some work has been done by Westermann and others (PNL-SA-9543, 1981) on the corrosion of galvanic couples of cast iron and cast steel with titanium, although the focus seems to have been on the iron and steel. Simulated Hanford groundwater flowing through crushed basalt at about 35 mL/hr, was the electrolyte. The tests were run at

temperatures of 150 and 250°C. The inlet oxygen concentration was kept between 6 and 8 ppm by sparging with a mixture of 20 μ oxygen and 80% argon; the outlet oxygen concentration was about 1 ppm. Further discussion of the autoclave system and simulated groundwater composition are given elsewhere in this series of reports.

3.7.3 Conclusions and Recommendations

As was noted in the previous section, there has been very little work applicable to a nuclear waste package on the galvanic corrosion of titanium or its alloys, probably because TiCode-12, the alloy under consideration, is expected to be more noble in a metallic sense than the other waste package components with which it is likely to couple galvanically. Nevertheless, some additional data requirements for the galvanic corrosion behavior of TiCode-12 have been suggested by Shao (BNL-NUREG-31771):

- The extent of the galvanic corrosion on both couple components, including a determination of dissolution and film growth rates.
- The cathode-to-anode ratio effect.
- The galvanic series in brine and basalt groundwaters for TiCode-12 and the other waste package components.
- The amount of hydrogen evolution during coupling.

All of these data requirements may be obtained by a continuation of the work on galvanic corrosion in simulated Hanford groundwater by Westermann and others (PNL-SA-9543, 1981) mentioned in the previous section. Galvanic couples of TiCode-12 and other likely metallic components of the waste package should be immersed in simulated basalt groundwater and brine under conditions expected in the repositories for periods of up to several years. This kind of experiment could be conducted using the autoclaves and auxiliary equipment described elsewhere in this program. The effect of radiation on galvanic corrosion would also be of interest and could be carried out in the radiation test facility also described elsewhere. The metal specimens comprising the galvanic couples should be weighed and their surfaces characterized at least by scanning electron microscopy and preferably by a combination of surface analysis techniques, both before and after exposure to the simulated repository environments; any weight changes of the specimen and the growth (or dissolution) of any surface films may be observed by these techniques. The testing of galvanic couples with several different area ratios should also be considered. The galvanic series for the metals and alloys likely to be used in a waste package under expected repository conditions in brine and basaltic groundwaters may be determined by potentiometric measurements of the single-electrode potential for each of these metals and alloys relative to some standard electrode such as the calomel electrode. Measurement of the hydrogen or other gas evolution at the low rates of galvanic corrosion expected is difficult and should not be conducted unless other evidence of galvanic corrosion is obtained. Placement of an inverted container or other collection

device (possibly for several years) over a galvanic couple of interest in an autoclave-simulated repository environment would be the most direct way to obtain evidence of hydrogen evolution, but this would not be an easy experiment to carry out. If a significant portion of any evolved hydrogen were to be retained by the metal, tests for hydrogen embrittlement, discussed elsewhere in this program, would be appropriate.

It has been recommended that consideration be given to the evaluation of possible galvanic effects on stress corrosion (Soo, P., 1982). Such testing could be carried out through the use of double U-bend type specimens in which the appropriate dissimilar metals are placed in contact (see Section 3.6.3.1 above). Galvanic enhancement of the dealloying of nickel-aluminum bronzes by titanium has been reported (Zanis, C. A., 1974); galvanically enhanced dealloying of TiCode-12, while unlikely, should be looked for during the course of galvanic corrosion studies on TiCode-12 (see Section 3.8 below).

3.8 Tests For Selective Leaching

3.8.1 Introduction

Selective leaching, or as it is often termed, dealloying, is a corrosion process by which one component of an alloy is preferentially removed from the alloy leaving an altered residual composition and structure (Heidersbach, R., 1968). As in the case of galvanic corrosion, dealloying has not been considered significant in the context of nuclear waste package performance because it is considered likely that it can be avoided by proper materials selection (NUREG/CR-2333, 1982). Selective leaching was addressed and dismissed by the MCC Workshop on Corrosion of Engineered Barriers as a form of localized corrosion encountered only with materials such as brasses, aluminum bronze, and gray cast iron, none of which are primary candidates for waste containment (PNL-3720, 1981). Additional data requirements, however, on the possible dealloying of TiCode-12 are suggested by Shao (BNL-NUREG-31771, 1981). In this portion of the report, a brief account will be given of testing for selective leaching which has been done on titanium alloys. Recommendations for future investigation of selective leaching of TiCode-12 will then be made.

3.8.2 Current Status of Selective Leaching Testing of Titanium Alloys

Selective leaching is not an expected failure mode for titanium alloys (PNL-3720, 1981) and for this reason it has generally not been the main focus of corrosion experiments on such alloys. Some evidence for dealloying has been observed during the course of testing for other modes of corrosion.

For example, Tomashov and co-workers (1974) conducted a study of the passivation and corrosion behavior of titanium and some of its alloys by electrochemical, gravimetric, analytical, metallographic, and X-ray and electron diffraction methods. As part of this study, the dissolution of Ti-15 Mo alloys with different histories of heat treatment (and thus different crystalline microstructures) were carried out in 40% H_2SO_4 at 65 to 100°C. Chemical analyses of the solutions to which the specimens had been exposed to determine

the ratio of dissolved Ti to dissolved Mo were carried out as well as gravimetric determinations of the overall corrosion rates. The molybdenum content of the solution was only 3.3% of the dissolved metal, a result implying some kind of preferential dissolution of the titanium.

In the context of nuclear waste packages, at SNL an Auger depth profile was obtained for TiCode-12 which had been immersed in concentrated NaCl brine with a pH of 1 at 200°C for three weeks (SAND81-1585, 1981). Evidence was obtained of nickel enrichment at the surface relative to the bulk metal concentration.

3.8.3 Conclusions and Recommendations

Additional data requirements for the selective leaching behavior of TiCode-12 have been suggested by Shao (BNL-NUREG-31771, 1982):

- Better definition of the range of conditions under which TiCode-12 and its welds will be prone to selective leaching.
- Further depth profiling studies using surface analytical techniques such as Auger spectroscopy.
- Better definition of the microstructure and examination of the stabilities of the phases making up this microstructure in order to evaluate the extent of selective texture attack.
- Further studies of the mechanisms which lead to near-surface composition gradients.
- The effects of component enrichment or depletion or overall corrosion resistance.
- Determination of the mechanism of corrosion and any changes in these with time as the enrichment or depletion of components proceeds.

Surface analysis and metallographic examination of TiCode-12 specimens and, if possible, chemical analyses of the solutions to which these specimens were exposed, all of which could be conducted as part of the long term testing for uniform corrosion, would provide most of the above data and, in particular, would indicate whether TiCode-12 is susceptible to selective leaching under repository conditions. Uniform corrosion test methods are addressed in by Jain in Section 3.3 of the present report. We recommend that selective leaching be considered during the course of uniform corrosion testing of TiCode-12.

3.9 Tests for Hydrogen Embrittlement

3.9.1 Introduction

Titanium and its alloys are known to show considerable degradation in their mechanical properties in the presence of hydrogen. In TiCode-12, 30-50 ppm hydrogen is normally present after the manufacturing process and large additional amounts can be absorbed when the container is exposed to radiolysis products in the repository. Even small concentrations of hydrogen may cause failure in a stressed container so that testing for hydrogen embrittlement failure modes is mandatory.

The general area of hydrogen embrittlement covers a very large volume of scientific research including a variety of testing methods. Figure 3.26 (taken from Nelson, H. G., 1974) describes a model for hydrogen interaction with an alloy. When hydrogen enters from an outside environment, the interaction on the surface will play an important role. For example, on TiCode-12 having an oxide film, the oxide may act as a barrier for hydrogen penetration into the metal (Caskey, C. R., 1974; Shah, K. K., 1974). However, it is possible that in some areas the oxide film is broken or dissolved (as in a crevice) and the oxide-free alloy surface may readily absorb hydrogen or form a hydride if the hydrogen concentration is sufficiently high. The hydride can continue to supply hydrogen via diffusion into the bulk even after its primary source has ceased to operate. Also, specimen texture, exposure, atmosphere, and preparation techniques can change the oxide characteristics and hence the hydrogen uptake rate. Hydrogen present from mill processes will diffuse easily within the structure, probably at a faster rate along the grain boundaries.

Unlike iron-based alloys, the embrittlement of a titanium alloy occurs primarily due to the formation of a hydride phase within the matrix; other mechanisms shown in Figure 3.26 are of minor importance. A stress pattern, such as triaxial stresses in the container may serve as a driving force for hydrogen to diffuse from the bulk and concentrate locally around metallurgical imperfections. Thus, a hydride phase may be formed when the local concentration of hydrogen exceeds the solubility limit. Since diffusion is a time dependent phenonenon, the embrittlement of TiCode-12 due to the hydride phase will also be time dependent and can have a long incubation period depending on temperature, stresses, and the concentration of hydrogen. This makes it hard to predict the long term effects of hydrogen on the mechanical properties of TiCode-12. Also, small concentrations of hydrogen which may seem to be unimportant from short term laboratory tests, can cause embrittlement after extended periods due to the problem of delayed fracture. Therefore, a conservative approach in testing the mechanical properties and subsequent design parameters of the TiCode-12 container is warranted.

The presence of significant quantities of hydrogen in TiCode-12 or in the surrounding environment may be deleterious with respect to delayed failure and brittle fracture. Therefore, any measurement technique (ASTM STP 543, 1976) which evaluates these two effects will provide relevant information. Different

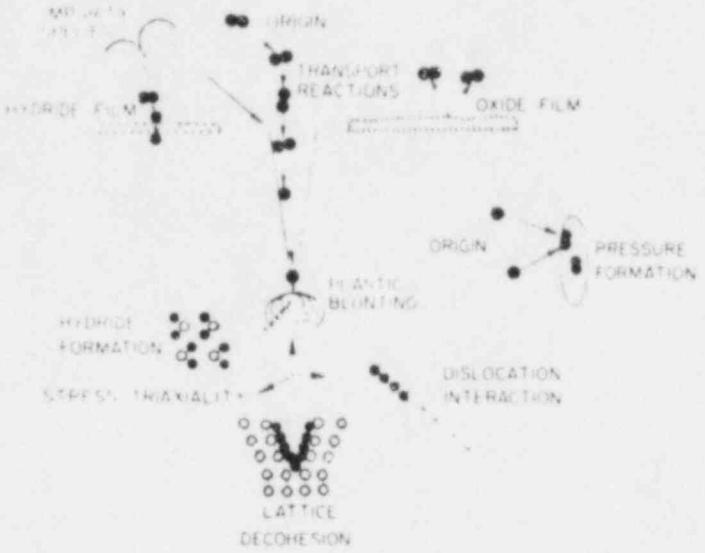

Figure 3.26 Interaction of hydrogen with an alloy (Nelson, H. G., 1974).

testing techniques have varying ability to quantify hydrogen embrittlement effects (see Figure 3.27) (Gray, H. R., 1974). Simple techniques such as disk pressuring (Fidelle, J. P., 1974 a,b) or the measurement of reduction in area are sufficient to demonstrate whether a given material is susceptible to adverse effects of hydrogen. However, the data obtained from these methods may be of limited importance in determining the performance of the TiCode-12 container. On the other hand, the technique of fracture mechanics is expected to yield quantitative data which can be used in evaluating the failure of TiCode-12. Accordingly, in its summary report (PNL-3720, 1981), the MCC Workshop has recommended static and dynamic fracture mechanics tests to quantify the hydrogen effects. The present report will mostly address these tests.

3.9.2 Variables Affecting Hydrogen Embrittlement

The main concern from the presence of hydrogen is that a TiCode-12 container might fracture during the containment period even though the applied load is much less than its ultimate strength. Archbold and others (PNL-4127, 1981; PNL-4157, 1982) have discussed in detail the hydrogen effects related to failure of titanium and its alloys (not TiCode-12 in particular) and have identified the following factors which determine the kinetics of cracking:

- Concentration of hydrogen with respect to the solubility limit - this limit itself will be determined by the temperature, stresses, microstructure, etc. The larger the content of hydrogen above the solubility limit at a given temperature, the faster will be the formation of hydrides and embrittlement.

- Absorption of hydrogen from environment - radiolysis of water will continuously produce hydrogen which can be absorbed by the container.

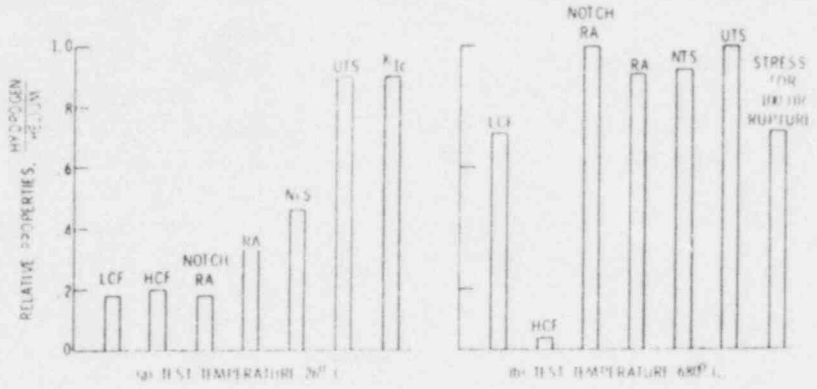

Figure 3.27 Comparison of mechanical properties of Inconnel 718 determined in hydrogen and helium at a pressure of 35 MN/m^2 (5000 psi) (Gray, H. R., 1974). Alloy annealed at 1038°C; notched specimens, K_t = 8; LCF, 1 to 2% strain; HCF, R = 0.1, (a) 180 ksi, (b) 140 ksi.

The production rate of hydrogen will depend on the intensity of irradiation and the chemistry of the groundwater. The hydrogen absorption rate will depend upon the container-surface conditions. When the radiolysis produces atomic hydrogen at the surface, it will probably enter the alloy more readily than molecular hydrogen gas. This fact should be kept in mind for laboratory tests simulating repository conditions.

- Strain rate in comparison with the diffusivity of hydrogen - in general a slower strain rate gives more time for hydrogen diffusion and hence more pronounced embrittlement. However, when hydrogen diffusion is not the rate determining step, the strain rate dependence will become less important. Some titanium alloys have shown (Irving, P. E., 1972) increased embrittlement at very high strain rates as a consequence of the strain rate sensitivity of the flow and fracture stresses of titanium hydrides rather than the metal itself.

- Internal flaws, cracks and stresses - the flaws and cracks present from the production process may not be easy to control and may enhance the embrittlement. Therefore, in this respect the test specimens should be representative of the final container material. Residual stresses resulting from the fabrication procedure including any welding should be taken into consideration during testing.

- Temperature - this variable affects both the solubility limit as well as the diffusivity of hydrogen. Therefore, its effect on embrittlement is not easy to predict, and testing should be carried out over the temperature range expected in a repository.

- Microstructure - TiCode-12 is a near-alpha titanium alloy. It has a small amount of beta-phase presumably present as a continuous network along the grain boundaries (NUREG/CR-2317, Vol. 1, No. 3, 1982). The beta-phase has higher hydrogen solubility and low susceptibility for hydride formation (BNL-NUREG-31773, 1982; Paton, N. E., 1974), and therefore is less susceptible to hydrogen embrittlement. Depending on the concentration of hydrogen, the fracture of TiCode-12 occurs at alpha-beta boundaries or through alpha grains (NUREG/CR-2317, Vol. 1, No. 4, 1982). In short, as shown for commercially pure titanium (Puttlitz, K. J., 1981), the phase morphology, grain size, properties of the grain boundary etc. are important parameters. Hence microstructural analysis should be included for all embrittlement testing. Any preferred orientation appearing in the actual container should also be given due consideration. Welding of the container is likely to change the microstructure in the heat affected zone. Therefore, separate testing of welded specimens will be needed.

- Irradiation - the direct effect of this variable on hydrogen embrittlement is not known, but it is likely that the radiation can help in the formation of the hydride phase.

Fatigue cracking due to cyclic loading and stress corrosion cracking are other important aspects of hydrogen embrittlement testing. However, cyclic loading is not expected in a repository and should not be of great importance except as an accelerating test. Stress corrosion cracking is considered to be a serious mode of failure and has been discussed in Section 3.6.

3.9.3 Accelerated Testing

From the available information on the hydrogen effects in titanium and its alloys (BNL-NUREG-31773, 1982), it is evident that the amount of hydrogen present in a commercial TiCode-12 sample may be low enough to show significant embrittling effects within the laboratory time scale. However, it is difficult to assert that such small concentrations can be ignored for the repository time scale. Additional amounts of hydrogen may also be absorbed by the alloy during radiolysis (NUREG/CR-2333, Vol. 4, Section 5, 1982) of the groundwater. Clearly, the laboratory testing conditions need to be made more severe to accelerate the embrittlement mechanism. In the case of corrosion failure discussed in the previous sections, testing could be accelerated by increasing the temperature or lowering the solution pH. Since hydrogen embrittlement is known to be a low-to-moderate temperature range phenomenon, increasing the test temperature will not necessarily accelerate it. The effect of pH falls under the category of stress corrosion cracking, and is discussed elsewhere in this study. Increasing the concentration of hydrogen will expedite the embrittling process and hence is a natural choice for acceleration purposes.

As for any other test acceleration procedures, one must be cautious in extrapolating the accelerated test data to real situations. Acceleration by increasing the hydrogen concentration can easily change the mechanisms of embrittlement and an extrapolation to lower concentration may not be appropriate. From Table 3.9 it may be seen that the functional relationship be-

Table 3.9 Effect of hydrogen concentration on K_{ITh} of Ti-6Al-4V (Meyn, D. A., 1981).

Hydrogen, ppm by Weight	K_{ITh}* (MPa$\sqrt{m}$)
8	92
36	65
53	67
122	64
215	66

*K_{ITh} is the lowest value at which sustained crack growth occurred.

tween the hydrogen concentration and the threshold stress intensity factor, which is a measure of embrittlement, is not linear. In spite of the ambiguity in extrapolating such results to lower concentrations, it may be noted that in general, the result should be a conservative estimate.

The concentration of hydrogen in an alloy sample can be increased by one of the following three procedures:

1. Heating a test specimen in a suitable hydrogen environment at a higher temperature where the solubility as well as diffusivity is larger - once the specimen has absorbed the desired amount of hydrogen, it can be cooled and tested at lower temperatures. This method is more appropriate for the materials (e.g., TiCode-12 which predominantly comprises alpha phase) which have low diffusivity, and thus cannot have homogeneous distribution of hydrogen at the room temperature. Furthermore, one can control the composition of the charging gas.

2. Cathodically charging the specimen - here, hydrogen from an H^+ containing acidic medium collects on the specimen surface and diffuses in. This method is simpler to use but is not appropriate for thick specimens.

3. Performing the embrittlement test in hydrogen gas - this approach is appropriate for determining hydrogen environmental embrittlement.

3.9.4 Fracture Toughness Parameters

Fracture toughness is a generic term to describe the resistance to extension of a crack.* Therefore, a parameter is needed to define this property quantitatively using available information from a prescribed testing procedure. This parameter should conform to the conditions expected for a container in a repository, and preferably be easy to determine.

The majority of the fracture toughness tests involve plane strain samples. The resistance of the material to sustained load fracture is then described by the threshold value of the stress intensity factor (K_{Th}) below which a crack will not propagate during a specific time. This parameter has obvious uncertainties of having a lower value if the test time is increased. There may also be some dependence on test specimen design, etc. In spite of some ambiguity, K_{Th} has been extensively used in screening various materials. By correlating plane strain fracture toughness (K_{Ic}) and dynamic tear energy with yield strength, ratio analysis diagrams (NRL-7780, 1974) have been developed and may be used for interpreting the fracture resistance of materials in terms of damage tolerant design. Evaluation of fracture toughness using the threshold parameters has been a widely tested method and hence also better understood. The BNL group has adopted (NUREG/CR-2317, Vol. 2, No. 1, 1982) this approach to evaluate the fracture toughness of TiCode-12, and from preliminary experiments determined K_{Th} to be approximately 4.5 MPa $\sqrt{m}$.

A general criticism on the use of K_{Th} as a fracture toughness criterion is that it is applicable only when plane strain conditions of elasticity are valid (PNL-4127, 1981). Thick compact tension specimens can approximately meet these conditions, but a thin TiCode-12 container probably will not. With the possibility of substantial plastic deformation during testing and use in the repository, a different set of test methods has been suggested (Priest, A. H., 1975), particularly the J-integral and R-curve methods. The J-integral is a mathematical expression and gives the critical parameter J_{Ic} to represent the material toughness at or near the onset of crack extension. A threshold value of J_{Ic} (J_{Th}) is defined analogous to K_{Th} and as long as minimum specimen size requirements are met, it is a specific material property (Landes, J. D., 1972). For materials which fracture in a ductile fashion on a microscale, J_{Th} is expected to give more conservative values for fracture toughness than K_{Th} and hence is a preferred parameter (Landes, J. D., 1977). However, a big disadvantage in determining J_{Ic} is that it involves the measurement of crack growth in a series of experiments, which is a tedious procedure.

The R-curve represents the resistance to fracture during incremental extension of a crack. The crack resistance is described in terms of the stress intensity factor K_R and can be obtained from a variety of tests (Priest, A. H., 1975; ASTM Designation E561-81, 1981). In principle, R-curve analysis can predict critical fracture stress and flaw size of an untested specimen at

---

*A glossary of the commonly used terms in fracture testing is described in the Annual Book of ASTM Standards, Part 10, Designation E616-81.

instability even when plane strain conditions are not satisfied. However, experimental knowledge of such predictions is very limited and the method is more complex than the determination of K_{Th}.

From the present understanding and reliability in translating the laboratory data of K_{Th}, J_{Th}, and R-curve analysis to actual design, it is suggested that extensive testing on TiCode-12 should be focused on K_{Th} measurements. Some supplemental testing should, however, be carried out to demonstrate that K_{Th} is not too unrealistic compared to the results obtained from J-integral data.

3.9.5 Test Methods

The MCC Workshop has considered (PNL-3720, 1981) the methods to test hydrogen effects in engineered barrier materials. These are divided into two broad categories: static test methods and dynamic test methods. An experiment may be performed using bend (Priest, A. H., 1975), compact tension (Priest, A. H., 1975), wedge opening load (Wei, R. P., 1972), or cantilever beam tests (Wei, R. P., 1972). Some details of these tests are described in Section 3.6.

The C-type and U-bend tests considered appropriate (see Section 3.6) for stress corrosion cracking (SCC) are, however, not recommended for hydrogen embrittlement due to lack of triaxial stress conditions. Among the suggested test methods, some are easy to use but appropriate for screening of available materials. Having selected TiCode-12 as the container material, such tests will not be necessary. Then, the MCC recommended tests will be as mentioned in the sections below.

3.9.5.1 Static Test Methods

These methods include:

- Slow crack growth using a fixed load on compact tension specimens. Determine K_{Th} or J_{Th}.
- Slow strain rate using compact tension specimens. Determine K_{Th} or J_{Th}.
- Same procedure as in the previous two tests, but on center cracked sheet specimens. This method may be useful for determining texture effects. Also, a longitudinally cracked tube can instead be used under load control for the same purpose.

In general, these methods use a specimen which has been previously fatigue cracked to provide stress intensification in a reproducible manner; a short fatigue crack extends from a notch machined in the specimen. The relative length of the crack, the dimensions of the notch and the specimen, and the procedure to produce a fatigue crack are prescribed by ASTM (ASTM Designation 399-81, Annex A2, 1981). In some cases, if crack initiation and

growth require an excessive number of fatigue cycles, ASTM recommends using a very sharp notch tip, statically pre-loading the specimen in such a way that the notch tip is compressed in a direction normal to the intended crack plane, or using a chevron notch.

To determine K_{Th}, one needs to find out the value of plane strain fracture toughness K_{Ic} below which there is no observable crack growth. ASTM has set a standard test method (ASTM Designation 399-81, 1981) for the determination of K_{Ic}. For the determination of both K_{Th} or J_{Th}, an important step is to measure the crack length under different conditions. There are a variety of methods which yield directly or indirectly the value of crack length as it grows. These are summarized by Deans and others (1979) and listed in Appendix A.

A test not mentioned in ASTM procedure or MCC recommendations uses a double cantilever beam specimen and is recommended by Archbold and others (PNL-4157, 1982) as a predictive test for monitoring and predicting delayed failure due to hydrogen embrittlement as well as SCC. This technique has been used by Boyer and Spurr (1978) with the specimen configuration shown in Figure 3.28.

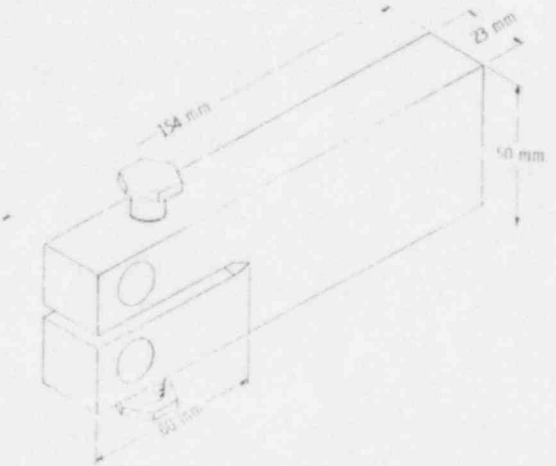

Figure 3.28 Specimen for double cantilever beam technique (Boyer, R. R., 1978).

The specimens are fatigue pre-cracked and loaded to desired stress levels in an Instron machine before starting to measure the crack growth. Here, the value of stress intensity decreases as the crack length increases. This method has the advantage of relatively low cost specimens which can be easily used under various conditions. Furthermore, an Instron machine is needed only to pre-load the specimen and subsequent loading is maintained by the bolts. Several specimens can be tested concurrently. This will, however, not permit any variation in strain rate as it affects the crack growth. For Ti-6Al-4V alloy, this method was found to be useful to detect texture related effects (Boyer, R. R., 1978).

The MCC recommended test when plane strain conditions are not present is the determination of threshold value of J-integral which is defined (ASTM Designation E813-81, 1981) by:

$$J = [W\,dy - T\cdot(\partial\bar{u}/\partial x)]\,ds$$

where:

- W = Loading work per unit volume, or for elastic bodies, strain energy density
- x,y,z = Rectangular coordinates
- ds = Increment of the contour path
- T = Outward traction vector on ds
- $\bar{u}$ = Displacement vector at ds
- $T\cdot(\partial u/\partial x)ds$ = The rate of work input from the stress field into the area enclosed by Γ, the path of the integral which contains the crack tip.

The standard method for determining J_{Ic} which is the value of J at crack initiation is described in the ASTM manual (ASTM Designation E813-81, 1981). Here the purpose is to obtain load vs crack displacement curve by loading the specimen to different displacement values in a series of tests. The displacement at each step may be measured by heat tinting the specimen. Clarke and others (1976) have developed a fully autographic method to determine J_{Ic} using one specimen and periodic partial unloading. In this case, the reciprocal of the unloading slopes (in load vs load time displacement plot) normalized for elastic modulus and specimen geometry, predicts the crack size using an elastic compliance calibration.

R-curve determination is another approach to evaluate the resistance to fracture during incremental slow crack extension from a sharp notch. MCC has not considered this method as best suited for the design of waste containers; nevertheless, it is a relevant test and its details are described in the ASTM manual (ASTM Designation E561-81, 1981).

In any of the test methods using thick specimens, one should be cautious of any errors due to "tunneling". This happens when the crack front penetrates deeper in the middle of the sample than on the surface. Thus, crack growth conditions may become more severe in the interior of the specimen and lead to a failure, while the observations from the surface give erroneous results.

3.9.5.2 Dynamic Test Methods

Except for the applied load, dynamic tests use the same kind of specimen, data analyses, etc. as do the static methods. Here, a cyclic stress is applied whose intensity varies between a minimum (e.g., zero) and a maximum value (K_{max}) at a frequency <30 Hz. The results may be expressed in terms of ΔK_{Th} below which the material will not fail irrespective of the total

number of cycles. In general, this parameter will give more conservative estimate of fracture toughness of a material, otherwise each dynamic method has the same advantages or disadvantages as the corresponding static method.

3.9.5.3 Weld Tests

It was mentioned earlier that due to the changes in microstructure or additional stresses, the area around a weld may be more susceptible to hydrogen embrittlement and fail earlier than the rest of the container. This adverse effect may also deteriorate toughness and SCC resistance of TiCode-12. A general description of specimen preparation, welding configuration and testing method is given in the ASTM manual (ASTM Designation G58-78, 1981). To evaluate the potential of hydrogen assisted delayed cracking, a weld bead is prepared (Dickinson, D. W., 1979) between a helically notched cylindrical test specimen after inserting it into a plate of the same material. The stress intensification for hydrogen diffusion is provided by the notch and the welded structure is tested in a static mode. Toughness of the weld may be determined by having a notched specimen and stressing it in a bending mode. Charpy V-notch tensile tests will also give information about toughness. Weymueller (1977) has discussed the merits of these tests.

An as-welded TiCode-12 component may have developed strong internal stresses due to inhomogeneous cooling. These stresses can considerably decrease the life of the container and may lead to early failure. Important methods to measure internal stresses are listed by Archbold and Polonis (PNL-4127, 1981). Since the present goal is not to characterize internal stresses but to evaluate their adverse effect on the container performance, these test methods may not be necessary. Previously described hydrogen embrittlement tests performed on welded specimens will include the effects of internal stresses also. However, if internal stresses become a major concern of failure, proper annealing treatment after welding should be considered to relieve them. This may improve ductility and toughness of the welded zone (Simpson, R. P., 1975).

3.9.6 Conclusions and Recommendations

Hydrogen in TiCode-12, present internally from manufacturing processes or absorbed during repository exposure, is likely to deteriorate mechanical properties of the container to the extent that hydrogen embrittlement is a potential failure mode. The most important property of concern is the crack growth under sustained load conditions. Fracture mechanics tests are considered to be appropriate to evaluate hydrogen effects.

Due to possible small hydrogen concentrations in as-received specimens, accelerated testing will be needed. Temperature, strain rate, microstructure, irradiation, etc. may influence the extent of the effect of hydrogen on the mechanical properties of TiCode-12, but their dependence may not be monotonic and difficult to determine. Therefore, to accelerate the testing procedure, the specimens may be charged with additional hydrogen from an outside source.

Several experiments will be needed to be able to extrapolate laboratory data to expected hydrogen contents in the repository.

The determination of K_{Th} or ΔK_{Th} for plane strain conditions is an appropriate starting point to evaluate the hydrogen effects. Some experiments to determine J_{Th} will be useful in determining how much difference it will make if elastic-plastic conditions are present. The double cantilever beam test (Boyer, R. R., 1978) is also an attractive test method especially when many specimens need to be tested with a limited number of testing machines.

3.10 References

AESD-TME-3113, "Engineered Waste Package Conceptual Design - Defense High Level Waste (Figure 1), Commercial High Level Waste (Form 1), and Spent Fuel (Form 2) Disposal in Basalt," Westinghouse Electric Corporation, September 1981.

ASTM, Annual Book of ASTM Standards, Part 10, Metals - Physical, Mechanical, Corrosion Testing, American Society for Testing and Materials, Philadelphia, 1981 a.

ASTM, Annual Book of ASTM Standards, Part 45, Nuclear Standards, Standard Specification B265-79, American Society for Testing and Materials, Philadelphia, 1981 b.

ASTM Designation 399-81, "Fatigue Precracking of K_{Ic} Fracture Toughness Specimens," Annual Book of ASTM Standards, Part 10, Annex A2, 1981.

ASTM Designation E561-81, "Standard Practice for R-Curve Determination," Annual Book of ASTM Standards, Part 10, 1981.

ASTM Designation E813-81, "Standard Test for J_{Ic}, A Measure of Fracture Toughness," Annual Book of ASTM Standards, Part 10, 1981.

ASTM Designation E399-81, "Plane-Strain Fracture Toughness of Metallic Materials," Annual Book of ASTM Standards, Part 10, 1981.

ASTM Designation G1-81, "Standard Practice for Preparing, Cleaning and Evaluating Corrosion Test Specimens," Annual Book of ASTM Standards, Part 10, 1981.

ASTM Designation G3, "Conventions Applicable to Electrochemical Measurements in Corrosion Testing," and "Method for Making Potentiostatic and Potentiodynamic Anodic Polarization Measurements," Annual Book of ASTM Standards, Part 10, 1981.

ASTM Designation G5, "Conventions Applicable to Electrochemical Measurements in Corrosion Testing," and "Method for Making Potentiostatic and Potentiodynamic Anodic Polarization Measurements," Annual Book of ASTM Standards, Part 10, 1981.

ASTM Designation G46-76, "Examination and Evaluation of Pitting Corrosion," Annual Book of ASTM Standards, Part 10, 1981.

ASTM Designation G58-78, "Preparation of Stress Corrosion Test Specimens for Weldments," Annual Book of ASTM Standards, Part 10, 1981.

ASTM STP 543, "Hydrogen Embrittlement Testing," 1976.

Bania, P. J. and S. D. Antolovich, "Activation Energy Dependence on Stress Intensity in Stress-Corrosion Cracking and Corrosion Fatigue," in Stress Corrosion - New Approaches, Special Technical Publication 610, H. L. Craig Jr., Ed., American Society for Testing and Materials, Philadelphia, 1976, p. 157.

Bates, J. F., "Cathodic Protection to Prevent Crevice Corrosion of Stainless Steels in Halide Media," Corrosion, 29, 28, 1973.

Beck, T. R. and S. G. Chan, "Experimental Observation Analysis of Hydrothermal Effects on Growth of Small Pits," Corrosion, 37, 665, 1981.

Berry, W. E., "Testing Nuclear Materials in Aqueous Environments," Handbook of Corrosion Testing, W. H. Ailor, Ed., John Wiley and Sons, New York, 1971, Chapter 13.

BNL-NUREG-31754, "Uniform, Pitting and Crevice Corrosion, and Hydrogen Embrittlement Test Requirements for TiCode-12 High Level Waste Containers," H. Jain, Brookhaven National Laboratory, August 1982.

BNL-NUREG-31755, "Stress Corrosion Cracking, Galvanic Corrosion and Selective Leaching Test Requirements for TiCode-12 High Level Waste Containers," B. Siskind, Brookhaven National Laboratory, August 1982.

BNL-NUREG-31771, "Stress Corrosion Cracking, Galvanic Corrosion, and Selective Leaching Data Requirements for TiCode-12 High Level Waste Containers," J. Shao, Brookhaven National Laboratory, August 1982.

BNL-NUREG-31773, "Hydrogen Embrittlement Data Requirements for TiCode-12 High Level Waste Containers," T. M. Ahn, Brookhaven National Laboratory, August 1982.

BNL-NUREG-31775, "Crevice Corrosion Data Requirements for TiCode-12 High Level Waste Containers," B. S. Lee, Brookhaven National Laboratory, August 1982.

Boyer, R. R. and W. F. Spurr, "Characteristics of Sustained-Load Cracking and Hydrogen Effects in Ti-6Al-4V," Met. Trans. 9A, 23, 1978.

Braithwaite, J. W. and M. A. Molecke, "Nuclear Waste Canister Corrosion Studies Pertinent to Geologic Isolation," Nuc. and Chem. Waste Management, 1, 37, 1980.

Brigham, R. J., "On the Variability of Crevice Corrosion Initation in Ferric Chloride Exposure Tests," Corrosion, 37, 608, 1981.

Callow, L., J. Richardson and J. Dawson, "Corrosion Monitoring Using Polarization Resistance Measurements, Part I and II," Brit. Corr. J. 11, 123, 1976.

Caskey, G. R., Jr., "The Influence of a Surface Oxide Film on Hydriding of Titanium," Hydrogen in Metals, I. M. Bernstein and A. W. Thompson, Eds., American Soc. Metals, 465, 1974.

Clark, W. G., Jr. and J. D. Landes, "An Evaluation of Rising Load K_{ISCC} Testing," in Stress Corrosion - New Approaches, Special Technical Publication 610, H. L. Craig Jr. Ed., American Society for Testing and Materials, Philadelphia, 1976, p. 108.

Clarke, G. A., W. R. Andrews, P. C. Paris and D. W. Schmidt, "Single Specimen Tests for J_{Ic} Determination," Mechanics of Crack Growth, ASTM STP 590, 1976.

Craig, H. L., Jr., D. O. Sprowls, and D. E. Piper, "Stress-Corrosion Cracking," in Handbook on Corrosion Testing and Evaluation, W. H. Ailor, Ed., John Wiley and Sons, New York, 1971, p. 231.

Danielson, M. J., "Application of Linear Polarization Techniques to the Measurement of Corrosion Rates in Geothermal Brines," Geothermal Scaling and Corrosion, ASTM STP 717, 1980, p. 41.

Day, K. J. and F. G. Dunkley, "Corrosion Testing and Determination of Corrosion Rates," Corrosion, Newnes Buttersworth, Boston, 1976, p. 30.

Deans, W. P. and C. E. Richards, "A Simple and Sensitive Method of Monitoring Crack and Load in Compact Fracture Mechanics Specimens Using Strain Gages," J. Testing and Evaluation, 7, 147, 1979.

Dear, S. W., and others, "Electrochemical Methods," Handbook of Corrosion Testing and Evaluation, W. H. Ailor, Ed., John Wiley and Sons, New York, 1971, Chapter 8.

Dickinson, D. W. and G. D. Ries, "Implant Testing of Medium to High Strength Steel - A Model for Predicting Delayed Cracking Susceptibility," Welding Research Supplement, 1979, p. 205s.

Diegle, R. B., "New Crevice Corrosion Test Cell," Materials Performance, 21, 43, 1982.

Epelboin, I. and others, "A. C. Impedance Measurement Applied to Corrosion Studies and Corrosion Rate Determination," Electrochemical Corrosion Testing, ASTM STP 727, 1981, p. 150.

Fidelle, J. P. and others, "Disk Pressure Technique," Hydrogen Embrittlement Testing, ASTM STP 543, 1974 a, p. 34.

Fidelle, J. P., R. Bernardi, R. Broudeur, C. Roux and M. Rapin, "Disk Pressure Testing of Hydrogen Environment Embrittlement," Hydrogen Embrittlement Testing, ASTM STP 543, 1974 b, p. 221.

Finley, H. F., "An Extreme Value Statistical Analysis of Maximum Pit Depths and Time to First Perforation," Corrosion, 23, 83, 1967.

Fontana, M. G. and N. D. Greene, Corrosion Engineering, McGraw Hill, New York, 1978.

France, W. D., Jr. and N. D. Greene, Jr., "Passivation of Crevices During Anodic Protection," Corrosion, 24, 247, 1968.

Gainer, L. G. and G. R. Wallwork, "An Apparatus for the Examination of Localized Corrosion Behavior," Corrosion, 35, 61, 1979.

Garner, A., "The Use of Free-Corrosion Potential-Time Transients to Distinguish Between Pitting and Crevice Corrosion After Potentiostatic Tests," Corrosion, 34, 285, 1978.

Gray, H. R., "Testing for Hydrogen Environment Embrittlement: Experimental Variables," Hydrogen Embrittlement Testing, ASTM STP 543, 1974, p. 133.

Greene, N. D. and M. G. Fontana, "An Electrochemical Study of Pitting Corrosion in Stainless Steels," Corrosion, 15, 32t, 1959.

Greiss, J. C., Jr., "Crevice Corrosion of Titanium in Aqueous Salt Solutions," Corrosion, 24, 97, 1968.

Gumbel, E. J., "Statistics of Extremes," Columbia University Press, 1958.

Hart, R. J., "Testing in Hot Brine Loops," Handbook of Corrosion Testing, W. H. Ailor, Ed., John Wiley and Sons, New York, 1971, Chapter 12.

Haruyama, S. and T. Tsuru, "A Corrosion Monitor Based on Impedance Method," Electrochemical Corrosion Testing, ASTM STP 727, 1981, p. 167.

Heidersbach, R., "Clarification of the Mechanism of the Dealloying Phenomenon," Corrosion, 24, 38-44, 1968.

Hickling, J. and N. Wieling, "Electrochemical Investigation of the Resistance of Inconel 600, Incoloy 800, and Type 347 Stainless Steels to Pitting Corrosion in Faulted PWR Secondary Water at 150 and 250°C," Corrosion, 37, 147, 1981.

Isaacs, H. S. and M. W. Kendig, "Determination of Surface Inhomogeneities Using a Scanning Probe Impedance Technique," Corrosion, 36, 269, 1980.

Isaacs, H. S. and B. Vyas, "Scanning Reference Electrode Techniques in Localized Corrosion," Electrochemical Corrosion Testing, ASTM STP 727, 1981, p. 3.

Ishikawa, Y. and others, "Pitting Corrosion Life Prediction of Machine Components by Means of Extreme Value Statistical Analysis," in Environmental Degradation of Engineering Materials in Aggressive Environments, Proceedings of Second International Conference on Environmental Degradation of Engineering Materials, September 21-23, 1981, Virginia Polytechnic Institute, Blacksburg, Virginia.

Irving, P. E. and C. J. Beevers, "Some Observations on the Deformation Characteristics of Titanium Hydride," J. Mat. Sci. 7, 23, 1972.

Jones, D. de G. and M. G. Masterson, "Techniques for the Measurement of Electrode Processes at Temperatures Above 100°C," Advances in Corrosion Sci. Tech., Vol. 1, M. G. Fontana and R. W. Staehle, Eds., Plenum Press, New York, 1970.

Landes, J. D. and J. A. Begley, "The Effect of Specimen Geometry on J_{Ic}," Fracture Toughness, ASTM STP 514, 1972, p. 24.

Landes, J. D. and J. A. Begley, "Recent Developments in J_{Ic} Testing," Dev. Fracture Mech. Test Method Standardization, ASTM STP 632, 1977, p. 57.

Lee, T. S., "A Method for Quantifying the Initiation and Propagation Stages of Crevice Corrosion," Electrochemical Corrosion Testing, ASTM STP 727, 1981, p. 43.

Lizlovs, E. A., "Polarization Cell for Potentiostaic Crevice Corrosion Testing," J. Electrochem. Soc. 117, 1335, 1970.

MacDonald, D. D., B. C. Syrett and S. S. Wing, "The Use of Potential - pH Diagrams for the Interpretation of Corrosion Phenomena in High Salinity Geothermal Brines," Corrosion, 35, 1, 1979.

MacDonald, D. D. and M. C. H. McKubre, "Electrochemical Impedance Techniques in Corrosion Science," Electrochemical Corrosion Testing, ASTM STP 727, 1981, p. 110.

MacDougal, B., D. M. Mitchell, and M. J. Graham, "The Use of Electrochemical and Surface Analytical Techniques to Characterize Passive Oxide Films on Nickel," Corrosion, 38, 85, 1982.

Macki, J. M. and R. L. Kochen, "The Galvanic Corrosion Behavior of Uranium Alloys in Hydrochloric Acid and Ocean Waste," RFP-1592, DOW Chemical Company, Golden, Colorado, 1971. Under AEC Contract No. AT (29-1)-1106.

Mansfeld, F. D. H. Hengstenberg, and J. V. Kenkel, "Galvanic Corrosion of Al Alloys, I. Effect of Dissimilar Metal," Corrosion, 30, 343-353, 1974.

Meyn, D. A., "Effect of Hydrogen Content on Inert Environment Sustained Load Crack Propagation Mechanisms of Ti-6Al-4V," Environmental Degradation of Engineering Materials in Hydrogen, Lab. Study of Environmental Degradation of Engineering Materials, Virginia Poly. Inst. Blacksburg, 1981.

Murphy, T. J., "Utilization of Anodic Breakdown of Titanium Alloys as a Method of Characterization," in Proc. Int. Conf. Titanium, 217, 1970.

National Assocociation of Corrosion Engineers, Electrochemical Techniques for Corrosion, 1977.

NAVSHIPRANDLAB REPT. 8-730, "Potentiostatic -Ellipsometric Studies of Titanium - Aluminum Binary Alloys in 3.5% Sodium Chloride Solution," O. P. Arora and J. P. Gudas, April 1971. AD725504.

Nelson, H. G., "Testing for Hydrogen Embrittlement: Primary and Secondary Influences," Hydrogen Embrittlement Testing, ASTM STP 543, 1974, p. 152.

NRL-7780, AD785233, "Prevention and Control of Sub-critical Crack Growth in High Strength Metals," R. W. Judy and R. J. Goode, Naval Research Laboratory, August 1974.

NUREG/CR-2317, Vol. 1, Nos. 3,4; Vol. 2, No. 1, BNL-NUREG-51449, "Container Assessment - Corrosion Study of HLW Container Materials, Quarterly Progress Reports," T. M. Ahn and P. Soo, Brookhaven National Laboratory, 1982.

NUREG/CR-2333, Vol. 1, "Nuclear Waste Management Technical Support in the Development of Nuclear Waste Form Criteria for the NRC," R. Dayal and others, Brookhaven National Laboratory, February 1982.

NUREG/CR-2333, Vol. 4, BNL-NUREG-51458, "Nuclear Waste Management Technical Support in the Development of Nuclear Waste Form Criteria for the NRC," Task 4, Test Development Review, T. M. Ahn and others, Brookhaven National Laboratory, February 1982.

NUREG/CR-2780, Part 1, BNL-NUREG-51548, "Near-Field Repository Conditions in Basalt and Salt," B. Siskind and D. Hsieh, Brookhaven National Laboratory, May 1982.

NUREG/CR-2780, Part 2, BNL-NUREG-51548, "Uniform and Pitting Corrosion Data Requirements for TiCode-12 High Level Waste Containers," J. Shao and P. Soo, Brookhaven National Laboratory, May 1982.

Oldfield, J. W. and W. H. Sutton, "Crevice Corrosion of Stainless Steels," Brit. Corr. J. 13, 13, 1978.

Oldfield, J. W. and W. H. Sutton, "Crevice Corrosion of Stainless Steels," Brit. Corr. J. 13, 104, 1978.

Paton, N. E. and J. C. Williams, "Effect of Hydrogen on Titanium and its Alloys," Hydrogen in Metals, American Soc. Metals, 409, 1974.

Payer, J. H., W. E. Berry, and W. K. Boyd, "Constent Strain Rate Technique for Assessing Stress-Corrosion Susceptibility", in Stress Corrosion - New Approaches, Special Technical Publication 610, H. L. Craig Jr., Ed., American Society for Testing and Materials, Philadelphia, 1976, p. 82.

PB81-104564, "Laboratory Corrosion Studies in Low and High Salinity Geobrines of the Imperial Valley," S. D. Cramer and J. P. Carter, Bureau of Mines Rept., 1980.

Pitman, S. G., B. Griggs and R. P. Elmore, "Evaluation of Metallic Materials for Use in Engineered Barrier Systems," Scientific Basis for Nuclear Waste Management, Vol. 3, J. G. Moore, Ed., Plenum Press, New York, 1981.

PNL-3484, "Investigation of Metallic, Ceramic, and Polymeric Materials for Engineered Barrier Applications in Nuclear-Waste Packages," R. E. Westerman, Pacific Northwest Laboratory, October 1980.

PNL-3720, "Materials Characterization Center Workshop on Corrosion of Engineered Barriers - Summary Report," M. D. Merz and others, Pacific Northwest Laboratory, March 1981.

PNL-3000-10, "Nuclear Waste Management Quarterly Progress Report, April Through June 1981," Section 22, R. E. Westerman, Pacific Northwest Laboratory, September 1981.

PNL-3000-11, "Nuclear Waste Management Quarterly Progress Report, July Through September 1981," Section 22, R. E. Westerman, Pacific Northwest Laboratory, December 1981.

PNL-3915, "Investigation of Susceptibility of Titanium - Grade 2 and Titanium - Grade 12 to Environmental Cracking in a Simulated Basalt Repository Environment - Interim Report," S. G. Pitman, Pacific Northwest Laboratory, October 1981.

PNL-3990, "Materials Characterization Center Test Methods - Preliminary Version," J. E. Mendel, Pacific Northwest Laboratory, March 1982.

PNL-4127, "Assessment of Delayed Failure Models in Titanium and Titanium Alloys," T. F. Archbold and D. H. Polonis, Pacific Northwest Laboratory, December 1981.

PNL-4157, "Assessment of Predictive Models for the Failure of Titanium and Ferrous Alloys Due to Hydrogen Effects," T. F. Archbold, R. B. Bower and D. H. Polonis, Pacific Northwest Laboratory, April 1982.

PNL-SA-9543, "Development of Engineered Structural Barriers for Nuclear Waste Packages," R. E. Westerman and others, Pacific Northwest Laboratory, November 1981.

Posey, F. A. and E. G. Bohlmann, "Pitting of Titanium Alloys in Saline Water," Desalination, 3, 269, 1967.

Priest, A. H., "Experimental Methods for Fracture Toughness Measurement," J. Strain Analysis, 10, 225, 1975.

Puttlitz, K. J. and A. J. Smith, "The Influence of Microstructure on the Hydrogen Embrittlement of Pure and Commerically-pure Titanium," Hydrogen Effects in Metals, I. M. Bernstein and A. W. Thompson, Eds., AIME, 427, 1981.

RHO-BWI-ST-15, "Corrosion Tests of Canister and Overpack Materials in Simulated Basalt Groundwater," W. J. Anderson, Rockwell Hanford Operations, May 1981.

SAND79-2023C, "Titanium Alloy Corrosion in Nuclear Waste Environments," J. W. Braithwaite, N. T. Magnani and T. W. Mumford, Sandia National Laboratories, 1979.

SAND80-1738C, "The Slow Strain Rate Behavior of TiCode-12 (ASTM Grade 12) in Aqueous Chloride Solutions," L. Abrego and H. J. Rack, Sandia National Laboratories, April 1981.

SAND80-2416C, "Development of Reference Conditions for Geologic Repositories for Nuclear Waste in the USA," G. E. Raines and others, Sandia National Laboratories, 1980.

SAND81-1585, "Sandia HLW Canister/Overpack Studies Applicable for a Salt Repository," Molecke, M. and others, Sandia National Laboratories, August 1981.

Schlain, D., "Certain Aspects of the Galvanic Corrosion Behavior of Titanium," U.S. Bureau of Mines, Report No. 4965, April 1953.

Schultz, R. W. and L. C. Covington, "Effect of Oxide Films on the Corrosion Resistance of Titanium," Corrosion, 37, 585, 1981.

Sedricks, A. J., Corrosion of Stainless Steels, John Wiley and Sons, New York, 1979.

Shah, K. K. and D. L. Johnson, "Effect of Surface Pre-Oxidation on Hydrogen Permeation in Alpha Titanium," Hydrogen in Metals, I. M. Bernstein and A. W. Thompson, Eds., American Soc. Metals, 475, 1974.

Shalaby, Z. A., "Galvanic Coupling of Ti with Cu and Al Alloys in Chloride Media," Corrosion Science, 11, 767-778, 1971.

Shreir, L. L., "Localized Corrosion," Corrosion, Newnes Buttersworth, Boston, 1976, p. 130.

Simpson, R. P. and K. C. Wu, "Microstructure - Property Control with Postweld Heat Treatment," Welding Research Supplement, 54, 73s. 1975.

Soo, P., BNL to E. A. Wick, NRC, Subject: Review of the MCC-103S Stress-Corrosion Cracking Susceptibility Test Methods, June 30, 1982.

Sprowls, D. O., J. W. Coursen, and J. D. Walsh, "Evaluating Stress-Corrosion Crack-Propagation Rates in High-Strength Aluminum Alloys with Bolt Loaded Pre-Cracked Double-Cantilever Beam Specimens," in Stress Corrosion - New Approaches, Special Technical Publication 610, H. L. Craig Jr., Ed., American Society for Testing and Materials, Philadelphia, 1976, p. 143.

Stewart, D. B. and R. W. Potter II, "Application of Physical Chemistry of Fluids in Rock Salt at Elevated Temperature and Pressure to Repositories for Radioactive Waste," Scientific Basis for Nuclear Waste Management, Vol. 1, G. J. McCarthy, Ed., Plenum Press, New York, 1979

Swyler, K. J., R. W. Klaffky and P. W. Levy, "Recent Studies on Radiation Damage Formation in Synthetic NaCl and Natural Rock Salt for Radioactive Waste Disposal Applications," Scientific Basis for Radioactive Waste Management, Vol. 2, C. J. Northrop Jr., Ed., Plenum Press, New York, 1980.

Syrett, B. C., D. D. MacDonald and H. Shih, "Pitting Resistance of Engineering Materials in Geothermal Brines," Corrosion, 36, 131, 1980.

Tomashov, N. D. and others, "The Passivation of Alloys on Titanium Bases," Electrochem. Acta. 19, 159-172, 1974.

Wei, R. P., S. R. Novak and D. P. Williams, "Some Important Considerations in the Development of Stress Corrosion Cracking Test Methods," Materials Research and Standards, September 1972, p. 25

Weymueller, C. R., "Applying the Right Mechanical Test Method," Welding Design and Fabrication, 56, 92, 1977.

Wilde, B. E., "A Critical Appraisal of Some Popular Laboratory Electrochemical Tests for Predicting the Localized Corrosion Resistance of Stainless Alloys in Sea Water," Corrosion, 28, 238, 1972.

Zanis, C. A. and R. J. Ferrara, "Seawater Corrosion of Nickel-Aluminum Bronze," Trans Am Foundrymen's Soc. 82, 71-78, 1974.

4. PACKING MATERIAL TESTING REQUIRED TO DEMONSTRATE COMPLIANCE WITH 1000-YEAR RADIONUCLIDE CONTAINMENT

One component which appears in some generic high level waste package designs is the packing material. In most cases it is considered to be the material between the host rock and the other waste package components. Many functions have been assigned to this component in various waste package designs; these are presented in Table 4.1. As the waste package designs evolved, the number of functions assigned to the packing material was reduced. In the present review two of its several proposed functions are considered to be important for 1000-year containment.

- Control of the groundwater flow to the waste form and, after saturation, out of the waste package.
- Retardation of the migration of radionuclides.

The Westinghouse group goes further and eliminates the second function, taking the position that packing material, if used at all in a basalt repository, should serve the single function of groundwater control (AESD-TME-3113, 1981). On the other hand, in the case of a tuff repository, that group recommends that packing material (sodium bentonite) be used, if at all, for the sole purpose of radionuclide retardation (AESD-TME-3138, 1982). The Westinghouse group argues against the use of any packing material in a salt repository, basing this position on the assumption of very low water flow in salt (AESD-TME-3131, 1981). The testing of crushed salt as a packing material in a salt repository would require a separate treatment from that presented here.

In this section the question of whether packing material can be given full credit for 1000-year containment of all radionuclides is addressed. Specifically, those attributes most important to testing for the purpose of demonstrating 1000-year containment are identified; experimentally measurable properties associated with these attributes are evaluated to determine those that should be included in testing for compliance; available test methods that provide the necessary licensing information are discussed. Although the NRC definition of a waste package includes packing material as a component (10 CFR 60), a specific definition of packing material and/or a description of its functions are not given. Such information is important in evaluating the extent of the contribution of packing material as a component of the waste package. In the discussion below, both the groundwater flow control and the radionuclide retardation are addressed in separate sections. Other attributes of the packing material will be discussed as they pertain to its performance in achieving 1000-year containment. In the discussion of groundwater flow control in Section 4.1.1, the emphasis is on bentonite because of its swelling behavior and formation of a low permeability barrier. Radionuclide retardation is discussed in Section 4.1.2 both in terms of bentonite and synthetic zeolites because of their recognized superior ion-exchange capabilities. To date, most packing material testing has focused on the ability of candidate

Table 4.1 Functions which have been assigned to the packing material.[a]

Function	Generic Design[b]						
	PNL	DOE	AECL	BWIP	KBS	BNL	AESD
Limit water ingress to package	X	X	X	X	X	X	X
Absorb radionuclides or other chemicals	X	X	X	X	X	X	-
Absorb water	X	X	X	X	X	-	-
Aid heat transfer	X	X	X	X	X	-	-
Condition groundwater	X	X	X	-	X	-	-
Fill cracks in host rock	X	-	-	-	X	-	-
Fill gaps	-	-	-	X	X	-	-
Load equalization	-	X	-	-	-	-	-

[a]Adapted and expanded from AESD-TME-3131 (1981), Table D-1.

[b]The presence of an X indicates that function was included in the generic design. The column headings are acronyms of the organization presenting the particular design:

PNL Pacific Northwest Laboratory
DOE Department of Energy
AECL Atomic Energy of Canada Ltd.
BWIP Basalt Waste Isolation Project
KBS Nuclear Fuel Safety (Sweden)
BNL Brookhaven National Laboratory
AESD Westinghouse Advanced Energy System Division

(BNL does not present a generic design in this report but the packing material functions are discussed in the text.)

materials to retard migration of radionuclides. Recently, a concerted packing material testing program was initiated at PNL (PNL-3873, 1981). As part of this effort, the time required for water to initially penetrate the packing material and the rate of percolation through the packing material after saturation will be determined for candidate materials. Such an approach recognizes the potential of certain packing materials, mainly bentonite and possibly synthetic zeolites (because of particle size and shape control), to comply with the containment criterion based solely on their ability to minimize groundwater migration either to or away from the waste package.

In Section 4.2, below, there is a discussion of the mechanical property testing which may demonstrate that the packing material complies with the 1000-year containment criterion as specified in 10 CFR 60 and, in particular, a discussion of the testing for failure of the packing material to control groundwater flow into the waste package under specified failure scenarios. (It should be noted that, in principle, radionuclide release from the waste package could occur in the absence of a net flow of water by mechanisms such as diffusion.) The emphasis will be on bentonite packing material.

Finally, it should be noted that our discussion of packing materials is limited to the expandable argillaceous material, bentonite, and synthetic zeolites and how they might perform in a salt or basalt repository environment. This discussion will be extended to a tuff repository environment in future reports.

4.1 Testing for Movement of Water and Radionuclides Through Packing Materials

4.1.1 Radionuclide Containment Based on Groundwater Flow Control

4.1.1.1 Groundwater Flow Control

The design life of packing material can be divided into two periods (PNL-3873, 1981). The first period is one of complete water exclusion. The second period, after saturation of the packing material, is concerned with the movement of water through the packing material. For our purposes, the length of the first period depends on the time required for water to completely saturate the packing material. For a material such as bentonite, saturation refers to the maximum amount of water that can be absorbed for a given compaction density. This is to be distinguished from saturation of the repository. In the case of materials such as bentonite, the time is a complex function of clay properties. On the basis of some rather preliminary information, PNL has estimated that the time required for water to penetrate and saturate 20 cm of bentonite will be on the order of several thousand years (PNL-3873, 1981). During the second period, movement of water through the packing material will be controlled by the hydraulic properties of the materials and by the regional hydraulic gradient. Assuming conservative values for hydraulic conductivity and hydraulic gradient, the time required for a volume of groundwater equal to the volume of a typical HLW container-overpack to contact the container after groundwater finally reaches the container has been estimated to be approximately 1×10^5 years (PNL-3873, 1981).

A. First Period -- Time Required to Saturate Packing Material

Two of the attractive features of bentonite that are used to justify its selection as a candidate packing material are its ability to absorb large quantities of water (up to seven times its dry weight before reaching the liquid limit), and because these clays expand upon hydration, the formation of a low permeability barrier restricts movement through the bentonite to diffusional processes. However, the swelling behavior of bentonite complicates the ability to predict its long-term behavior. This is mainly because of the complex interdependence of swelling pressure with other packing material properties. In the discussion that follows, an attempt will be made to clarify some of the relationships among bentonite properties important to water migration.

A conceptual design for bentonite packing material may be similar to the 12-inch-thick annularly-shaped blocks discussed elsewhere (AESD-TME-3086, 1981). These blocks likely will have been been fabricated by compacting unsaturated clay. In the presence of water, the unsaturated clay will take additional water into the clay interlayers and expand. If the clay is confined (as it will be according to the proposed NRC waste package definition, 10 CFR 60), it will exert a force outward on its containment, known as the swelling pressure. The swelling pressure developed by a montmorillonite clay is a function of several variables including bulk density, water content, temperature, composition of interstitial water, and identity of the exchangeable cation within the clay structure (PNL-3873, 1981). In turn, the hydraulic conductivity (a constant relating fluid discharge rate to an existing hydraulic gradient) is a function of packing material compaction density and, thus, swelling pressure. The basic relationship is that the higher the density, the higher the swelling pressure will be with the result of a lower hydraulic conductivity. Ultimately, low hydraulic conductivity ranges are desired such that, coupled with reasonable regional hydraulic gradients, transport through fully saturated bentonite is diffusion-controlled. However, little information exists about the rate of hydration of confined, compacted bentonite. As explained elsewhere (PNL-3873, 1981), if the packing material can be viewed as a system of hypothetical concentric layers, during the first period of packing material life, groundwater will migrate into the interfacing layer of packing material and the clay in that layer will begin to hydrate and to exert a swelling pressure. Before groundwater can reach the second layer of packing material, it must migrate through the first layer which has at least started the hydration-swelling process and may have largely completed the process. It should be obvious from the discussion above that the determination of the time required to saturate bentonite must be conducted as a function of several variables. It is felt that the migration rate of the hydration process should be controlled by the rate at which water can be forced through previously saturated portions of clay (PNL-3873, 1981). Some initial results from PNL would seem to confirm this hypothesis (PNL-3000-10, 1981).

In reviewing the literature on the performance of bentonite as a candidate packing material under anticipated repository conditions, it became apparent that the data base required to demonstrate 1000-year containment is severely lacking. Furthermore, the number of properties of bentonite that

will require some degree of testing along with the variables (and range of some of them) of which these properties are functions is relatively large. Detailed justification for all the properties and variables that have been identified as important in testing packing material performance would require an effort that is outside the scope of this report. Instead, a brief treatment of the major packing material properties will be given with reference made to pertinent discussions where the data exist.

B. Second Period -- Water Migration After Saturation

After the bentonite packing material has become fully saturated, water movement will be controlled by the hydraulic conductivity of the packing material and the regional hydraulic gradient. Again, because of the propensity of bentonite to swell upon hydration, the hydraulic conductivity may decrease to the point where diffusion may become the principal mechanism of transport through the clay. An hydraulic conductivity of $<10^{-11}$ cm/s for bentonite is necessary in order to achieve diffusion-controlled transport (AESD-TME-3113, 1981). The movement of water through solid media is generally given by Darcy's Law (PNL-3873, 1981). However, the hydraulic conductivity is calculated from the experimentally measured intrinsic permeability (Lohman, S. W., 1972). (Some confusion persists in the literature as concerns the terms and concepts used in hydrology. A brief explanation of hydraulic properties and related terminology is given elsewhere, BNL-NUREG-31049, 1982.) In turn, the permeability is a function of the composition and compaction density (i.e., porosity) of the packing material, temperature, groundwater composition, and hydraulic gradient, among others. There is evidence in the literature that bentonite may exhibit non-Darcian behavior, especially at low hydraulic gradients (Pusch, R., 1979b). Thus, in order to determine the long term behavior of hydraulic properties of the packing material, it will be necessary to measure the permeability at the low hydraulic gradients anticipated in actual repositories (BNL-NUREG-31049, 1982).

4.1.1.2 Testing the Ability of Packing Material to Control Groundwater Migration

The study and performance testing of candidate packing materials have been in progress in the U. S. and abroad for several years. In March 1980, a concerted packing material testing program, sponsored by ONWI, was initiated at PNL (PNL-3000-6, 1980). Part of this program is focused on devising laboratory test procedures to measure packing material performance properties that support and quantify necessary packing material attributes (PNL-3873, 1981). Although the test methods described below are discussed largely in terms of the water flow control performance of bentonite, they are generic enough to be applicable to other candidate packing materials. As noted above, no attempt will be made to provide detailed justification for all the properties and variables (listed in Table 4.2 below) judged important in testing packing materials for 1000-year containment. Rather, the following topics will be discussed in the sections below: (1) methods available for providing information on the most important properties (e.g., permeability, swelling pressure) relevant to groundwater flow control. This discussion will include comments on

Table 4.2 Packing material properties and variables important in testing for 1000-year groundwater flow control.

Packing Material Attribute - Groundwater Flow Control

First Period - Time to Saturation

Packing Material Properties and Variables	Test Method Status		
	Available	Unavailable	Under Development
Compaction Density	X		
• Compaction Pressure	X		
• Water Content	X		
• Packing Material Composition	X		
Swelling Pressure	X		
• Compaction Density	X		
• Water Content	X		
• Water Composition	X		
• Water Eh, pH[b]			
• Identity of Exchangeable Cations	X		
• Hydraulic Gradient[b]			
• Temperature Profile and Gradient[c]			X
• Radiation Treatment[b]			
Rate of Packing Material Hydration	X		
• Compaction Density	X		
• Swelling Pressure	X		
• Hydraulic Conductivity	X		
• Hydraulic Gradient	X		
• Initial Water Content	X		
• Temperature Profile and Gradient[c]		X	
• Rehydration After Thermal Cycling	X		
• Radiation Treatment[b]			
• Packing Material Composition	X		
• Packing Material Thickness	X		

Second Period - Migration After Saturation

Packing Material Properties and Variables	Test Method Status		
	Available	Unavailable	Under Development
Hydraulic Conductivity[a] (Permeability)	X		
• Packing Material Composition	X		
• Compaction Density	X		
• Swelling Pressure	X		
• Water Composition	X		
• Water Eh, pH[b]			
• Hydraulic Gradient	X		
• Temperature Profile and Gradient[c]			X
• Radiation Treatment[b]			
Packing Material Stability			
• Physical and Chemical Characterization	X		
• Thermal Stability (Dry and Hydrothermal Conditions)	X		
• Pressure Effects on Phase Stability	X		
• Water Composition, Eh and pH[d]		X	
• Radiation Treatment	X		
• Wet/Dry Cycling	X		
• Synergistic Interactions		X	

[a] First period also depends on hydraulic conductivity.
[b] Dependence of packing material property on this particular variable is yet to be determined.
[c] Test methods (and their status as listed in the table) for appropriate temperature ranges are available; however, no methods exist that account for temperature gradients.
[d] Unavailable here implies that the Eh and pH ranges that will occur under actual repository conditions, and over which testing should be conducted, are not known with any degree of certainty.

some of the properties being investigated as they pertain to licensing needs; (2) external variables, i.e., repository conditions, and the ranges of interest that have been, or should be, included in designing methods for testing packing material performance; and (3) other considerations important to packing material performance (e.g., thermal conductivity, morphological stability, compatibility with host rock, etc). The status of test methods available, unavailable, or under development for demonstrating 1000-year containment and ranges of some of the variables to be considered in testing are given in Tables 4.2 and 4.3, respectively. By available, we mean that, although certain test methods have been developed by DOE and others, most, if not all, have yet to be subjected to interlaboratory scrutiny for technical community acceptance as, for example, MCC test methods.

Packing material properties, and the variables upon which they depend, identified as important in testing for regulatory compliance based on the ability to control groundwater flow are summarized in Table 4.3. A property important to both time periods of groundwater flow control is hydraulic conductivity, which is a function of compaction density (AESD-TME-3113, Appendix A, 1981). For expandable clays, two variables apparently important to compaction density are: (1) the pressures used to compress granulated powders into blocks, and (2) the initial water content. The structural pattern of bentonite is characterized by aggregates separated by voids regardless of compaction pressure. However, voids become smaller and the aggregates more deformed at higher pressures (Pusch, R., 1981), thus yielding a denser form. The range of compaction pressures that will require investigation will largely be dictated by: (1) the compacted form's ability to maintain its physical shape during emplacement (thus necessitating some mechanical stability testing) and (2) the smear density* required to achieve diffusion-controlled transport. The compaction density is also being investigated as a function of water content of the unpressed clay (PNL-3873, 1981). However, some questions arise concerning the significance of these particular experiments. Firstly, due to the thermal environment that packing material may experience for the first few hundred years (BNL-NUREG-31049, 1982), the water content of the compacted bentonite may be close to zero, regardless of its initial water content. Assuming repository conditions are such that the water in the bentonite exists as a vapor during the thermal period and that this water vapor is contained within the outermost waste package boundary, packing material performance should be examined as a function of rehydration as water returns to the liquid state. Thus, the use of expandable clays with the proper degree of hydration (PNL-3000-9, 1981) as packing material will have to be carefully assessed in any testing program. Secondly, the ability of bentonite to function as a barrier to water intrusion depends on the swelling pressure developed for a given "water-saturated" density. The water content after saturation should not have anything to do with the initial water content unless, for the pressure applied in compacting the bentonite powder, water saturation has been

*The final density of a material such as bentonite after swelling into assembly gaps, fractures, etc.

Table 4.3 Ranges and limits of parameters important in testing packing material for groundwater flow control.

Packing Material Property or Variable	Range or Upper Limit
Compaction Pressure[a]	55-211 MPa
Water Content[b]	0-28 weight percent
Compaction Density[c]	1.8-2.6 g/cm^3
Hydraulic Conductivity	$\leq 10^{-11}$ cm/sec
Swelling Pressure	d
Repository Conditions	**Range or Upper Limit**
Groundwater Composition	e
Groundwater Eh, pH	f
Temperature	30-300°C
γ-Radiation Dose,	10^{10} Rads
Dose Rate	10^6 R/hr
Pressure	$\leq$35 MPa[e]
Hydraulic Gradient[g]	$\leq$1 cm/cm

[a]Range listed is that reported for Na and Ca bentonite (PNL-3873, 1981). Ranges for other candidates will depend on type of material and mechanical stability requirements.

[b]Refers to initial water content; not likely to exceed 10 weight percent for actual designs (AESD-TME-3113, Appendix A, 1981). Range listed is that reported for Na and Ca bentonite.

[c]Lower limit is minimum acceptable value required to achieve diffusion-controlled transport (AESD-TME-3113, Appendix A, 1981). Range listed is for same materials as above.

[d]Maximum swelling pressures are uncertain (PNL-3873, 1981); however, diffusion-controlled transport in bentonite is achieved at a swelling pressure as low as 5 MPa (Dayal, R., 1981).

[e]See reference BNL-NUREG-31049 (1982).

[f]Accurate ranges have yet to be determined for salt and basalt. Ranges that are reported (BNL-NUREG-31049, 1982) have either been calculated from thermodynamic data or measured under unrealistic repository conditions.

[g]For basalt, it is stated that low (<1) hydraulic gradients will exist (PNL-3873, 1981). Firstly, site-specific gradients are still open to question. Secondly, the engineered system will quite likely perturb the host rock gradient in the immediate vicinity of the waste package; how and to what extent is not clear. Because of time constraints, measurements at realistic hydraulic gradients may only be feasible for relatively permeable packing materials. Therefore, present experiments use hydraulic gradients which are several orders of magnitude greater than those likely to be formed in the candidate host rock strata; the applicability of such measurements to repository conditions has not been established.

achieved. This is simple enough to determine experimentally. Test methods for determining compaction density as a function of compaction pressure and water content have been described elsewhere (PNL-3873, 1981). Initial results for sodium and calcium bentonite have been reported for a range of compaction pressures (55-221 MPa) and water content (0-28 weight percent). It has been observed that, at constant compaction pressures, maximum bentonite densities were obtained at 5-8 weight percent water.

PNL has designed and constructed a permeability cell which, coupled with the other components of their water/radionuclide migration system, provides information on packing material hydraulic conductivity, radionuclide retardation, and swelling pressure. The system is also being used to determine the rate of packing material hydration. The system, described in detail elsewhere*, is sufficiently flexible in design to provide the necessary information concerning packing material attributes (listed in Table 4.1) as a function of most of the variables that affect packing material performance. In order to provide permeability data within a reasonable time period, PNL conducts tests at larger hydraulic gradients than would be expected in an actual repository. There is evidence in the literature that, for low permeability materials such as bentonite, fluid flow deviates from Darcy's Law at very low hydraulic gradients. Generally, the groundwater migration through a compacted, hydrated clay will be less than the rate predicted by Darcy's Law. In order to predict the long term behavior of bentonite with any degree of confidence, it is important to know how the hydraulic conductivity varies as a function of gradient. Pusch (1979b) has described an experimental arrangement that measures flow rates through saturated, compacted bentonite as a function of successively reduced hydraulic gradients. The data obtained explicitly showed the dependence of permeability on hydraulic gradient and time. The hydraulic heads used in these experiments were some 40-100 times lower than those reported by PNL (PNL-3873, 1981). Furthermore, PNL reported that hydraulic conductivities were independent of the hydraulic head over the range investigated (Westsik, Jr., J. H., 1981).

Experiments have been initiated (PNL-3000-10, 1981) in order to elucidate the mechanism of clay hydration. Water breakthrough times (what constitutes "breakthrough" was not defined) are being measured for 5-cm by 0.5-, 1.0-, 2.0-, and 3.0-cm bentonite cylinders, 2.1-2.2 g/cm^3 compaction density, 7.5 weight percent initial water content. The most important factors affecting the time required to completely saturate a packing material such as bentonite have been discussed, i.e., the swelling pressure developed upon hydration; the resultant permeability after saturation (a function of swelling pressure which, in turn, depends on compaction density and initial water content); and the hydraulic head in the vicinity of the packing material. Preliminary results indicate that water movement through clay occurs via two mechanisms: (1) Darcian flow and (2) either diffusion or vapor transport (PNL-3000-11, 1981).

*(PNL-3873, 1981; PNL-3000-8, 1981; Westsik, Jr., J. H., 1981)

4.1.1.2.1 Repository Conditions Important in Testing Packing Material Performance

Although a considerable amount of information has been generated concerning the properties and performance of candidate packing materials, not much of it relates directly to anticipated nuclear waste repository conditions. This is especially true of the ability of packing materials to control the flow of groundwater. Part of the present BNL effort is to identify repository conditions that are important in testing waste package performance and the ranges of these parameters that represent the repository environment (BNL-NUREG-31049, 1982). The expected repository conditions and ranges of interest that should be considered in testing packing materials for 1000-year containment via groundwater flow control will be discussed in this section.

The ability of packing material to retain its hydraulic properties during the required time period may be greatly affected by the thermal environment. The packing material will experience a temperature cycle from an initial repository ambient temperature (a low of 34°C reported for salt, BNL-NUREG-31049, 1982) to as high as 250-300°C and then a slow return to ambient as fission products decay and the surrounding host rock cools. Thus, it is important that the temperature dependence of the chemical and physical properties on which packing material attributes are based be known over these temperature ranges. The discussion at hand is concerned with reversible changes in properties resulting from temperature variations as distinguished from temperature induced transformations that affect packing material stability. These effects will be addressed in a later section. Of immediate importance to groundwater flow control is how the rate of water movement through packing material is affected by increased temperatures. The ability to exclude water from the waste form and retard its flow out of the waste package is influenced by temperature because of a decrease in water viscosity, increased diffusion rates, and possible changes in the swelling pressures developed in clay minerals (PNL-3873, 1981; AESD-TME-3113, Appendix A, 1981). Other parameters, important to overall packing material performance, that are affected by temperature variations include thermal conductivity and ion exchange capacity.

Current plans at PNL call for the measurement of hydraulic conductivities (PNL-3000-9, 1981; PNL-3000-11, 1981) and swelling pressure (PNL-3000-11, 1981; PNL-3000-7, 1980) as a function of temperature. Other physical properties that will be studied as a function of temperature (25 to 250°C) include thermal conductivity, specific heat, bearing capacity, and stress/strain relations. A rigid-volume flow cell (PNL-3000-8, 1981) has been designed for temperature measurements from 25 to approximately 150°C. A second permeability meter system, a high temperature stress/strain flow system, has been described that will allow measurement of hydraulic properties up to 250°C under a confining pressure of 250 bars (25 MPa) (PNL-3000-8, 1981). In the results reported to date (PNL-3000-10, 1981; PNL-3000-11, 1981), no mention has been made of determining the rate of water migration through the packing material as a function of temperature. Any systematic elucidation of the mechanism of clay hydration should include temperature dependence. Further-

more, an understanding of the long term performance of packing material, in terms of groundwater flow control, necessitates that water migration rates be known over the temperature ranges of interest. Because of their low thermal conductivity, a significant thermal gradient may exist for several years across a given thickness of packing material such as bentonite. This gradient will change as a function of time and degree of water saturation of bentonite. Such factors will affect the rate of water migration through packing material (AESD-TME-3113, Appendix A, 1981). At this time, we know of no tests that account for the effect of thermal gradients on packing material performance. Finally, there is some concern that water may be irreversibly lost from bentonite at elevated temperatures (AESD-TME-3113, Appendix A, 1981). Initial results of experiments conducted at PNL on bentonite samples that had been held at 100, 200, and 300°C (1 atm) for 60 days indicate that bentonite readily rehydrates when exposed to moisture at room temperature (PNL-3000-11, 1981).

After repository closure, pressure can be developed from the hydraulic head present (basalt case only) and the rock overburden, or lithostatic, pressure. The effect of hydraulic gradient on Darcian flow has been discussed in Section 4.1.1.2. Other concerns over the effect of repository pressure on packing material stem from the thermal stability of some packing material minerals as a function of imposed water pressure and the possibility that swelling pressure may be functionally related to hydraulic pressure. The stability of packing material mineral phases will be discussed in a later section. In the presence of groundwater, confined, compacted bentonite will expand and fill the available pore volume within the clay body. Under high hydraulic gradients, expansion will continue until the swelling pressure is balanced by forces opposing collapse, including the applied water pressure. However, it has recently been reported that swelling pressure and hydraulic pressure may be additive (AESD-TME-3113, Appendix A, 1981). Given that swelling pressures as high as 20-30 MPa have been measured in the laboratory for bentonite (PNL-3873, 1981), this observation is of great concern if the waste package design pressure limit is 11 MPa (hydrostatic pressure at 1100 m, BNL-NUREG-31049, 1982) for basalt (AESD-TME-3113, Section 5, 1981). Much work remains to be done in this area, especially as concerns how temperature and time affect pressures, and whether or not swelling pressure is functionally related to hydraulic pressure (AESD-TME-3113, Appendix A, 1981).

The swelling pressure of bentonite is largely governed by the ionic strength and cationic charge of the electrolyte between the montmorillonite platelets (PNL-3873, 1981). This being the case, it is important that the hydraulic properties of expandable clay materials be investigated as a function of groundwater compositions. Compositions and ranges for salt and basalt groundwater are given elsewhere (BNL-NUREG-31049, 1982). The presence of impurity cations in groundwater can affect the chemistry of bentonite and, hence, some properties such as swelling pressure, to some degree. A discussion of the effect of type and quantity of adsorbed cation on the swelling volume of montmorillonite is given elsewhere (Dayal, R., 1981). While it is apparent that the redox status of the aqueous system (given by pE, pH) can affect the stability of candidate packing materials (see discussion below), it is not clear how or if the hydraulic properties of packing material function-

ally and reversibly depend on groundwater Eh and pH. Groundwaters used in testing packing material properties that contribute to groundwater flow control should account for the pH and Eh excursions that might occur as a result of the hydrothermal and radiation environments that will exist under oxic and anoxic conditions.

4.1.1.2.2. Factors Important to Packing Material Stability

A study of the hydraulic properties of candidate packing materials will be precluded if such materials undergo degradation under repository environmental conditions resulting in significant compromise of groundwater flow control attributes. Several factors may affect the chemical stability of packing materials in a nuclear waste repository, including temperature, pressure, hydrothermal conditions, groundwater composition, Eh and pH, and the radiation field associated with high level waste. How packing material stability may be affected by these repository conditions and the status of stability testing is discussed in this section.

Prior to subjecting candidate materials to simulated repository conditions, physical and chemical characteristics should be firmly established. Current efforts at PNL (PNL-3000-10, 1981) concerning material characterization include X-ray diffraction, differential thermal analysis (DTA), and chemical analysis. Changes in the chemistry, morphology, and crystallinity of solid phases will be detected by the techniques of electron microscopy (PNL-3873, 1981). Initial DTA scans of sodium and calcium bentonite indicate that kinetic effects can strongly influence water loss behavior (PNL-3000-10, 1981), thus precluding the use of existing published DTA curves for predicting water loss behavior for these materials. The point here is that, while a sizable amount of information on the physical and chemical characteristics of some candidate packing materials exists in the literature, a certain amount of reinvestigation may be required in order to establish acceptable "baseline" data.

Most of the candidate packing materials should be inherently stable at the elevated temperatures anticipated in salt and basalt repositories in an unconstrained atmosphere. However, some concern has been expressed over the long term thermal stability of bentonite (AESD-TME-3113, Appendix A, 1981). After absorbed and interlayer water is driven off at temperatures $\leq 300^{o}C$, impurity cations such as Ca^{2+}, Mg^{2+}, and K^{+} present in and around the clay may occupy preferred positions in the bentonite lattice, resulting in irreversible structural changes. Diagenetic clay alteration has been reported to occur at temperatures as low as $40^{o}C$ (Dayal, R., 1981). Also, the thermal stability of mixtures of packing materials is not well documented. Dry heating (up to $250^{o}C$) experiments are currently under way for several candidate packing materials and mixtures (PNL-3000-10, 1981). Alteration of solid phases will be determined using petrographic microscopy, X-ray diffraction, and scanning electron microscopy techniques.

Many of the mineral phases of candidate packing materials have limited stability at elevated temperatures and, because many are hydrated, thermal

stability limits vary as a function of imposed water pressure (<100 MPa) (PNL-3873, 1981). The direction of the PNL testing program on packing material stability is to set upper limits on the amount of packing material degradation that is acceptable over the required containment period under repository conditions rather than attempting to establish thermodynamic stabilities (PNL-3873, 1981; PNL-3000-9, 1981). This will be accomplished via a testing program that consists of accelerated tests at higher temperatures (up to 400°C) and long term (at least several years duration)(PNL-3000-9, 1981) tests at anticipated repository temperatures. Part of the PNL stability testing will consist of hydrothermal treatment of packing material samples (PNL-3000-7, 1981). High temperature, pressurized autoclaves will be used that allow for fluid sampling during the test duration. Test parameters will include time (1 to 12 months), temperature (up to 250°C), pressure (30 MPa), packing material composition, and groundwater composition (to include a basalt and a granite composition and a WIPP site brine). Low pressure (~10 MPa) data for determining pressure effects on phase stability will be collected from tests conducted in Parr bombs under saturated steam pressure (PNL-3000-9, 1981). After hydrothermal treatment, the aqueous fluids will be analyzed for major cations, anions, pH, and Eh. Reacted materials will be characterized by petrographic microscopy, X-ray diffraction, scanning electron microscopy, electron probe analysis, and bulk chemical analysis.

Packing material stability can be affected by groundwater composition, Eh and pH. The effect of these parameters on stability has been discussed elsewhere and will not be treated in any detail here (PNL-3873, 1981; AESD-TME-3113, Appendix A, 1981; Dayal, R., 1981). Briefly, groundwater composition may be important in packing material mineral alteration. However, little is known about the rate and extent of chemical alteration of candidate packing materials in the presence of anticipated groundwaters and other expected repository conditions. It is also not known if or how such alteration will affect packing material properties. The PNL hydrothermal testing program should provide answers to some of these questions. Groundwater pH strongly affects the solubilities of both silicon and aluminum and is a major determinant of the stability of silicate phases (PNL-3873, 1981). The redox status of aqueous systems is given by Eh, and is a measure of the electric potential necessary to cause oxidation or reduction of a material or dissolved species. Equilibrium Eh is determined by several factors, including oxygen fugacity (construct to express the free energy of a real gas). Thus, the prevailing Eh of a system determines the stable oxidation state of polyvalent elements, (RHO-BWI-ST-7, 1980) and could affect the stability of certain mineral phases. Ample information exists in the literature on mineral stability in terms of redox potential and pH (PNL-3873, 1981). However, what is not known with any degree of certainty are the ranges of Eh and pH that will occur under repository conditions. Field measurements of Eh are extremely difficult (PNL-3873, 1981; RHO-BWI-ST-7, 1980); therefore, it is normally calculated from thermodynamic data. In these calculations for basalt, it is assumed that iron-bearing minerals in the rock control oxygen fugacity (RHO-BWI-ST-7, 1980). Thus, the rate at which the repository environment returns to equilibrium anoxic conditions is not known. The period during which oxidizing conditions prevail is important to canister/overpack corrosion. Several factors can also affect the

prevailing groundwater pH, e.g., temperature, flow rate, water:rock ratio, and radiation field. As part of their packing material stability testing program, PNL intends to monitor the Eh and pH of fluids used in hydrothermal experiments. This program will include measurements as a function of radiation environment (see below). Additional testing should address how Eh and pH are affected by the presence of other waste package components (e.g., borosilicate glass) and host rock, and by the possible generation of corrosion and/or radiolysis products.

One repository parameter that was not included in the discussion in Section 4.1.2.1 was the radiation dose associated with the high level waste. This is because effects due to radiation appear to be more directly related to chemical stability than hydraulic properties of packing material. A discussion of the radiation stability of packing materials is given elsewhere (PNL-3873, 1981; BNL-NUREG-51458, 1982). Briefly, effects due to gamma radiation (up to 10^{10} R) can manifest themselves in essentially two ways: (1) structural damage or loss of crystallinity, including radiolysis of structural water, and (2) radiolysis of water and dissolved species which may affect the Eh and pH of the aqueous phase within the packing material and surrounding host rock (PNL-3873, 1981). The magnitude of radiolysis effects is a function of radiation dose and dose rate, temperature, water chemistry, and mobility of radiolysis products. At this time, little is known about the radiation stability of candidate packing materials. Present plans call for exposure of samples to ^{60}Co gamma radiation in dry and aqueous environments (PNL-3000-7, 1980). Synergistic effects due to elevated temperatures were not explicitly addressed but should be included in the radiation testing. Solid phase characterization and aqueous fluid analyses will be conducted using the same techniques described above for the thermal stability tests.

4.1.1.2.3 Additional Considerations Regarding Packing Material Performance

In this section are listed some other factors that should be, or are being, considered in testing the ability of packing material to control groundwater flow for 1000 years. Discussions of how these factors affect packing material performance and test methods available that account for them are detailed elsewhere. Reference to the literature will be made, where appropriate.

1. The thermal conductivity of the packing material is important because it is largely responsible for the overall temperature of the waste package (PNL-3873, 1981; AESD-TME-3113, Appendix A, 1971; BNL-NUREG-31049, 1982). The thermal history of the waste package is important to both the stability and performance of the packing material. Current plans at PNL include the measurement of thermal conductivity as a function of water content and compaction density (PNL-3000-7, 1980).

2. During the thermal period of high level waste disposal, the packing material may be exposed to several wet/dry cycles. Such cycling could result in cracks or fissures, thus affecting groundwater flow

control (Dayal, R., 1981; Sethi, A. J., 1981). Other effects that may result from wet/dry cycling are anisotropic swelling and separation of multi-component (e.g., bentonite/sand) packing material mixtures (Beall, G. W., 1981; Davis, M. S., 1982). While some data and test methods have been reported (Sethi, A. J., 1981) that address wet/dry cycling, such considerations are not part of any comprehensive packing material testing program.

3. Packing material performance and/or stability may be affected due to synergistic interactions among waste package components or between the packing material and host rock under repository conditions. Such interactions have been addressed elsewhere (AESD-TME-3086, 1981). The type of testing that is required would be similar to the whole package testing schemes that have been designed to evaluate the effect of synergistic interactions on the chemical durability of certain nuclear waste forms (BNL-NUREG-51458, 1982). Studies of the interaction of candidate packing materials with several simulated nuclear waste solids under hydrothermal conditions have been initiated (Sasaki, N., 1981). Initial results indicate that reactions of packing materials with simulated wastes can immobilize certain radionuclides by forming new phases.

4.1.2 Single Component (Packing Material) Compliance With 1000-Year Containment Based on Radionuclide Retardation

The discussion of the properties of synthetic zeolites with respect to their use as packing material and their potential as a single component to comply with 1000-year containment is similar to that for bentonite, although the mechanisms involved may be somewhat different. For example, synthetic zeolites differ from bentonite in that they lack its high degree of plasticity and positive swelling pressure upon hydration. In many cases, however, they display superior retardation factors (or distribution coefficients, K_d's)* for radionuclides such as Cs or Sr as compared to bentonite. Some synthetic zeolites may also display superior resistance to wet/dry cycling or hydrothermal conditions that may occur in nuclear waste repositories**. Although synthetic zeolites may differ greatly with respect to stability towards dehydration/rehydration cycles at elevated temperatures, we will assume for the rest of the discussion that only synthetic zeolites with high silica content such as mordenite or clinoptilolite, which demonstrate good thermal stability, are under discussion. Synthetic zeolites, like bentonite, will not effectively absorb anionic radionuclide species such as TcO_4^- and I^-, although it has been suggested that special zeolites such as lead or silver zeolites might serve this purpose (BNL-NUREG-51458, 1982; Strickert, R., 1980).

---

* (PNL-3873, 1981; PNL-3000-6, 1980; Westsik, Jr., J. H., 1981; PNL-3000-7, 1980; BNL-NUREG-51458, Vol. 1, Vol. 4, 1982; Ahn, T. M., 1980; Breck, D. W., 1974; Barrer, R. M., 1978; Neretnieks, I, 1977; Komarneni, S., 1980).

**(Coombs, D. S., 1959; Jacobsson, A., 1977; Komarneni, S., 1981, 1982.)

4.1.2.1 Retardation of Selected Chemical Species

Initially, the dehydrated zeolite will retard the motion of groundwater by sorption. Subsequently, the zeolite will slow the movement of the groundwater by its relatively low permeability. Obviously, the "effective" permeability will be a function of the form and compaction density of the zeolite or mixture of zeolites used. It has been suggested (BNL-NUREG-51458, Vol. 1, Vol. 4, 1982; Ahn, T. M., 1980) that an advantage of using synthetic zeolites rather than natural zeolites or bentonite is that they are available in varying sizes and shapes and can be made with very uniform size distribution so that, with careful selection of sizes and shapes, the hydrological properties could be adjusted in a controlled and predictable fashion. Although the permeability could be relatively low, it will not be effectively "zero" on hydration as may be the case with bentonite. Consequently, the rationale for using zeolites as opposed to bentonite lies primarily in their superior retardation factors (BNL-NUREG-51458, Vol. 1, Vol. 4, 1982; Ahn, T. M., 1980) for selected radionuclides. As stated in a previous report (Ahn, T. M., 1980), synthetic zeolites could independently achieve 1000-year containment based on their sorption properties for a number of the important radionuclides (but not all). Better analytical testing data for distribution coefficients or retardation factors are needed as will be discussed in the next section.

Although other physical properties of zeolites such as mechanical strength or thermal conductivity (which, in turn, depends on moisture content) may enter into design considerations, they have been dealt with elsewhere*. Properties of typical zeolites along with other packing materials, have been extensively discussed in the references already listed in this section. Much of the previous work dealt with zeolites as a component in a multicomponent packing material system and, hence, also is not relevant to the present discussion.

4.1.2.2 Testing the Ability of Packing Material to Retard the Migration of Selected Chemical Species

This section of the report will deal with analytical testing methods for distribution coefficients and retardation factors of selected packing materials, bentonite and synthetic zeolites. Some of these methods are already in existence and have been applied to packing materials. Others could be used with slight modifications. These methods will be referenced and briefly discussed. In almost all cases, these methods have not been tested over the full range of hydrothermal and dynamic environments corresponding to the possible ranges of conditions in deep nuclear waste repositories in basalt or salt. These methods have been discussed in the references previously listed in this section and in further references from Sandia (SAND81-0277A, 1981; SAND81-1377C, 1981; SAND79-1109, 1980). The experimental modifications involved will not be discussed in any detail, but should be kept in mind by the informed reader. For other properties, satisfactory methods for these packing materials

*(BNL-NUREG-51458, Vol. 1, Vol. 4, 1982; Ahn, T. M., 1980; Jacobsson, A., 1977; Radhakrishna, H. S., 1981).

may not exist and may represent licensing information needs for NRC. In these cases, the variables will be mentioned and some of the important conditions and requirements that should be addressed when designing the tests will be referred to briefly.

Unless stated otherwise, it will be assumed that the same test method for a selected property can be applied to both bentonite and selected synthetic zeolites, although the ranges of testing and minor experimental conditions may be different. If a test method or variable is applicable to only one packing material, this limitation will be stated. In other cases, more than one test method may be required to cover adequately the full range of conditions to be expected in a nuclear waste repository. Each property of interest will be defined along with related variables and conditions affecting this property before discussing specific analytical test methods.

4.1.2.2.1 Sorption and its Measurement

Sorption represents the primary means by which radionuclide transport is retarded in a zeolite packing material (BNL-NUREG-51458, Vol. 1, Vol. 4, 1982; Ahn, T. M., 1980) and is an important mechanism in bentonite, though secondary to diffusion*. Sorption is usually interpreted as being due to reversible mechanisms such as ion-exchange and surface adsorption; however, irreversible processes such as precipitation and fixation also occur but normally are not experimentally determined. Not all chemical reactions serve to retard radionuclide migration. Highly soluble radionuclide complexes with inorganic ligands or radiocolloid formation may actually accelerate migration. Retardation mechanisms are functions of many factors including, but not necessarily limited to, the following: temperature, groundwater concentration and composition, solid-solute ratios, pH, Eh, radionuclides and their concentrations, surface area, cation exchange capacity, particulates and complexing agents present, and equilibration time or groundwater flow rates.

Laboratory tests usually measure distribution ratios, R_d, for a specific chemical species in order to estimate the degree to which a chemical species migrating through a material will be removed from the solution by the material. Assuming that equilibrium conditions prevail for mass transport, $R_d \simeq K_d$, where K_d is called the distribution coefficient:**

* (PNL-3000-6, 7, 1980; PNL-2872, 1979; PNL-3349, 1979; SAND81-0277A, 1981)

**If true chemical equilibrium is obtained, R_d and K_d are the same thing. Although K_d implies an equilibrium condition for reactions which may not be realistic because of time dependence or kinetics of specific reactions or because of irreversible reactions, the terms are often used interchangeably. However, R_d is the actual property that is measured in a laboratory test and K_d is the theoretical construct on which it is based. Although R_d may approach K_d very closely, for all practical purposes, in a well-designed experiment and since true chemical equilibrium cannot be guaranteed, R_d is a more accurate term. The use of R_d in sorption experiments has also been addressed elsewhere (Westsik, Jr., J. H., 1981).

$$R_d \simeq K_d = \frac{\text{mass of solute in or on solid phase per unit mass of solid phase}}{\text{concentration of solute in solution}} \text{ (units} = \frac{mL}{g})$$

In Sandia reports (SAND81-0277A, 1981; SAND81-1377C, 1981; SAND79-1109, 1980) Nowak has calculated that candidate packing materials such as bentonite in a 1-ft-thick barrier can delay by 10^4 to 10^5 years the breakthrough of transuranics (assuming K_d's for these materials = 9000 mL/g) and by 10^3 years major cationic (but not anionic) fission products (assuming K_d's = 200 mL/g). Breakthrough was defined by Nowak as the appearance of a migrating species at approximately 1% of its initial concentration. Both delay periods would approach NRC's 1000-year containment criterion. These delays can be achieved provided that: (1) the K_d's are at least as high as indicated; (2) the interstitial groundwater velocity through the barrier is = 1 ft/yr; (3) the effective porosity of the packing material is ≤ 0.1; and (4) no channels or cracks develop in the packing material. Both bentonite and synthetic zeolites have the potential to meet these criteria except that, as previously stated, other getters might be needed for anions or for Sr^{+2} in the presence of concentrated brines. In the case of bentonite, there is a possibility of cracks forming from wet/dry cycling scenarios.

A. Static Methods

Static methods used to measure K_d or R_d by a batch method (PNL-3349, 1980; PNL-2872, 1979; PNL-SA-7928, 1979) apply to specific radionuclides and specific sets of laboratory conditions and assume that equilibration times are sufficiently long to attain a steady state. A high K_d value implies low rates of radionuclide migration relative to groundwater flow rates. A standard ASTM method (ASTM D 18, 1982) for determination of distribution ratios by the short term batch method is now under development. In batch testing, concentrations of the radionuclide in solid and liquid phases which are in contact with each other are measured by appropriate analytical instrumentation. In addition to the limitation that effects due to hydrologic flow are not examined in static batch K_d methods, the solution-to-solid ratio is also higher than the in situ case. Since only the total concentration of each radionuclide is usually determined, the concentrations of the separate oxidation states are not known. These concentrations are needed in order to predict the behavior of multiple oxidation state radionuclides in the packing material. In some cases, behavior of separate oxidation states may be studied in appropriately buffered systems such that one radionuclide oxidation state predominates. Static experiments have the least error where sorption of the radionuclide from solution is neither very high nor very low; consequently, batch K_d experiments are most useful for K_d values between 1.25 and 400 mL/g (PNL-3349, 1980). Despite their limitations, static measurements, because of their relatively low cost and simpler procedures, remain useful for screening purposes.

Recent reports (BNL-NUREG-51458, Vol. 1, 1982; PNL-3349, 1980) list proposed standard batch K_d procedures and discuss factors affecting retardation

of radionuclide migration, variables to be considered when setting up the experiments and possible sources of error. The static method would utilize a suspension of packing material to be evaluated in groundwater that is spiked with one or more radionuclides. It is necessary to provide continuous agitation of the suspension prior to sampling and analysis. One serious source of error leading to unrealistically high K_d values may be container wall adsorption of radionuclides such as Pu or Am; however, this may be corrected by appropriate experimental design.

B. Dynamic Methods

A strictly empirical approach to packing material testing can be taken by dynamic or flow-through methods using continuous imput, pulsed input, or thin-layer chromatography. The column flow-through method as applied to both continuous and pulsed input was discussed in a previous report (BNL-NUREG-51458, Vol 1, 1982) based on work by Relyea and others (PNL-3349, 1980; PNL-2872, 1979; PNL-SA-7928, 1979) and other researchers (LA-8088-PR, 1980; BNL-NUREG-51315, 1981; SAND79-2468, 1980). From such measurements, the retardation factor, R_F, of a packing material/radionuclide system can be determined. This factor is given by $R_F = V_w/V_n$, where V_w is the water velocity and V_n is the radionuclide velocity through the packing material. If ideal chromatographic sorption behavior is assumed, K_d and R_F can be related by a single expression (PNL-3349, 1980):

$$R_F = 1 + \frac{\rho_b K_d}{\varepsilon}$$

where ρ_b (g/cm^3) is the bulk density and ε the effective porosity of the packing material. Thus, if there is no radionuclide sorption, $K_d = 0$ and $R_F = 1$, and the radionuclide migrates at the same velocity as the groundwater. The effective porosity which, due to isolated or dead-end pores, is less than the bulk porosity can be calculated by dividing the volume corresponding to peak breakthrough of some nonsorbing tracer (such as tritium) by the column volume. Controversy exists with respect to the non-sorbing nature of tracers such as tritium, ^{22}Na, and anions used to estimate groundwater velocity through the packing material since sources of error (loss, chemical reaction, or sorption) may exist which would retard the tracers relative to the groundwater. Unfortunately, dynamic tests, while more realistic in estimating retardation factors relevant to repository conditions, are much more complex and thus subject to many sources of error (PNL-3349, 1980; LA-8088-PR, 1980; BNL-NUREG-51315, 1981; SAND79-2468, 1980) and as yet no standard, generally accepted, methods have been devised. However, some preliminary tests can be referenced (BNL-NUREG-51458, Vol. 1, 1982; PNL-3349, 1980).

Some comparisons of batch and column methods (e.g., Meyer and others (PNL-SA-6957, 1977) for Cs^+ on Na^+-saturated montmorillonite) indicated that similar K_d values were obtained. Other experiments indicated that the two methods are not always equivalent, with batch K_d's generally, but not always, larger. For relatively soft materials, such as bentonite, batch and

column methods are more likely to agree since this packing material is not affected by the grinding agitation in the batch method. According to Relyea (PNL-3349, 1980), with harder materials, agitation of the slurry during a batch test may actually grind rock particles and cause their dissolution, resulting in the formation of new minerals with more surface area or higher sorptive capacity, and the introduction of competing ions into the solution.

4.1.2.2.2 Factors Requiring Consideration in Experiment Design

As noted elsewhere (PNL-3873, 1981; PNL-3349, 1980), dynamic column flow experiments must be designed to minimize wall effects and to seal column edges to prevent fluid channelling along the walls. Given the highly sorptive nature of some radionuclides and the very low flow rates which must be investigated (10^{-8} cm/sec), accelerated tests using faster flow rates are often required and series of separate tests must be performed to make sure that the retardation capacity of the column is independent of flow rate over the range to be investigated.

Variables such as pH and Eh must be carefully controlled and experiments carried out over an appropriate range of these and other previously listed variables. To control Eh properly, it will be necessary to conduct experiments under controlled atmospheric (nitrogen or argon) conditions. To simulate likely nuclear waste repository hydrothermal conditions, temperature and pressure effects must also be studied. Although it is known that sorption properties of packing material are affected by changes in temperature in a complex way, so far, few direct measurements have been made on packing materials at elevated temperatures and standard methods do not yet exist for doing so. Temperature studies remain to be carried out for radionuclides and the packing materials of interest over a range of realistic repository and groundwater conditions.

Existing experimental data indicate that some important radionuclides such as ^{129}I, ^{99}Tc, ^{237}Np, and ^{226}Ra are not well sorbed on bentonite (BNL-NUREG-51458, 1982; Strickert, R., 1980; PNL-SA-6957, 1977; Allard, B., 1977). Although zeolites can, to some degree, be tailored to fit the radionuclide to be sorbed, evidence indicates that anionic species will also not be well sorbed by zeolites unless unusual (Pb or Ag) cation species are used. Komarneni and Roy (1980) and Neretnieks (1977) have studied the sorption capacity of both natural and synthetic zeolites from the perspective of their use as packing material in a nuclear waste repository using the batch sorption method. For Cs^{+}, Sr^{+2}, Ba^{+2}, and Rb^{+2}, the sorption of 95 to 99% of the ions in solution was achieved by natural zeolites. Because of their greater uniformity in pore size, the synthetic zeolites tested did not perform as well overall. This handicap could be surmounted by use of appropriate mixtures. Neretnieks (as quoted in PNL-3000-6, 1980) tested the sorption of Eu^{+3}. Since it was adsorbed well by all the zeolites tested, it was inferred that Am^{+3} would also be adsorbed efficiently. Data obtained under oxic conditions should not be considered representative of the sorptive behavior for the actinides (because of their complex solution chemistry and

multiple oxidation states), especially for the TRU elements in the repository environment after return to anoxic conditions. Therefore, data are needed over the full range from oxic to completely anoxic.

When considering a sorbent for use in a nuclear waste repository as packing material, it is important to consider the fixation properties of the sorbent (e.g., its ability to prevent radionuclides from desorbing) as well as its sorptive capacity. Clays such as bentonite appear to sorb reversibly without fixing any of the radionuclides permanently. Komarneni and Roy (1980) found that selected mixtures of zeolites could show excellent fixing as well as sorptive capacities for four radionuclides: Cs^{+}, Sr^{+2}, Ba^{+2}, and Rb^{+2}.

In packing materials with very low hydraulic conductivities such as bentonite, transport through the packing material may be essentially by diffusion. Because of the very slow flow rates and radionuclide transport rates, accelerated tests must be devised. However, it may be difficult to prove that they can be extrapolated to represent the real conditions. Where the radionuclide migration could be expected to be very small, a special technique such as that developed by S. Fried (1980) (sectioning with a refrigerated microtome) could be utilized. The diffusion characteristics and related radionuclide retardation factors for highly compressed clays are not well known (PNL-3000-6, 7, 1980; SAND81-0277A, 1981; SAND81-1377C, 1981; SAND79-1109, 1980). It may be that, for bentonite, K_d's as measured in slurries are largely irrelevant given a high degree of clay compaction.

Mathematical modeling by mass-balance equations was used by authors such as Nowak (SAND81-0277A, 1981; SAND79-1109, 1980) (for bentonite) and Ahn, Wilke, and Dayal (BNL-NUREG-51458, Vol. 4, 1982) (for zeolite)* to model both transport and retardation processes involved in radionuclide migration. The results of the calculations by Ahn and others (1980) indicated that a 3-ft-thick bed of synthetic zeolite packing material would provide total containment of activity released continuously from a 208-L glass monolith for a period of up to 1000 years. Such estimations must be employed very cautiously, since simplifying assumptions must be made and possible synergistic effects as well as practical engineering problems must be considered. For example, Ahn and others (1980), did not consider effects of radiation and thermal stability and did not address retention of long lived anionic species. The main purpose of such a calculation is that it indicates what systems are worthy of further experimental testing under realistic repository conditions. In any case, better data relevant to repository conditions are required to make such calculations more meaningful.

4.1.3 Summary and Conclusions

The question of whether packing material can alone be given full credit for 1000-year containment of all radionuclides has been addressed. The

*"Evaluation of Synthetic Zeolites as Backfill in a HLW Repository," T. M. Ahn, R. Dayal and R. J. Wilke, Appendix to a Letter from D. G. Schweitzer, BNL, to E. A. Wick, NRC, dated September 12, 1980.

approach taken in evaluating the status of the ability of packing materials to comply with the proposed containment criterion can be summarized as follows: (1) Attributes most important to testing to demonstrate 1000-year containment were identified; (2) experimentally measurable properties associated with these attributes were evaluated to determine those that should be included in testing for compliance; and (3) test methods that provide the necessary licensing information and the status of their development were discussed. For the purpose of this report, only two candidate packing materials were discussed, bentonite and synthetic zeolites.

The two most important attributes that a packing material should possess in order to demonstrate compliance with the containment criterion are groundwater flow control and retardation of radionuclide migration. While bentonite and synthetic zeolites possess both attributes to some degree, compliance with the containment criterion by bentonite is most likely to be achieved via groundwater flow control because of the propensity of this material to swell upon hydration and form a low permeability barrier. Under such conditions, movement of radionuclides and common groundwater ions may be diffusion controlled. Synthetic zeolites, on the other hand, display superior ion-exchange capabilities for selected radionuclides. Based on existing data, it has been determined that a 3-ft-thick bed of synthetic zeolites may provide total containment of the activity released from a 208-L glass monolith (Ahn, T. M., 1980). From our review of available information, however, it was determined that not much of the data on the performance and properties of candidate packing materials relate directly to anticipated nuclear waste repository conditions. Thus, the behavior of packing materials in a repository environment is only speculative at this time. Our conclusions regarding compliance of candidate packing materials with the containment criterion and the status of test development are summarized below.

4.1.3.1 General Conclusions

- Packing material properties and performance have not been tested under the range of conditions expected in a repository. For this reason, full credit for 1000-year containment of all radionuclides cannot be given to packing material at this time.

- Although some test methods are available for quantifying the important packing material attributes, no standard, generally accepted methods appear to exist or be in use within the technical community. Some degree of test methodology standardization (e.g., an MCC-type approach) and interlaboratory data generation and statistical comparison seem essential.

- A specific definition of packing material and/or a description of its intended functions are not available at this time (10 CFR 60). Such design-specific information is essential in formulating appropriate test methods and establishing primary packing material attributes. Whether or not packing material can fulfill some of the functions identified in this report will depend on this information.

4.1.3.2 Specific Conclusions

- From a groundwater flow control point of view, the design life of packing material can be divided into two time periods: (1) The time required to completely saturate the material and (2) the time for water to migrate through the packing material after saturation.

- Because of the swelling behavior of bentonite upon hydration and the complex interdependence of swelling pressure with other packing material properties, the first time period is a complex function of clay properties. In order to predict the long term behavior of expandable clays, more extensive testing is required to address these properties and the variables upon which they depend. The situation will probably be less complicated for non-expanding materials such as synthetic zeolites.

- Little information exists on the rate of hydration of confined, compacted bentonite under repository conditions. However, the most important packing material properties that should be considered in determining this rate have been identified: swelling pressure, the resultant permeability after saturation, and the regional hydraulic gradient.

- After saturation, groundwater flow through a material such as bentonite will depend on the hydraulic conductivity through the material. For fully saturated bentonite, diffusion-controlled transport will dominate if the hydraulic conductivity is $<10^{-11}$ cm/s. Otherwise, fluid flow should be given by Darcy's Law. However, there is some evidence that compacted bentonite may exhibit non-Darcian behavior at low hydraulic gradients. Thus, prediction of the long term behavior of fluid motion through saturated bentonite will require elucidation of the principal mode(s) of transport (Darcian, non-Darcian, or diffusion), and determination of diffusion rates for radionuclides and groundwater ions and the functional dependence of hydraulic conductivity on hydraulic gradient.

- The compaction density of bentonite is important to both time periods of groundwater flow control. In turn, the compaction density is a function of water content. However, because of the anticipated repository thermal environment and the swelling pressure developed upon saturation, the significance of experiments that address the degree of clay hydration (PNL-3000-9, 1981) should be carefully re-evaluated. This is a specific instance in which site-specific and design-specific information would be useful in dictating experimental scope and direction.

- As far as testing of packing material performance under anticipated repository conditions is concerned, a significant information gap exists. Some examples are as follows: (1) how the rate of water

movement through packing material is affected by increased temperatures is not known; (2) the effect of thermal gradients across a given packing material thickness on packing material performance is not known or considered in any proposed testing programs; (3) the functional dependence of swelling pressure on hydraulic pressure has yet to be determined. Such an investigation should also address how temperature and time affect pressures; (4) the hydraulic properties of a material such as bentonite are strong functions of groundwater composition. Testing of packing material performance must include the full range of constituents that may comprise the groundwater chemistry, accounting for radiolysis and corrosion products; and (5) it has yet to be determined how or if the hydraulic properties of packing material functionally and reversibly depend on groundwater Eh and pH. Groundwaters used in testing packing material properties that contribute to groundwater flow control should account for the pH and Eh excursions that might occur as a result of the hydrothermal and radiation environments that will exist under oxic and anoxic conditions.

- Several questions remain to be answered concerning the stability of candidate packing materials under anticipated repository conditions. Some of the factors that should be addressed in establishing packing material stability include: (1) The physical and chemical characteristics of the material, e.g., these characteristics can vary from lot to lot for bentonite (AESD-TME-3086, 1981), (2) the long term thermal stability of bentonite, synthetic zeolites, and multi-component mixtures has yet to be determined. Testing must be conducted under both dry and hydrothermal conditions in order to establish stability limits as a function of imposed water pressure; (3) little is known about the rate and extent of chemical alteration of candidate packing materials in the presence of anticipated groundwater compositions. It is also not known if or how such alteration will affect packing material properties and performance; (4) groundwater Eh and pH can affect packing material stability; however, the ranges of these parameters that will occur under repository conditions are not known with any degree of certainty; (5) much work remains to be done in the area of radiation stability of packing materials (BNL-NUREG-30631, 1981; BNL-NUREG-28682, 1980). Possible synergistic effects due to elevated temperatures and groundwater radiolysis should be accounted for in the radiation testing; and (6) while some data are available on the effect of wet/dry cycling on packing material stability, such considerations are not part of any comprehensive testing program.

- Although the basic approach for testing such variables as retardation factors seems appropriate, few if any tests have been made under the full range of realistic repository conditions, i.e., flow rates, hydrothermal conditions, radiation field, anoxic conditions, etc.

- Candidate packing materials (synthetic zeolites and bentonite) should be tested for their radionuclide retardation properties (see Table 4.4) for all the radionuclides of interest during the first 1000 years

Table 4.4 Packing material properties and variables important for testing radionuclide retardation.

Packing Material Property and Variables	Test Method Status			Interlaboratory Testing	Remarks
	Available	Unavailable	Under Development		
Distribution Coefficient (K_d) or Distribution Ratio (R_d)	X			Preliminary	ASTM Draft methods (ASTM D 18, 1982) ready to be tested in interlaboratory comparison. PNL Relyea method** has been tested in preliminary interlaboratory comparison.
• Temperature	X				
• Groundwater Concentration and Composition	X				
• pH	X				
• Eh			X*		Must be tested over range from oxic to completely anoxic conditions.
• Solid Composition	X				
• Packing Material Surface Area	X				
• Solid-Solution Ratio	X				
• Radionuclide Concentration	X				Must be tested for each radionuclide over range of concentrations. Must also be tested for radionuclide mixtures.
• Equilibration Time	X				
• Corrosion Products			X		
• Radiation Effects			X		BNL***
Retardation Factor (R_f)			X	Not ready for testing as standard method	Still preliminary state of testing, not ready for consideration as standard method, suitable for interlaboratory testing according to Relyea** and Ahn****.
• Groundwater Flow Rate Substituted for Equilibration Time	X				
• Other Variables (same as K_d)		See above for K_d			

* (Hirschfeld, T., 1982)
** (PNL-3349, 1980; PNL-2872, 1979; PNL-SA-7928, 1979)
*** (BNL-NUREG-30631, 1981; BNL-NUREG-28682, 1980)
****(BNL-NUREG-51458, Vol. 4, 1982)

under realistic conditions to be expected in a basalt or salt repository (see Table 4.3). It is especially important that measurements be performed under appropriate conditions of temperature, pressure, pH, chemical composition and under controlled atmospheres which can vary from oxic to completely anoxic conditions.

- Radionuclide retardation tests should include, but not be limited to, static tests to determine R_d's for screening purposes. These tests require use of appropriately spiked* solid samples of packing material in contact with groundwater under realistic chemical and thermal conditions with continuous agitation. It is important to continue sampling until the process of equilibration** is completed within experimental error.

- Dynamic column flow tests must be conducted over the range of conditions to be expected in the repository with special emphasis on compaction density, temperature, flow rates, pressure, chemical composition of groundwater, pH and Eh. Wall effects must be minimized (perhaps by going to wide columns) and column edges sealed to prevent channeling. Compatibility of chamber materials and possible leaching effects of groundwater on sections of apparatus in contact with the groundwater must be taken into account.

- For very low groundwater flow rates and/or strongly sorbed radionuclides, a few preliminary tests have been devised. This is an area that requires more development. The concept of accelerated testing at higher flow rates extrapolated into the low flow rate region also requires further development. Finally, pore water chemistry should be examined as a part of all tests. In cases where radionuclide breakthrough cannot be observed in the laboratory time scale, information on pore water chemistry is necessary to determine the rate and extent of radionuclide migration.

- Since use of multicomponent packing material systems is highly probable to adequately retard all of the radionuclides of interest, dynamic column flow tests must also be conducted on appropriate mixtures or layers of packing materials to check for possible synergistic effects,

---

* Spike - to add a known amount of a substance, chemical or radionuclide to a known amount of solution or material, usually for purposes of calibration or in order to run a controlled experiment.

**Equilibration - to bring a chemical system (either solution or solid-liquid mixture or suspension) into chemical equilibrium so that the relative amounts of chemical compounds or ions are not changing with time. By chemical equilibrium is meant the condition existing when a chemical reaction and its reverse action proceed at equal rates. Since some reactions may take place very slowly or may take place very slowly until some threshold condition is reached, ample time must be allowed to be certain of equilibrium.

especially under hydrothermal conditions. Possible effects due to other components of the waste package must also be included in test conditions, perhaps by doping the groundwater with possible corrosion products from the container or waste form leachates.

- Distribution ratio and retardation factor data may be applied to mass balance type models. These models can be used to estimate radionuclide breakthrough times and release rates which can then be used to evaluate packing material performance in terms of the NRC criteria. Because of the many approximations and simplifications which necessarily enter in developing these mathematical models, these predictions, where possible, should be tested empirically using site-specific and design-specific criteria under field conditions.

4.2 Testing for Mechanical Failure of Bentonite as a Packing Material

4.2.1 Failure Modes and Scenarios

Movement of groundwater through mechanically intact packing materials is expected to be controlled either by the hydraulic conductivity, or for sufficiently low values of this parameter ($<10^{-11}$ cm/s in the case of bentonite), by diffusion (Section 4.1.1.1, above). Mechanical failure of the packing material will facilitate the movement of groundwater through this barrier. The following mechanical failure modes have been considered:

- Fracturing
- Hydrologic erosion
- Creep
- Liquefaction.

The first three have been classified by the DOE as packing material "degradation modes", but it is also noted that hydrologic erosion is most credibly a potential result of man-made intrusion into a geologic waste repository such as, for example, solution mining in the vicinity of a salt dome repository. Furthermore, it is indicated that creep of the packing material into cracks or voids in the surrounding geology should be viewed as a beneficial occurrence since potential pathways for the intrusion of groundwater can be sealed off as a result (DOE/NWTS-13, 1981). This failure mode is, therefore, perhaps more properly termed "loss of creep" or embrittlement. As noted by Wheelwright, (PNL-3873, 1981) the self sealing properties of proposed packing materials such as bentonite clays result from a combination of their plasticity and swelling pressure. Failure by fracturing may result from a loss of plasticity through embrittlement as the water content of the packing material is reduced below the plastic limit as well as from any accompanying shrinkage of the material. Changes in plasticity and volume may also result from mineralogical transformation of the packing material from one material to another. Possible causes of water content reduction and mineralogical transformation are discussed below. The fourth failure mode, liquefaction, may result from an increase in the water content which causes the liquid limit of the packing material to be exceeded; the liquid limit signifies the moisture content at which

the material flows under an applied force (Baver, L. D., 1972). Therefore, the plastic limit, liquid limit, and shrinkage are important parameters which must be considered in the testing of bentonite packing material. These parameters are defined in Section 4.2.2, below. The effects of the repository environment on these parameters must also be considered.

Wet-dry cycling of the packing material is one possible result of the high temperature (on the order of 250°C) to which it may be subjected as the radionuclide decay heat from the waste is dissipated(NUREG/CR-2780, 1982). As the temperature of bentonite, for example, is raised above 25°C at atmospheric pressure it is thought that the water adsorbed on the surfaces of the clay particles is driven off. It is believed that at temperatures between 100 and 300°C the water located between the unit cell layers of the minerals constituting the clay is expelled and that at approximately 300°C dehydration of the crystalline lattice occurs, possibly resulting in irreversible changes in the mineral structure. If these mineralogic changes result in embrittlement and shrinkage of the packing material, the integrity of this material may be compromised by cracking and fracturing, thus creating pathways for groundwater intrusion into the waste package (AESD-TME-3113, 1981). The wet-dry cycling scenario thus consists of an initial drying of the "wet" packing material by nuclear decay heat followed by a rewetting as groundwater intrudes at a later time. Dry periods of up to hundreds of years are thought to be plausible, (RHO-BWJ-SA-145, 1981) but, depending on the relative rates of cooling and approach to equilibrium pressure, the dry period may be much shorter.

An alternative scenario may be considered in which drying of the packing material at an elevated temperature does not occur. For example, if the waste package is emplaced just prior to closure of the repository, the pressure on the waste package may approach the maximum equilibrium pressure (about 33 MPa for expanding packing material in a basalt repository) rapidly enough so that drying of the packing material does not occur because of the elevation of the boiling point of water with increasing applied pressure. (In effect, the waste package is in a pressurized system.) Changes in the mineralogic structure and, consequently, in the liquid limit and plastic limit properties as well as in the volume of the packing material are likely. The high temperature mineralogic transformations of bentonite and other packing materials are discussed in another BNL report in this program by Eastwood (BNL-NUREG-31770, 1982).

4.2.2 Current Status of Test Methods

Standard test methods have been specified by the American Society for Testing and Materials (ASTM) for the liquid limit, plastic limit, and the shrinkage factors of soils and have been designated by the ASTM as D423-66, D424-59, and D427-61, respectively (ASTM, 1981). These test methods were devised for use in the contexts of civil engineering and agronomy and thus are merely a starting point for the discussion of testing relevant to nuclear waste disposal. Note the use in these ASTM test methods of the term "soil", which is more general than "clay".

The liquid limit of a soil is the water content, expressed as a percentage of the weight of the oven-dried soil, at the boundary between the liquid and the plastic states. For the purposes of the ASTM test, this boundary between states is arbitrarily defined as the water content at which two halves of a soil sample cake separated by a groove will flow together for a distance of 1/2 inch (12.7 mm) when a cup containing the sample is dropped 25 times for a distance of 1 cm at the rate of 2 times per second. The experimental apparatus thus consists of a cup which can be lifted and dropped under standardized conditions. The soil-and-water sample is placed in the cup and formed into a cake, a groove is made in the sample, and the number of times the cup must be dropped in order for the groove to close over a distance of 1/2 inch is noted. The water content at the liquid limit is usually determined by conducting the above procedure for a range of water contents and plotting the number of times the cup must be dropped against the water content of the samples (ASTM, 1981; Gillot, J. E., 1968).

The plastic limit of a soil is the water content, once again expressed as a percentage of the mass of oven-dried soil, at the boundary between the plastic and semisolid states. For the purpose of the ASTM test method, this is arbitrarily defined as the lowest water content at which the soil can be rolled into 1/8-inch- (3.2-mm-) diameter threads which do not break into pieces. In accordance with this definition, the method consists of rolling out a thread of the moist soil on a suitable surface such as a ground-glass plate or a piece of glazed or unglazed paper (ASTM, 1981). The shrinkage limit of a soil is the maximum water content at which a reduction in water content will not cause a decrease in the volume of the soil mass. This parameter is generally obtained by extrapolation from a graphical plot of soil volume against moisture content. The soil volume may be obtained by measuring the volume of mercury displaced upon immersion of the soil sample. (ASTM, 1981; Gillot, J. E., 1968).

The liquid and plastic limit tests were used by Sethi and co-workers (1981) to investigate changes in the properties of bentonite clays which had been subjected to a program of thermal treatment in order to simulate wet-drying cycling. Each wet-dry cycle consisted of taking a wetted sample, drying it in an oven, and removing it from the oven for rewetting with distilled water or for testing. Clay samples sealed in airtight Teflon* containers were also subjected to this thermal program (with a maximum moisture loss of less than 1.0%). Information about the three clays tested by these authors is presented in Table 4.5. To simulate the local repository moisture conditions, the initial wetting consisted of equilibrating the sample at its initial liquid limit with fluids simulating granitic or basaltic groundwaters (Table 4.6). A schematic of the thermal program is given in Figure 4.1. Thermal cycling was conducted at three temperatures: 75, 100, and 150°C; the average duration of a wet-dry cycle was temperature dependent, lasting about four, three, or two days, respectively. The cycling was continued for periods of

*Teflon is a registered trademark of DuPont for polytetrafluoroethylene.

Table 4.5 Some basic characteristics of the three clays used by Sethi, Bird, and Yong (1981).

Clay Designation and Origin	Soluble Cations (meq/100 g)				Exchangeable Cations (meq/100 g)					C.E.C.** (meq/100 g)	Organic Matter (Percent)	Surface Area (m^2/g)
	Na	Ka	Ca	Mg	Na	K	Ca	Mg	ESP*			
800-002 Pembina Mountain Clays, Winnipeg	1.3	0.1	1.5	0.3	2.2	0.6	11.9	51.4	3	73.8	7.7	794
800-003 Crude Bentonite, Dresser Industries Rosalind, Alberta	4.9	0.1	0.0	0.1	29.3	0.5	13.2	8.4	53	55.1	6.6	535
80-004 Avonlea Company	19.3	0.1	1.7	0.4	34.4	1.3	4.7	16.2	64	53.6	11.5	615

*ESP = Exchangeable sodium percentage.
**C.E.C. = Cation exchange capacity.

Table 4.6 Synthetic groundwater formulations used by Sethi, Bird, and Yong (1981).

Ionic Species	Concentration (mg/L)	
	Basaltic	Granitic
Na^+	30	8
K^+	9	3.5
Ca^{2+}	6.5	13
Mg^{2+}	1	5
HCO_3^-	58	22
SO_4^{2-}	23	9
Cl^-	16	9
F^-	0.7	0.6
NO_3^-	7.7-8.2	5.9-7.0

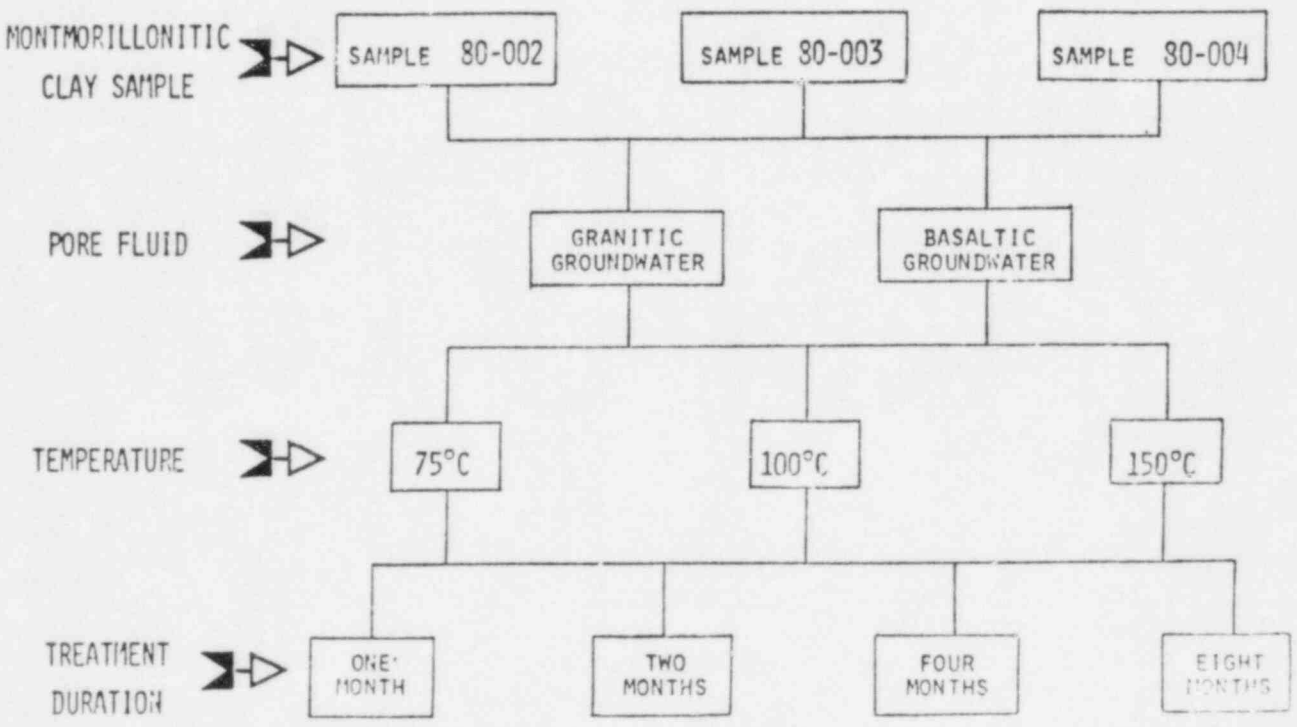

Figure 4.1 Schematic of the program of thermal cycling used by Sethi, Bird, and Yong. (1981)

one to eight months (but only one month for the samples in sealed containers). The liquid and plastic limit tests were conducted as per the ASTM methods described above. The results of the tests are presented in more detail in the original paper and are also discussed by Snead (BNL-NUREG-31839, 1982) but the general trends observed with increasing wet-dry cycling were increasing liquid limit values for the calcium-rich sample (designated 80-002 in Table 4.5), and decreasing liquid limit values for the other two samples.

The ASTM tests discussed above are suitable for use only under ambient temperature and pressure conditions and are not intended for use under the more severe conditions expected in a repository environment. The testing itself is done under ordinary ambient conditions even if the samples tested have been exposed to a repository-like environment as in the work by Sethi and coworkers (1981). Another problem with the latter work is the short length (on the order of days) and repetition (seven to twenty six times) of the wet-dry cycling. As noted in Section 4.2.1, above, wet-dry cycling, if it occurs at all, is likely to consist of one dry period lasting for perhaps years.

In addition, it is difficult to obtain reproducible results using these test methods. For example, in the liquid limit test the following factors have been found to contribute to variations in the results (Russell, E. R., 1970): (1) the difficulty of cutting a groove in some soils; (2) the tendency of soils of low plasticity to slide rather than flow plastically; (3) the tendency of some soils to liquefy with shock rather than to flow plastically; (4) the sensitivity to small differences in apparatus; and (5) sensitivity to operator technique.

In Section 4.2.1 above, it was noted that plasticity is one component of the self-sealing ability of a clay, the other component being the swelling pressure. Some studies of this self-sealing property have been sponsored by KBS* in Sweden. For example LeBell (1978) studied the swelling of compacted bentonite using a special cell constructed of glass plates mounted in a metal frame. The glass plates were separated by a 0.5 mm-thick spacer in order to create an artificial crack which was connected to a 2.6 cm^3 cavity in which a sample of compacted bentonite was placed (Figure 4.2). The whole cell was then immersed in a synthetic groundwater solution (Table 4.7) and the swelling of the bentonite was recorded photographically as a function of time. This work appears to have been done under ambient temperature and pressure conditions.

Pusch (1978), also under the auspices of KBS, measured the extrusion of highly compressed (50 MPa) bentonite which had been flooded with synthetic groundwater or a dilute (2%) saline solution. The bentonite was confined in a rigid steel container with slots simulating joints in the surrounding rock. The container consisted of a series of rings with notches of various depths so that the stack of rings forms a cylinder with slots ranging from 0.05 to 0.5 mm wide through which water was allowed to enter and through which the swelling bentonite could be extruded (Figure 4.3). The extrusion of the bentonite

*Kaernbraenslesaekerhet (Nuclear Fuel Safety) of Sweden

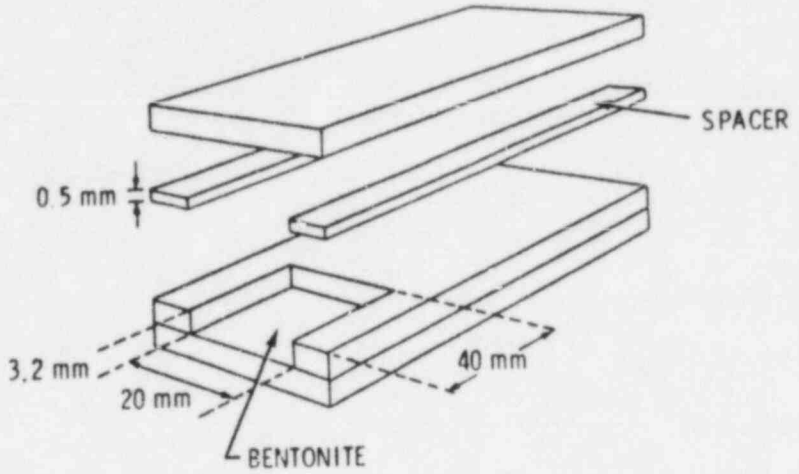

Figure 4.2 Cell for investigating swelling and extrusion of bentonite used by PNL-3873 (1981).

Table 4.7 Synthetic groundwater solution used by LeBell (1978).

Dissolved Component	Concentration (mg/L)
HCO_3^-	197.3
Ca^{2+}	33
Mg^{2+}	7
Na^+	124
K^+	5
Mn^{2+}	0.5
SiO_2	20
NH_4^-	0.2
NO_3^-	1
Cl^-	30
F^-	1
NO_2^-	0.1
SO_4^{2-}	18.6
Fe^{3+}	0.4
OH^-	31.8

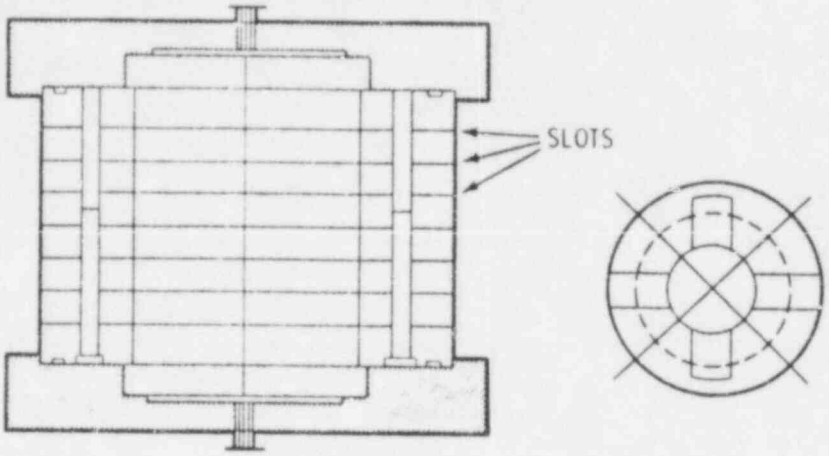

Figure 4.3 Device for investigation of swelling and extrusion properties for bentonite used by Pusch (1978).

was determined at various time intervals (on the order of days) by means of thin metal blades which were pushed through the slots. It was found that the extrusion rate increased with increasing joint width and was approximately the same for both water compositions investigated. The temperature conditions were unspecified.

An apparatus somewhat similar to LeBell's was used by Chan at Ontario Hydro to measure the extrusion properties or, in Chan's terminology, the injectability of bentonite and kaolin grouting materials into a fissure. The cell consisted of an aluminum base plate 20 cm by 61 cm by 1.2 cm and a similarly sized piece of transparent Lexan* separated by a shim material 0.25-mm thick. An inlet fitting through which the clay was injected was placed at one end of the Lexan to allow flow of the clay in one direction. The shim material was omitted at the other end so that it would be open to the atmosphere during injection. Pressures on the clay were slowly increased in steps from zero to a maximum of 105 KPa. When a particular pressure value was applied, the material was injected into the gap slowly and then stopped. After a five-minute hold time, the shape of the leading edge of the clay was traced on the surface of the Lexan material. At the end of a test, photographs and a paper tracing of the leading edge contours were taken in order to obtain areas, and then volumes, of the injected material at each pressure. The resulting data consisted of plots of pressure vs volume of injected material for several bentonite-water and kaolin-water materials. Note that this study appears to have been carried out at room temperature (Chan, H. T., 1981).

Chan also studied the hydrologic erosion of these clay materials. In his erosion test, two acrylic tubes 6 cm in length and 1.27 cm in diameter were joined to form a single tube. The two tubes were separated by a filter paper

*Lexan is a registered trademark of General Electric for a polycarbonate resin material.

disk. One section of the 12-cm tube was filled with the clay material. Filters and an end cap were then attached. A small hole with a diameter of about 1 or 2 mm was then made very close to the edge of the filter paper disc; during testing, the tube would be oriented with this hole at the top. The second section of the 12-cm tube was then filled with deionized water, and filters and an end cap were attached here as well. The section containing the clay material was always the inflow end of the tube during the erosion test. When water was allowed to seep through the clay material in the first section of the tube, some of this material was eroded into the adjacent section through the hole in the filter paper disc separating the two sections. By maintaining a hydraulic head of 260 cm of water as the driving force for the flow through the tube, it was found that the bentonite was completely washed through the hole within minutes; in order to decrease the rate of erosion the hydraulic head was reduced to 60 cm of water. It was expected that observations of the amount of clay material eroded from the first into the second tube section and of the change in the flow rate through the sample would yield information about the susceptibility of the two clay materials to hydrologic erosion. As a result of these experiments, it was found that kaolin was much more susceptible than bentonite to hydrologic erosion. A more detailed account may be found in the original report (Chan, H. T., 1981).

Hydrologic erosion of mixtures of sodium bentonite clay and quartz sand (20%-80% by weight) was investigated by Pusch (1979a). The clay packing material was placed in two columns consisting of threaded steel cylinder sections. (See Figure 4.4). The two columns were connected at their tops to a vessel with simulated groundwater which could be put under pressure by compressed air in order to establish the desired hydraulic gradient. One of the columns in each series of tests was used to simulate the case of an initially heterogeneous packing material by filling two of the sections with quartz sand only. In order to obtain values for the hydraulic conductivity of the packing material, the quantity of percolated water was determined by collecting it in flasks at the bottom of the columns. After the percolation tests (and it is not indicated how it was determined that a percolation test was completed), the steel cylinder sections were disconnected and a large number of water content and clay content determinations were made (by unspecified methods) in order to investigate the uniformity of the percolation and to ascertain whether transport of clay particles had occurred. Tests with water pressures of up to 300 kPa and hydraulic gradients of up to 100 were conducted.

The testing discussed up to this point has been carried out with the purpose of measuring specific properties of the packing material. The testing program in progress at PNL includes a much more direct approach. Noting that the ability to slow or stop the migration of water between the host geology and the waste container system is a primary attribute of an effective packing material, the PNL workers have given a high priority to the measurement of the flow of water through this material. It is intended that the permeability of the packing material be determined as a function of the composition, density, and the radiation and thermal histories of the material as well as of the composition of the permeating fluid (PNL-3873, 1981).

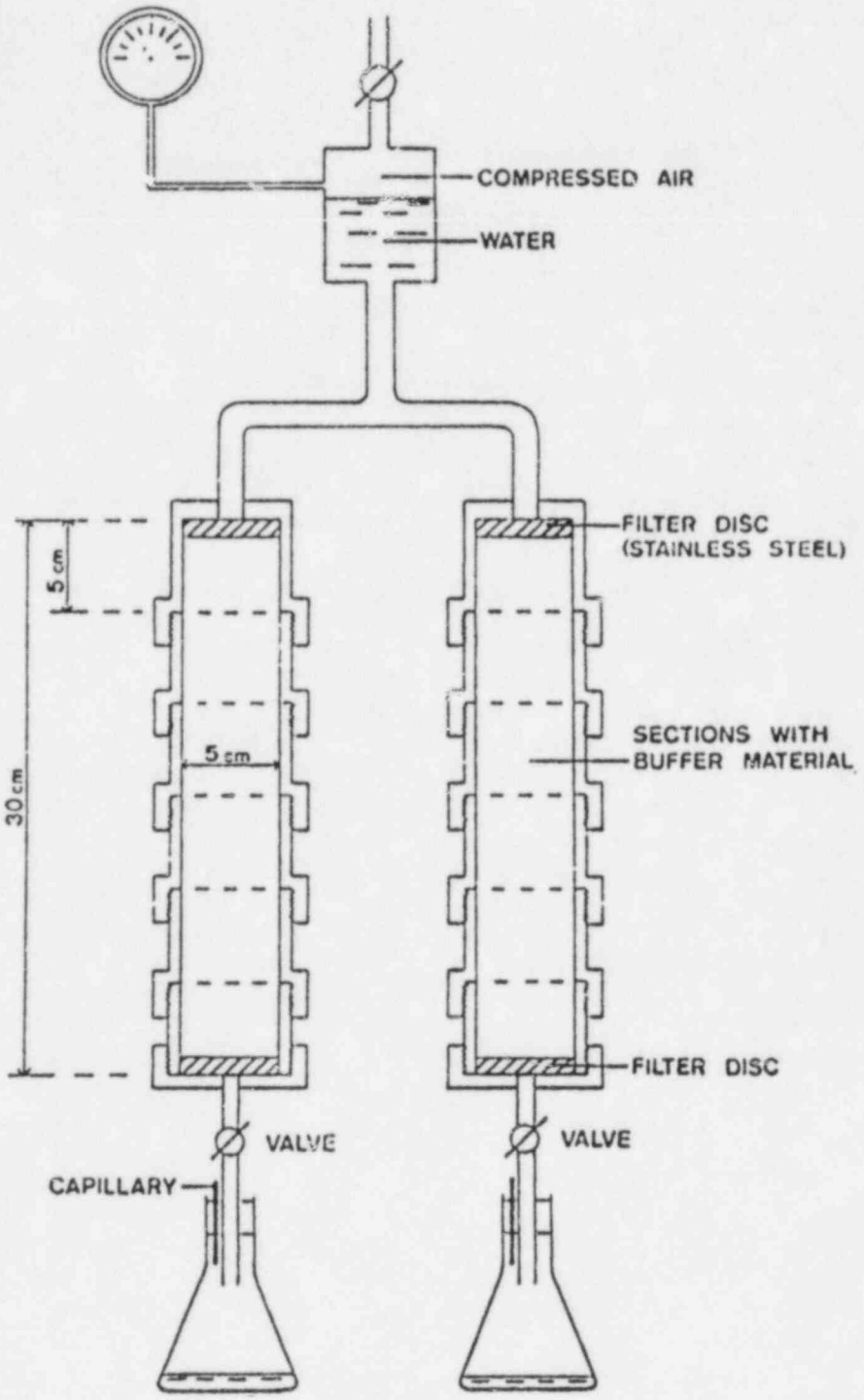

Figure 4.4 Hydrologic erosion test device used by Pusch (1979a).

A schematic of the apparatus for measuring the permeability as well as the swelling pressure and radionuclide migration is shown in Figure 4.5. (Radionuclide migration is discussed in Section 4.1.2, above). The permeating fluid, e.g., synthetic groundwater, is pumped from the reservoir to the permeability cell in a pulse-free flow. The actual pressure in the system is controlled by the back-pressure relief valve and is monitored by the pressure transducer. The permeability cell itself is shown in Figure 4.6 and includes a load cell to monitor the swelling pressure of candidate packing materials as they saturate with the permeating fluid. Initial testing done with this system is described by Wheelwright (PNL-3873, 1981).

4.2.3 Summary and Conclusions

In the discussion in Section 4.2.2, above, of the ASTM tests for several properties of soils (including clays), it was indicated that these tests were suitable for use only under ambient temperature and pressure conditions but that the mechanical failure modes which might be deduced from these properties were of concern under repository conditions. While the definitions of and the testing methods for the liquid, plastic, and shrinkage limits of soils could be extended to clay materials under repository conditions, such an extension of the testing methods, while undoubtedly a worthy undertaking, is likely to be a complex and time-consuming process which could cause undue delay in the licensing of a repository. Measurements of the self-sealing ability of a packing material, such as those done by KBS, are more pertinent to the problems of mechanical failure under repository conditions. Such experiments at higher temperatures and longer time periods are recommended. The KBS group has assumed packing material temperatures of less than 100°C; the U.S. planners are assuming temperatures as high as 250 to 300°C (BNL-NUREG-31770).

It is also recommended that direct measurements of the rate of flow of the permeating fluid (synthetic groundwater or brine, as applicable) through the candidate packing materials be continued and extended. There are problems, however, with the PNL apparatus as described by Wheelwright in PNL-3873 (1981). Significant mechanical failure of the material during the time period of the experiment would be indicated by a measurable flow of the fluid through the permeability cell at realistic hydraulic gradients, for example, ≤ 1 cm/cm at steady-state flow as opposed to 10^4 or 10^5 cm/cm typical of the PNL measurements. The use of hydraulic gradients several orders of magnitude greater than those expected in the candidate last rock strata is an accelerating technique for mechanically intact materials of low permeability. Because of time constraints, measurements of permeability at realistic hydraulic gradients may be feasible only for relatively permeable packing materials or for those which have lost their mechanical integrity. Such unrealistically large hydraulic gradients may cause closing of cracks and fractures, and thus mechanical failure may occur but not be detected. Also, there is no permeability standard for fine-grained soils such as clay in the ASTM procedures, although the ASTM permeability test method for granular soils, D2434-68 (ASTM, 1981) is often misused for clays (Eastwood, D., 1982). In any case, the applicability of measurements using unrealistically large values of the

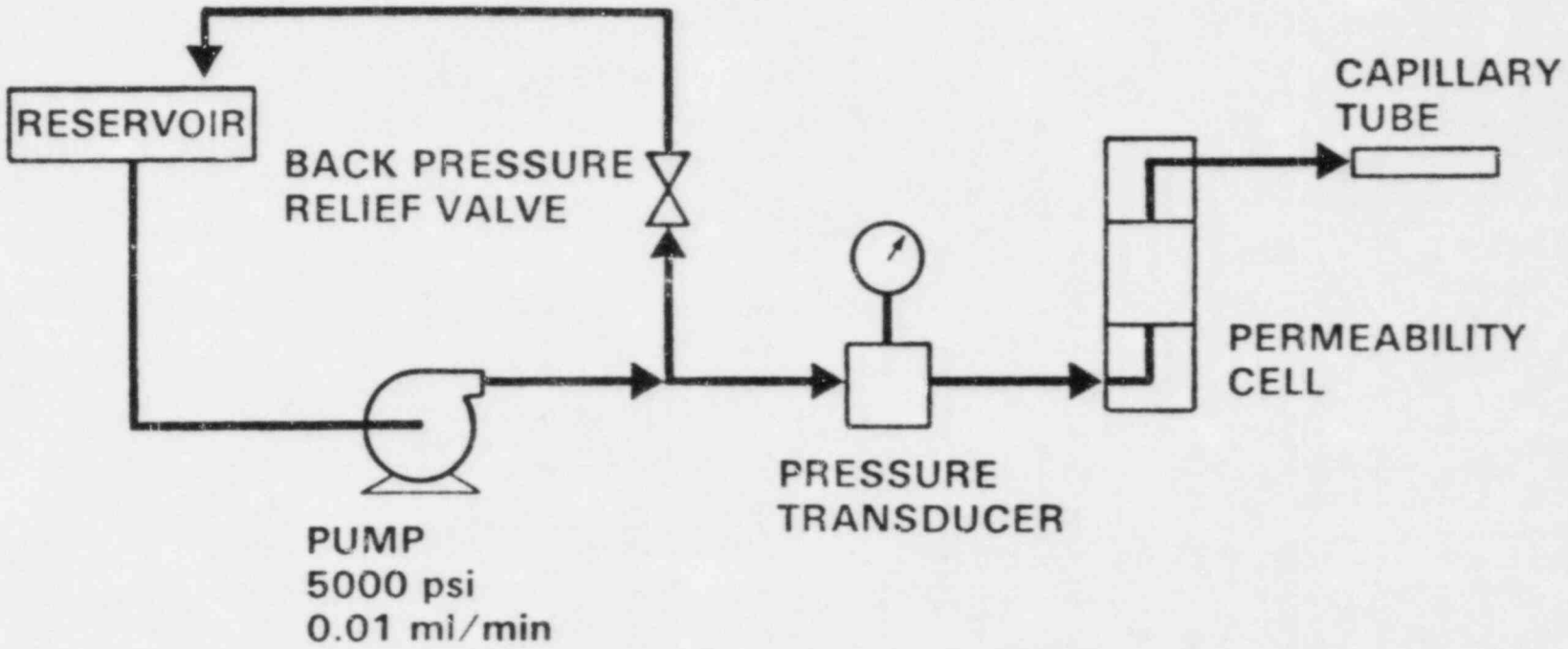

Figure 4.5 Schematic of PNL permeability apparatus (PNL 3873, 1981).

hydraulic gradient to repository conditions has not been established. A discussion of the measurement of the hydraulic conductivity of fine-gained soils is given by Olson and Daniel (1981).

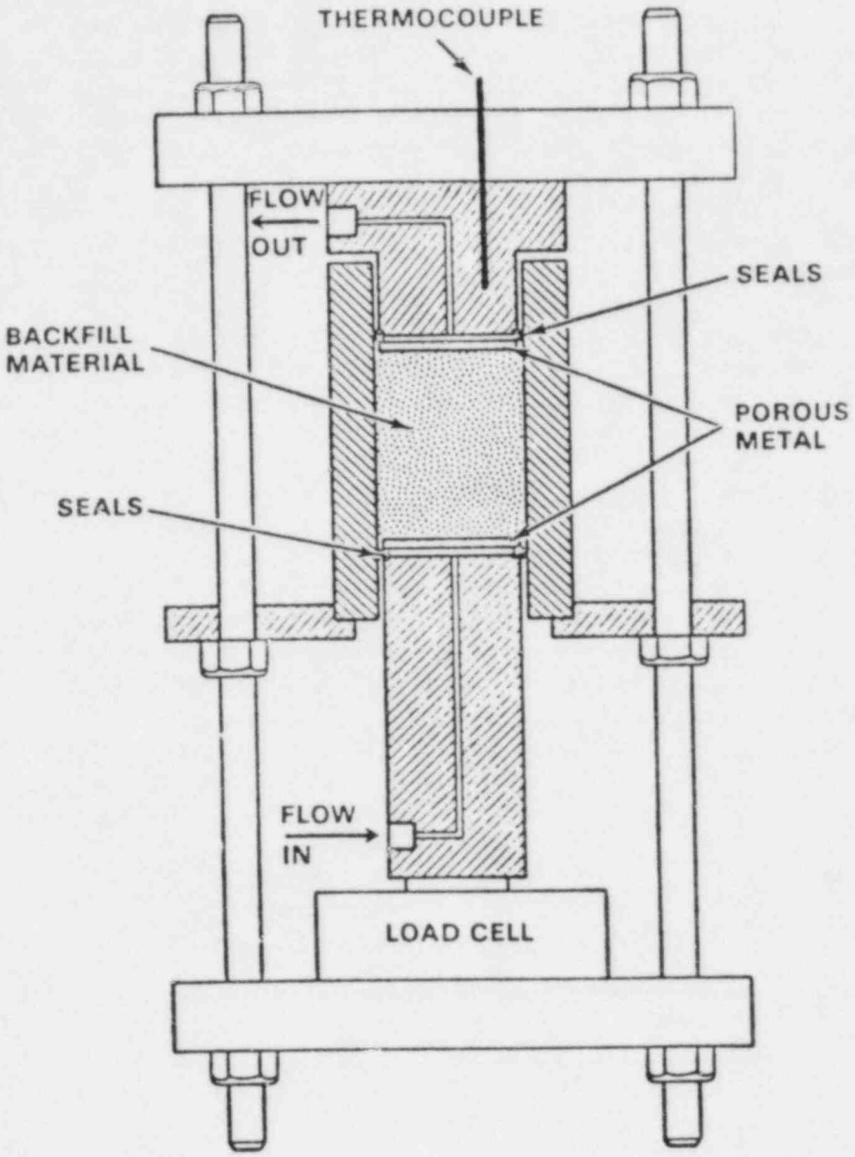

Figure 4.6 PNL permeability cell (PNL-3873, 1981).

It is therefore suggested that measurements of the transport of water through candidate packing materials be conducted using apparatus similar to the PNL system but capable of simulating the expected repository environment. In addition to applying a more realistic hydraulic gradient across the sample, it should be possible to heat the material in the cell to realistic repository

temperatures and temperature gradients. For example, mechanical failure may result from differential thermal expansion across a temperature gradient. Also, the permeating fluid should have the expected Eh, pH, and composition of the repository groundwater or brine. The composition is of particular importance because cationic constituents such as K^+ can replace the exchangeable cation, often Na^+, in packing materials such as bentonite, thus causing changes in the susceptibility of the material to mechanical failure. In another BNL report in this program, Eastwood discusses the available information about the chemical changes in packing materials (BNL-NUREG-31770, 1982). Simulation of the expected radiation environment during the course of the suggested measurement of fluid transport would be useful in order to study the effects on the packing material due to radiolysis-induced changes in the pH, Eh, and composition of the permeating fluid.

It was recommended above that the hydraulic gradient not be used as an accelerating parameter. Because of sluggish reaction rates for the mineralogical transformations, long term laboratory experiments should be performed under conditions to be expected in the repositories even though experiments lasting for several years may not be adequate to demonstrate definitively the absence of mechanical failure for the full 1000-year containment period. Potentially deleterious structural changes in packing materials may be detectable by techniques such as X-ray diffraction or scanning electron microscopy (Sasaki, N., 1982) long before macroscopic mechanical failure becomes evident. It is recommended that such techniques be used as an adjunct to measurements of the penetration of the permeating fluid through the packing material. Such experiments are planned at Argonne National Laboratory by Couture (1982). If possible, mineralogical characterization of a packing material should be conducted while the material is under simulated repository conditions.

4.3 References

AESD-TME-3086, "Engineered Waste Package Conceptual Design - Defense High Level Waste (Form 1) Disposal in Salt," Westinghouse Electric Corporation, March 1981.

AESD-TME-3113, "Engineered Waste Package Conceptual Design - Defense High Level Waste (Form 1), Commercial High Level Waste (Form 1), and Spent Fuel (Form 2) Disposal in Basalt," Westinghouse Electric Corporation, Section 5 and Appendix A, September 1981.

AESD-TME-3131, "Engineered Waste Package Conceptual Design - Defense High Level Waste (Form 1), Commercial High Level Waste (Form 1), and Spent Fuel (Form 2) Disposal in Salt," Westinghouse Electric Corporation, Appendix D, November 1981.

AESD-TME-3138, "Conceptual Waste Package Designs for Disposal of Nuclear Waste in Tuff," Westinghouse Electric Corporation, Appendix E, May 1982.

Allard, B., H. Kipatsi and J. Rydberg, "Sorption of Long-Lived Radionuclides in Clay and Rock," KBS-TR-55, Kaernbraenslesaekerhet (Sweden), 1977.

Allard, B., H. Kipatsi and B. Torsternfelt, "Sorption of Long-Lived Radionuclides in Clay and Rock - Part 2," KBS-TR-98, Kaernbraenslesaekerhet (Sweden), 1978.

ASTM, Annual Book of ASTM Standards, Part 19, Natural Building Stones; Soil and Rock, American Society for Testing and Materials, Philadelphia, 1981.

ASTM Draft, "Test Method for Distribution Ratios by the Short-Term Batch Method," private communication to D. Eastwood, BNL, American Society for Testing and Materials, D-18 Committee on Soil and Rocks, Meeting in Ft. Lauderdale, FL, January 1982.

Barrer, R. M., Zeolites and Clay Minerals as Sorbents and Molecular Sieves, Academic Press, New York, NY, 1978.

Baver, L. D., W. H. Gardner and W. R. Gardner, Soil Physics, 4th Ed., (John Wiley and Sons, New York, 1972).

Beall, G. W., A. G. Lamkin and K. L. Kelly, "Critical Factors Affecting the Use of Montmorillonite as a Nuclear Waste Backfill Material," presented at NBS Workshop on Research and Development Needs in Backfill for Underground Nuclear Waste Management, Gaithersburg, MD, April 13-14, 1981.

BNL-NUREG-28682, "Review of Recent Studies of the Radiation Induced Behavior of Ion Exchange Media," K. J. Swyler, R. E. Barletta and R. E. Davis, Brookhaven National Laboratory, 1980.

BNL-NUREG-30631, "Irradiation of Zeolite Ion-Exchange Media, Draft Report," K. J. Swyler and R. E. Barletta, Brookhaven National Laboratory, December 1981.

BNL-NUREG-31049, "Near-Field Repository Conditions in Basalt and Salt," B. Siskind and D. Hsieh, Brookhaven National Laboratory, March 1982.

BNL-NUREG-51315, "Evaluation of Isotope Migration - Land Burial Water Chemistry at Commercially Operated Low Level Radioactive Waste Disposal Sites," K. S. Czyscinski and A. J. Weiss, Brookhaven National Laboratory, 1981.

BNL-NUREG-51458, Vol. 1, "Nuclear Waste Management Technical Support in the Development of Nuclear Waste Form Criteria for the NRC - Task 1: Waste Package Overview," R. Dayal and others, Brookhaven National Laboratory, February 1982.

BNL-NUREG-51458, Vol. 4, "Nuclear Waste Management Technical Support in the Development of Nuclear Waste Form Criteria for the NRC - Task 4: Test Development Review," T. M. Ahn and others, Brookhaven National Laboratory, February 1982.

BNL-NUREG-31770, "Chemical Failure Modes of Bentonite and Zeolites for Use as Discrete Backfill in Nuclear Waste Repositories," D. Eastwood, Brookhaven National Laboratory, August 1982.

BNL-NUREG-31837, "Data Requirements for Mechanical Failure of Bentonite in a Discrete Backfill for Basalt and Salt Repositories," C. L. Snead, Jr., Brookhaven National Laboratory, August, 1982.

Breck, D. W., Zeolite Molecular Sieves - Structure, Chemistry and Use, Wiley Interscience, New York, NY, 1974.

Chan, H. T., "Laboratory Study of Clay-Type Grouting (Sealing) Materials - Progress Report," Report No. 81-20-K, Ontario Hydro Research Division, February 1981.

Coombs, D. S., A. Ellis and W. S. Frye, "The Zeolite Facies, with Comments on the Interpretation of Hydrothermal Synthesis," Geochimica et Cosmochimica Acta, 17, 53-107, 1959.

Couture, R. A., "Modification of Backfill Materials Under Repository Conditions," Statement of Work for the Nuclear Regulatory Commission, FIN A2239, Argonne National Laboratory, May 12, 1982.

Davis M. S. and D. G. Schweitzer, Brookhaven National Laboratory, Letter to E. A. Wick, NRC. Subject: Review of Westinghouse Reports AESD-TME-3086 and -3087, March 1981, dated January 5, 1982.

Dayal, R. and R. J. Wilke, "Role of Clay Minerals as Backfill in Radioactive Waste Disposal," submitted for publication in Proceedings of the VII International Clay Conference, Pavia and Bologna, Italy, September 1981.

DOE/NWTS-13, "Nuclear Waste Package Materials Degradation Modes and Accelerated Testing," U. S. Department of Energy, September 1981.

Eastwood, D., Brookhaven National Laboratory, Memorandum to File, "Joint ASTM (American Society for Testing and Materials) Meeting of D-19 (Water), D-18 (Soil and Rock), and D-34 (Waste Disposal) held in Orlando, January 24-29, 1982," February 8, 1982.

Fried, S. and others, "Measurement of Penetration Depths of Plutonium and Americium in Sediment from the Ocean Floor," Scientific Basis for Nuclear Waste Management, Vol. 2, C. M. J. Northrup Jr., Ed., (Plenum Press, New York, 1980), p. 647.

Gillott, J. E., Clay in Engineering Geology, (Elsevier, Amsterdam, 1968).

Hirschfeld, T. and T. Deaton, Lawrence Livermore Laboratory, "Remote Fiber Optic Fluorometry: Specific Analyte Optrodes," Abstract 404 of invited paper presented at Pittsburgh Conference on Analytical Chemistry and Applied Spectroscopy, Atlantic City, NJ, March 1982.

Jacobsson, A., "A Short Review of the Formation, Stability, and Cementing Properties of Natural Zeolites," KBS-TR-27, Kaernbraenslesaekerhet (Sweden), 1977.

Komarneni, S. and R. Roy, "Super Overpack: Tailor-Made Mixtures of Zeolites and Clays," in Scientific Basis for Nuclear Waste Management, Vol. 2, C. J. Northrup, Ed., (Plenum Press, New York, 1980), p. 411.

Komarneni, S. and R. Roy, "Hydrothermal Transformation in Candidate Overpack Materials and their Effects on Cesium and Strontium Sorption," Nucl. Tech. 54, 118-122, 1981.

Komarneni, S. and R. Roy, "Interactions of Backfill Materials with Cesium in a Bittern Brine under Repository Conditions," Nucl. Tech. 56, 575-579, 1982.

LA-8088-PR, "Laboratory Studies of Radionuclide Distribution Between Selected Groundwater and Geological Media, Annual Report, October 1, 1978 - September 30, 1979," B. R. Erdal and others, Los Alamos National Laboratory, 1980.

LeBell, J. C. "Colloid Chemical Aspects of the 'Confined Bentonite Concept'," KBS-TR-97, Kaernbraenslesaekerhet (Sweden), 1978.

Lohman, S. W., "Ground-Water Hydraulics," Geological Survey Professional Paper 708, U.S. Government Printing Office, Washington, DC, 1972.

Neretnieks, I., "Retardation of Escaping Nuclides from a Final Repository," KBS-TR-30, Kaernbraenslesaekerhet (Sweden), 1977.

NUREG/CR-2780, BNL-NUREG-51548, "Near-Field Repository Conditions in Basalt and Salt - Final Report," B. Siskind and D. Hsieh, Brookhaven National Laboratory, May 1982.

Olson R. E. and D. E. Daniel, "Measurement of the Hydraulic Conductivity of Fine-Grained Soils," in Permeability and Groundwater Contaminant Transport, T. F. Zimmie and C. O. Riggs, Eds., American Society for Testing and Materials, Philadelphia, 1981.

PNL-3000-6, Section 23, "Nuclear Waste Management Quarterly Progress Report, April through June 1980," E. J. Wheelwright, Pacific Northwest Laboratory, September 1980.

PNL-3000-7, Section 17, "Nuclear Waste Management Quarterly Progress Report, July through September 1980," E. J. Wheelwright, Pacific Northwest Laboratory, November 1980.

PNL-3000-8, Section 17, "Nuclear Waste Management Quarterly Progress Report, October through December 1980," E. J. Wheelwright, Pacific Northwest Laboratory, March 1981.

PNL-3000-9, Section 20, "Nuclear Waste Management Quarterly Progress Report, January through March 1981," E. J. Wheelwright, Pacific Northwest Laboratory, June 1981.

PNL-3000-10, Section 21, "Nuclear Waste Management Quarterly Progress Report, April through June 1981," E. J. Wheelwright, Pacific Northwest Laboratory, September 1981.

PNL-3000-11, Section 21, "Nuclear Waste Management Quarterly Progress Report, July through September 1981," E. J. Wheelwright, Pacific Northwest Laboratory, December 1981.

PNL-3349, "Methods for Determining Radionuclide Retardation Factors: Status Report," J. F. Relyea, R. J. Serne and D. Rai, Pacific Northwest Laboratory, 1980.

PNL-3873, "Development of Backfill Material as an Engineered Barrier in the Waste Package System -Interim Topical Report," E. J. Wheelwright and others, Pacific Northwest Laboratory, September 1981.

PNL-SA-6957, "Systematic Study of Nuclide Sorption on Select Geological Media in Waste Isolation Safety Assessment Program," Task 4 Contractor Information Meeting Proceedings, R. E. Meyer and others, Pacific Northwest Laboratory, 1977.

PNL-2872, "Controlled Sample Program Number 2: Interlaboratory Comparison of Batch K_d Values," J. F. Relyea and R. J. Serne, Pacific Northwest Laboratory, June 1979.

PNL-SA-7928, "Sorption Behavior of ^{85}Sr, ^{137}Cs, and ^{95}Tc Under Normal Atmospheric and Reduced Oxygen Levels," J. F. Relyea, C. D. Washburne and R. W. Fulton, Pacific Northwest Laboratory, 1979.

Pusch, R., "Self-Injection of High Compacted Bentonite into Rock Joints," KBS-TR-73, Kaernbraenslesaekerhet (Sweden), 1978.

Pusch, R., "Clay Particle Redistribution and Piping Phenomena in Bentonite/Quartz Buffer Materials Due to High Hydraulic Gradients," SKBF-KBS-79-01, Kaernbraenslesaekerhet (Sweden), 1979a.

Pusch, R., "Water Percolation Effects on Clay-Poor Bentonite/Quartz Buffer Material at High Hydraulic Gradients," SKBF-KBS-79-17, Kaernbraenslesaekerhet (Sweden), 1979b.

Pusch, R., private communication to G. Bida, Brookhaven National Laboratory, 1981.

Radhakrishna, H. S., Research Division, Ontario Hydro, "Evaluation of Thermal Properties of Buffer Materials for a Deep Underground Nuclear Waste Disposal Vault," presented at NBS Workshop on Research and Development Needs in Backfill for Underground Nuclear Waste Management, Gaithersburg, MD, April 13-14, 1981.

RHO-BWI-ST-7, "Engineered Barrier Development for a Nuclear Waste Repository Located in Basalt," M. J. Smith, Rockwell Hanford Operations, May 1980.

RHO-BWJ-SA-145, "The Development and Testing of Waste Package Backfill Materials for a Nuclear Waste Repository Located in Basalt," M. I. Wood, Rockwell Hanford Operations, April 1981.

Russell, E. R. and J. L. Mickle, "Liquid Limit Values by Soil Moisture Tension," J. Soil Mechanics and Foundations Division, Proc. Am. Soc. Civil Eng. 96, 967, 1970.

SAND79-1109, "The Backfill Barrier as a Component in a Multiple Barrier Nuclear Waste Isolation System," E. J. Nowak, Sandia National Laboratories, 1980.

SAND79-2468, "Assessment of Potential Radionuclide Transport in Site-Specific Formations," R. G. Dosch, Sandia National Laboratories, August 1980.

SAND81-0277A, "Backfill Barriers for Nuclear Waste Repositories in Salt," E. J. Nowak, Sandia National Laboratories, March 1981.

SAND81-1377C, "Composite Backfill Materials for Radioactive Waste Isolation by Deep Burial in Salt," E. J. Nowak, Sandia National Laboratories, January 1981.

Sasaki, N. and others, "Backfill-Waste Interaction Under Radwaste Repository Conditions," paper presented at the International Symposium on the Scientific Basis for Nuclear Waste Management, Boston, MA, November 16-20, 1981.

Sasaki, N., S. Komarneni, B. E. Scheetz and R. Roy, "Backfill-Waste Interactions in Repository Simulating Tests," in The Scientific Basis for Nuclear Waste Management, S. V. Topp, Ed., Elsevier, Amsterdam, 1982.

Sethi, A. J., G. W. Bird and R. N. Yong, "Effect of Hydrothermal and Cyclic Wetting-Drying Treatment on Properties and Characteristics of Montmorillonitic Clays," presented at NBS Workshop on Research and Development Needs in Backfill for Underground Nuclear Waste Management, Gaithersburg, MD, April 13-14, 1981.

Strickert, R., A. M. Friedman and S. Fried, "The Sorption of Technetium and Iodine Radioisotopes by Various Minerals," Nucl. Tech. 49, 253-266, 1980.

Westsik, J. H., Jr. and others, Pacific Northwest Laboratory, "Permeability, Swelling and Radionuclide Retardation Properties of Candidate Backfill Materials," PNL-SA-9645, paper presented at the International Symposium on the Scientific Basis for Nuclear Waste Management, Boston, MA, November 16-20, 1981.

APPENDIX A

Summary of Methods of Crack Length Measurement (Deans, W. P., 1979).

Technique	Brief Description	Advantages	Disadvantages
Optical	relies on microscopes or telescopes, often aided by etched or scribed markings; almost all test piece geometries	inexpensive; does not require calibration; does not require specimen to behave in a linear elastic manner	only gives surface readings and usually underestimates average crack length because of crack curvature; not amenable to automation and hence time-consuming; requires surfaces to be accessible and in well-polished condition
Mechanical, COD	basis is to measure the COD, usually between points along the loading line or, in the case of bend and wedge opening loading specimens, at the front face [55-60]; displacement measured mostly by clip gages; for high temperature testing extension arms may be used to transfer the displacements to lower temperature regions for measurement; extension arms may be used via moving seals to measure displacements inside autoclaves; any test piece geometry that behaves in a linear elastic manner	cost depends on application and ranges from low cost in room temperature air to moderately expensive in high temperature aggressive environments; does not require the specimen to be visually accessible and can provide an average crack length figure; easily incorporated in automatic systems	calibration required in some cases: clip gages and to a lesser extent transducers not very robust
Mechanical, BFS	strains measured on the back face of CT or T-type WOL specimens by strain gages or possibly clip gages or transducers for large test pieces; possible use in single-edge-notched tension or three and four point bend specimens; all specimens must behave in a linear elastic manner	cost depends on application and ranges from very inexpensive in room temperature air tests to moderately expensive in high temperature aggressive environments; does not require the specimen to be visually accessible and can provide an average crack length figure; shows excellent characteristics for incorporation in automatic systems	calibration required for test pieces other than CT and T-Type WOL specimens
Electrical, strain gage filaments	electrically conducting wires are attached to the specimen so that they are broken by an advancing crack, providing stepwise changes in resistance [61-63]; can be used for all specimen geometries	low cost; easily adapted for automatic processes	only gives surface readings, not well suited for high temperatures and aggressive environments; difficult to locate gages and ensure crack always and only breaks filaments when crack tip passes through

Technique	Brief Description	Advantages	Disadvantages
Electrical, d-c potential drop (resistance)	a constant d-c current is passed through a specimen so that a change in crack length alters the potential difference of suitably placed contact points, usually in vicinity of the crack tip [55,64-67]; suitable for all test piece geometries	low cost; does not require any delicate instrumentation attached to the specimen; high stability for long term tests and some relaxation from linear elastic behavior easily accommodated; particularly well suited for automatic control and long term, high temperature testing; robust and simple; can give an average crack length value	some theoretical calibrations available but usual to carry out calibration tests; some uncertainty in stress corrosion and corrosion fatigue studies over possible interference with electrochemical conditions adjacent to crack tip; for decreasing K, constant COD tests crack faces may short electrically, thus underestimating crack length; bridging of crack surfaces by corrosion products may produce erroneous crack length readings; in some cases the grips may have to be electrically insulated from the testing machine; not well suited for very large specimens
Electrical, a-c potential drop (resistance)	similar to d-c potential drop	does not require any delicate instrumentation attached to the specimen; some relaxation from linear elastic behavior easily accommodated; well suited for automatic control and can give average crack length values; high sensitivity	moderate cost; wires have to be carefully placed and must not be moved during test; long-term stability difficult to achieve; bridging of crack surfaces by corrosion products may produce erroneous crack length readings; electrical insulation required
Electrical, eddy currents	an eddy current probe adjacent to a cracked surface produces an electrical signal, indicating the crack [68]; can be used with a servo-system or stepping motor that moves the probe so that a nil eddy current signal is maintained; used for center-cracked sheets but should be adaptable to other geometries.	easily adapted for automatic processes	may only be useful for surface measurements; expensive

Technique	Brief Description	Advantages	Disadvantages
Ultrasonic	involves transmission and reception of a high frequency sound beam intersected by a crack [69]; if probe is fixed the moving crack alters the proportion of the signal reflected by crack and the opposite boundary of the specimen; a more accurate version involves a stepping motor that moves the probe so that the strength of the signal reflected by the crack remains constant [70]; used mainly on WOL compact specimens	can be adapted for automatic processes; internal measurements of crack length; only method that can give crack profile; relaxation from linear elastic behavior easily accommodated	not well suited for small, thin specimens; expensive; cannot be used at high temperatures; not well suited to environmental testing; not a proven technique for specimens other than WOL compact specimens; difficult to achieve high resolution
Acoustic emission	involves attachment of sensing transducer to test piece that oscillates at its resonant frequency on receiving elastic stress waves from source of deformation [65]; detected emissions are then amplified, selectively filtered and conditioned, and then counted either on a periodic basis as a rate of emission or as a cumulative total; adaptable to any geometry	can be very sensitive for detecting onset of cracking	expensive, sophisticated equipment; filtering of extraneous noise from test machine and grips necessary during testing; poor correlation with crack length; signals are material-dependent

NRC FORM 335 (7 77)

U.S. NUCLEAR REGULATORY COMMISSION

BIBLIOGRAPHIC DATA SHEET

1. REPORT NUMBER *(Assigned by DDC)*
NUREG/CR-3091
BNL-NUREG-51630

4. TITLE AND SUBTITLE *(Add Volume No., if appropriate)*
Review of Waste Package Verification Tests
Semiannual Report Covering the period April-September 1982

2. *(Leave blank)*

3. RECIPIENT'S ACCESSION NO.

7. AUTHOR(S)
G.T. Bida, D. Eastwood, H. Jain, B. Siskind, P. Soo.

5. DATE REPORT COMPLETED
MONTH: November YEAR: 1982

DATE REPORT ISSUED
MONTH: April YEAR: 1983

9. PERFORMING ORGANIZATION NAME AND MAILING ADDRESS *(Include Zip Code)*
Department of Nuclear Energy
Brookhaven National Laboratory
Upton, New York 11973

6. *(Leave blank)*

8. *(Leave blank)*

12. SPONSORING ORGANIZATION NAME AND MAILING ADDRESS *(Include Zip Code)*
Division of Waste Management
Office of Nuclear Material Safety and Safeguards
United States Nuclear Regulatory Commission
Washington, DC 20555

10. PROJECT/TASK/WORK UNIT NO.

11. CONTRACT NO.
A3167

13. TYPE OF REPORT
Final Report

PERIOD COVERED *(Inclusive dates)*
April 1982 - September 1982

15. SUPPLEMENTARY NOTES

14. *(Leave blank)*

16. ABSTRACT *(200 words or less)*

This is part of an ongoing task to identify tests that may be used to verify that engineered waste package/repository systems meet the containment and controlled release performance objectives of 10 CFR 60. The report describes tests to verify that chemical and mechanical failure modes in TiCode-12 containers and bentonite and zeolite-based packing materials do not compromise the 300-1000 year containment period for these engineered barriers.

17. KEY WORDS AND DOCUMENT ANALYSIS

17a. DESCRIPTORS

17b. IDENTIFIERS/OPEN-ENDED TERMS

18. AVAILABILITY STATEMENT
Unlimited

19. SECURITY CLASS *(This report)*
Unclassified

21. NO. OF PAGES

20. SECURITY CLASS *(This page)*

22. PRICE
$

NRC FORM 335 (7 77)